Aus dem Institut für Neurophysiologie

der Medizinischen Fakultät Charité – Universitätsmedizin Berlin

DISSERTATION

Influence of microglial activation on neuronal survival and excitability

Zur Erlangung des akademischen Grades

Doctor of Philosophy (PhD)

Im Rahmen des

International Graduate Program Medical Neurosciences

vorgelegt der Medizinischen Fakultät

Charité – Universitätsmedizin Berlin

Von

Ismini Papageorgiou

aus

Athen, Griechenland

Gutachter/in: 1. Prof. Dr. Uwe Heinemann

2. Prof. Dr. med. F. Heppner

3. Prof. Dr. rer. nat. U.-K. Hanisch

Datum der Promotion: 22. März 2013

To

Maria, Vagelis

and

Panagiotis

ACKNOWLEDGEMENTS

It is a really trivial task trying to rank a long list of colleagues and friends, who all have contributed, materially or mentally, in the successful accomplishment of this work.

In order to avoid listing them after 'importance', I would rather introduce a chronological order and start with my teacher and professor at the Medical School of Patras, Dr. Aristidis Charonis. His devotion to science captured my interest and brought me in the world of 'blots, manuscripts and citations'. I thank him the most for believing in me and for encouraging me with indissoluble enthusiasm till today. Thanks, Aris!

I will always be grateful to my family, Maria, Vagelis and Panagiotis, to whom my dissertation is dedicated, for emotionally and financially supporting my decision to follow science far away from my hometown.

In 2007, as a beginner in the International program 'Medical Neurosciences', I started working in the group of my professor, supervisor and teacher, Dr. Uwe Heinemann. With his warm and friendly personality that accentuates his scientific image he played a decisive role in my career orientation towards the central nervous system. I thank him a lot for his influence, for being the same time inspirational and revolutionary critical and for quite often stretching his timetable with our long-lasting project reports.

In the group of Prof. Heinemann I met my former project leader and current professor at the University of Heidelberg, Dr. Oliver Kann. I thank him for trusting me in this project and for teaching me how to transform my ideas into scientific thought, how to design, organize, judge and, why not, reject a project if necessary. With him I have learned how to set the experimental rules and subsequently comply with them. I also thank him for carefully editing this manuscript, for providing me with his critical comments and for being always available for discussions.

From my close laboratory environment in the Institute of Neurophysiology, I would like to point out the contribution of Dr. Siegrun Gabriel, Dr. Christine Huchzermeyer and Dr. Richard Kovacs, who devoted so much time with me in troubleshooting the electrophysiology setup. Without them and without the excellent technical assistance of Kristin Lehmann, the realization of this project on time would have been impossible. Moreover, I am exceptionally grateful to our secretary, Sonja Frosinski, to Katrin Schulze and Andrea Schütz for the lab management, to Dr. Hans-Jürgen Gabriel and Bernd Schacht for their experienced technical support.

I would also like to acknowledge our collaborators from other institutes: my former classmate in the Master program and thereafter colleague, Gina Eom, and Prof. Frank Heppner from the Institute for Neuropathology Charité Universitätsmedizin, as well as Prof. Uwe-Karsten Hanisch, Dr. Denise van Rossum and Dr. Tommy Regen from the Department of Neuropathology University of Göttingen, for theoretically and technically consulting the molecular part of this project.

At this point I ought to emphasize the importance of being part of the International program Medical Neurosciences – first as a Master student and then as a PhD candidate. The program provided me and my classmates with the opportunity to visit different labs and supported us with the excellent office and scientific administration of Lutz Steiner, Lars Niehaus, Petra Wienzek, Ralf Ansorg, Chen Hu-Ping and Dr. Benedikt Salmen.

Last, but not least, I would like to express my warmest gratitude to my closest friends that decorated not only my scientific but also my personal life in Berlin: Dr. Benedikt Salmen and Dr. Nikolaus Maier for introducing to me Σplot and MatLab, and Andriani Fetani for her precise and systematic work in microglial quantitative morphology. Benedikt, Nikolaus and Andriana, I owe you a lot!

Heidelberg, September 2012

This work was financially supported by the Deutsche Forschungsgemeinschaft (DFG) with the SFB/TR3 transregional grant for Medial Temporal Lobe Epilepsies.

I. TABLE OF CONTENTS

II. LIST OF FIGURES

III. LIST OF TABLES

IV.LIST OF ABBREVIATIONS

aCSF	artificial cerebrospinal fluid
AP	action potential
CA	cornu ammonis
DG	dentate gyrus
ELISA	enzyme-linked immunosorbent assay
E-S coupling	fEPSP - fPopS coupling
fEPSP	field excitatory post-synaptic potential
fPopS	field population spike
IL-6	interleukin 6
ISI	interstimulus interval
KA	kainate
KIR	inward rectifying potassium channels
KOR	outward rectifying potassium channels
LFP	Local field potential
LPS	Lipopolysaccharide
MHC-II	Major histocompatibility complex class II
MUA	Multiunit activity
NMDA	n-methyl-D-aspartic acid
NO	nitric oxide

NO_2	nitrite
OD	optical density
PBS	phosphate buffered saline
PI	pulse index
PPD	paired pulse depression
PPF	paired pulse facilitation
PPI	paired pulse index
RD	reagent diluent
ROI	region of interest
SC	Schaffer collateral
TLR	toll like receptor
TNF-α	tumor necrosis factor alpha

1. INTRODUCTION

1.1. MICROGLIA AS RESIDENT INNATE IMMUNE CELLS IN THE CENTRAL NERVOUS SYSTEM

Microglial cells are resident tissue macrophages of the central nervous system (CNS) and constitute 5-20% of the total cell population (Mittelbronn et al., 2001; Streit, 2005; Ransohoff and Cardona, 2010). In contrast to other tissue macrophages and much more than dendritic cells (Carson et al., 1998; Banchereau et al., 2000; Reis e Sousa, 2006), microglia are highly ramified and cover distinct, non-overlapping domains with their processes (Ransohoff and Cardona, 2010; Verkhratsky, 2010).

Microglia were morphologically identified by Santiago Ramón y Cajal (1913), who introduced the term 'third element' to discriminate them from astrocytes ('second element') and neurons ('first element'). Later on, Pio del Rio-Hortega (1932) recognized two cell groups within Cajal´s 'third element': microglia and oligodendroglia (Streit, 2005; Wirenfeldt et al., 2011).

1.1.1. MESODERMAL PROGENITORS COLONIZE THE CENTRAL NERVOUS SYSTEM DURING EMBRYONIC LIFE

In contrast to other glial cells (astrocytes, oligodendroglia), who share with neurons a common ectodermal progenitor, microglia originate from the embryonic mesoderm. The mesodermal origin of microglia was hypothesized already by del Rio Hortega (1919, 1932) (Chan et al., 2007; Wirenfeldt et al., 2011). However, his hypothesis was recently validated with engineering of PU.1 knock-out mice, where deletion of a macrophage differentiation factor extinguished the peripheral macrophage population along with microglial cells from the CNS (McKercher et al., 1996). Further fate-mapping experiments confirmed that microglia derive from primitive blood marrow precursor cells that arise early in development from the embryonic yolk sac (Ginhoux et al., 2010).

Bone marrow precursor cells colonize the human CNS between the 6.5th and 8th gestational week (Rezaie et al., 1999; Wirenfeldt et al., 2011), at the developmental Carnegie state 18 – 20 (Witschy, 1962; Theiler, 1972; Hill, 2008). The equivalent of Carnegie´s stage 18-20 occurs between the 9th and 12th gestational day in the rat and between the 8th and 9th gestational day in the mouse (Clancy et al., 2007a, 2007b; EMAP eMouse Atlas Project, 2012). Indeed, the bone

marrow microglial precursors emerge from the mouse yolk sac on embryonic day 8 and invade the CNS one day later (Ginhoux et al., 2010).

Bone marrow precursors invade by crossing the meninges and colonize all parts of the brain, while concomitantly acquiring a ramified phenotype (Cuadros and Navascues, 1998; Chan et al., 2007; Monier et al., 2007). Two types of migration have been assigned to microglial precursors: tangential migration, which covers long distances and is associated with ameboid morphology (Marin-Teva et al., 1998), and radial migration across the cortical layers, which is followed by docking and ramification (Sanchez-Lopez et al., 2004). The same procedure is observed *in vitro* after microglial seeding on organotypic slice cultures (Hailer et al., 1997a; Hinze and Stolzing, 2011).

1.1.2. RESTING / SURVEYING MICROGLIA: VERSATILE CELLS WITH COMMITTED STATUS TO ENVIRONMENTAL FUNCTION

As dictated by their developmental lineage, microglial cells are tissue macrophages expressing a CNS-committed phenotype (Lawson et al., 1990; Biber et al., 2007; Kettenmann et al., 2011). This renders them highly responsive to pathological but also physiological homeostatic changes (Schwartz et al., 2006; Hung et al., 2010). Microglia in the undisturbed CNS are termed as 'resting'. However, the observation that microglial branches constantly palpate (Davalos et al., 2005; Nimmerjahn et al., 2005; Ohsawa and Kohsaka, 2011) has challenged the terminology 'resting' with the less static term 'surveying', which emphasizes their active role in the guarding the CNS homeostasis (Hanisch and Kettenmann, 2007).

1.2. MICROGLIAL ACTIVATION

Microglial activation does not emerge as a continuum, but as an assembly of independent phenotypic traits, which are triggered in a context-dependent manner (Lemke et al., 1999). The definition of the partially reversible (Hailer et al., 1997a, 1997b; Perry et al., 2010) morphological and functional changes occurring during activation depends on a wide range of parameters, which encompass the lack of a surrogate staging marker. Morphology (Davalos et al., 2005), motility (Gyoneva et al., 2009), secretion of cytokines (Hartlage-Rübsamen et al., 1999), free radicals (Dringen, 2005), arachidonic acid metabolites (Matsuo et al., 1995), and

changes in the membrane potassium conductance (Kettenmann et al., 1990; Schmidtmayer et al., 1994; Eder et al., 1995; Fischer et al., 1995) are some of those.

1.2.1. MORPHOLOGICAL CORRELATES OF MICROGLIAL ACTIVATION

Microglial activation is correlated with morphological changes in the cell´s soma and processes, which can be visualized by *Griffonia simplicifolia* isolectin B4 (Streit and Kreutzberg, 1987; Stence et al., 2001) or antibodies against markers such as Iba1 (Ito et al., 1998; Jinno et al., 2007; Shapiro et al., 2009) and CD11b (Roy et al., 2006; but see also Matsumoto et al., 2007 for CD11b marker selectivity). Activation using the Gram (-) bacterial endotoxin lipopolysaccharide (LPS) has been associated with round-shaped somatic transition (Nakamura et al., 1999) and process retraction (Stence et al., 2001; Davalos et al.,2005; Haynes et al., 2006; Orr et al., 2009; Hung et al., 2010; Fontainhas et al., 2011). In their resting/surveying status, microglial cells extend numerous branches (processes), therefore termed 'ramified microglia'. Activation is associated with rounding of the somatic shape, process retraction and transition to the process-devoid, 'ameboid' phenotype (Figure 1C). Exceptionally, immature microglia from juvenile animals exhibit ameboid morphology which is not correlated with pathology (Marin-Teva et al., 1998; Sanchez-Lopez et al., 2004; but see also Brockhaus et al., 1993, 1996). Intermediate states (Kreutzberg, 1996), such as the one depicted in Figure 1B, show that the transition from the ramified to the ameboid status is not an all-or-none phenomenon.

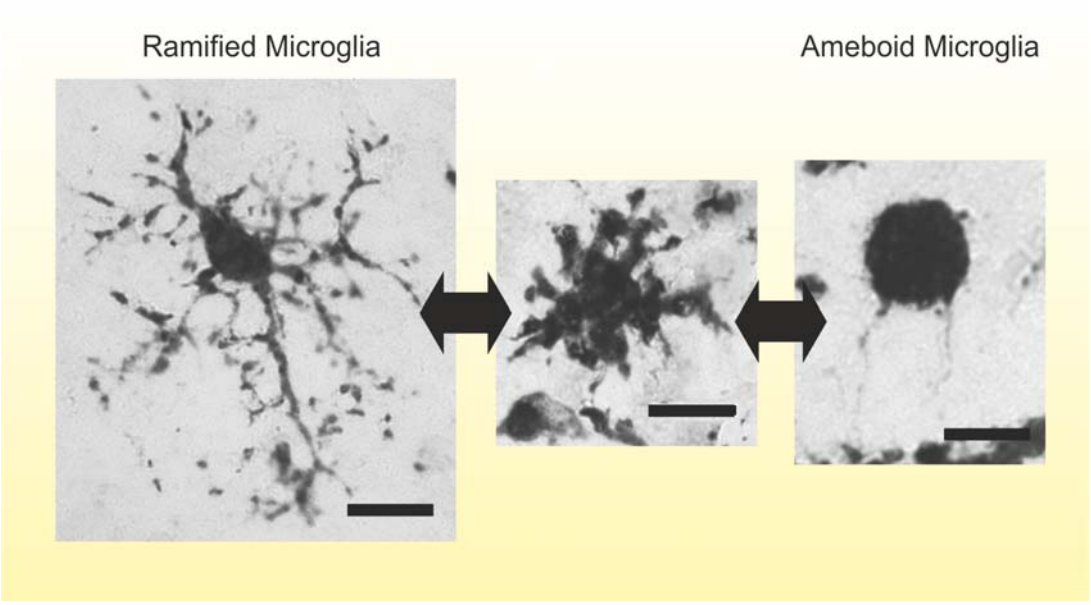

FIGURE 1: MICROGLIAL MORPHOLOGY, RAMIFIED AND AMEBOID MICROGLIA

Microglia in their resting/surveying state are highly ramified cells (left panel: ramified microglia). Activation stimuli trigger retraction of processes and enlargement of somata towards the transition to the ameboid phenotype (right panel: ameboid microglia). Iba1 immunohistochemistry, microglia sampled from the middle organotypic layers, scale bar = 15 µm.

1.2.2. MICROGLIAL MOTILITY AND MOBILITY

Inspite of being docked tissue macrophages, microglia exhibit a broad motility and mobility spectrum. Their branches are in constant palpating motion that occurs without somatic translocation, the latter being a trait of activation. Whereas the term 'motility' refers to palpation of processes (Nimmerjahn et al., 2005), 'mobility' describes positional changes and somatic migration. Microglial branch motility occurs in the undisturbed CNS and is suggested to serve environmental surveillance, whereas mobility is considered a hallmark of brain pathology such as brain trauma (Stence et al., 2001) and spreading depression (Grinberg et al., 2011). Interestingly, experimental exposure to LPS also triggers microglial mobility (Gyoneva et al., 2009).

1.2.3. MICROGLIA AS VECTORS OF INNATE IMMUNITY

The immune properties of microglial cells are constitutively suppressed in the CNS. However, upon homeostatic disruption microglia become competent phagocytes and perform all innate immunity functions necessary to initiate and perpetuate inflammation, such as antigen presentation, chemotaxis, cytotoxicity, phagocytosis and secretion of chemokines that recruit elements of the adaptive immune response.

Major histocompatibility complex molecules of class II (MHC-II), such as DR, DP, DQ, necessary for antigen presentation to CD 4(+) T-cells (Ulvestad et al., 1994b), but also pattern recognition receptors such as toll-like receptors (TLRs) (Bsibsi et al., 2002; Olson and Miller, 2004) are constitutively expressed at low levels and up-regulated upon activation. Moreover, activation prompts the synthesis and secretion of proinflammatory mediators. Cytokine

secretion from activated microglia has been confirmed in *in vivo* and *in vitro* preparations of human (Helmy et al., 2011a, 2011b) and murine brain (Hartlage-Rübsamen et al., 1999; Lemke et al., 1999; Mertsch et al., 2001; Zhang et al., 2008b). Cytotoxicity and parenchymal damage is mediated by the production of reactive oxygen and nitrogen species (Dringen, 2005), arachidonic acid metabolites (Matsuo et al., 1995) and extracellular matrix lytic enzymes such as matrix metalloproteinase (Gottschall et al., 1995a, 1995b; Cross and Woodroofe, 1999; Rosenberg et al., 2001) and elastase (Nakajima et al., 1992). Equally to macrophages, activated microglia remove apoptotic debris and opsonized targets via phagocytosis (von Zahn et al., 1997; Beyer et al., 2000; Ribes et al., 2009, 2010; Hughes et al., 2010).

1.2.4. MEMBRANE POTASSIUM CONDUCTANCE

Microglial activation *in vivo* and *in vitro* has been associated with changes in the passive membrane conductance and resting membrane potential. Resting/ramified microglial cells *ex vivo* exhibit little if any membrane current and their resting membrane potential is at the range of -20 mV (Boucsein et al., 2000). However, ameboid microglia from juvenile animals are relatively hyperpolarized (around -40 mV) and exhibit voltage-gated inward-rectifying potassium currents (Brockhaus et al., 1993; Schilling and Eder, 2007).

Microglial activation *in vivo* due to trauma (Boucsein et al., 2000), ischemia (Lyons et al., 2000) or status epilepticus (Avignone et al., 2008) is associated with changes in the membrane conductance and modified expression of the inward and outward (delayed) rectifying potassium channels (Kettenmann et al., 2011).

The ‘resting’ phenotype of microglial cells in primary cultures resembles the *in vivo* juvenile pattern of dominating voltage-gated inward rectifying potassium currents (Kettenmann et al., 1990). Upon LPS-triggering, an outward (delayed) rectifying potassium current, reminiscent of that observed *in vivo*, is additionally expressed (Ilschner et al., 1995; Nörenberg et al., 1994).

1.2.5. MICROGLIAL ACTIVATION STIMULI: STRANGER OR DANGER

Microglial cells are under constitutive suppression by signals expressed in the undisturbed CNS (Biber et al., 2007). Homeostatic imbalance and extinction of the suppressing signals is permissive for microglial activation (Cardona et al., 2006).

As vectors of innate immunity in the CNS, microglia can be activated by a variety of extrinsic and intrinsic stimuli. Importantly, disruption of the blood brain barrier, which mediates the physical separation of the CNS parenchyma from the plasma components, is immediately sensed by microglia and associated with their transition to ameboid phagocytes. Some examples of microglial triggering stimuli are listed here:

- Extrinsic factors, like foreign particles (Block et al., 2004), and pathogens, the latter ranging from Gram (+) and Gram (-) bacteria (Prinz et al., 1999) to viruses (Weissenböck et al., 2000; Ovanesov et al., 2006) and prions (Siskova et al., 2000; Thellung et al., 2007).
- Intrinsic stimuli such as temperature changes (Sugama et al., 2011), synuclein (Zhang et al., 2005; Austin et al., 2006), alpha-beta amyloid aggregates (Garcao et al., 2006; Zhang et al., 2011a) and signals released from degenerating neurons (Rupalla et al., 1998; Zhou et al., 2005) such as chromogranin A (Ciesielski-Treska et al., 1998) and μ-calpain (Levesque et al., 2010).
- Disruption of the blood brain barrier, extravasation of plasmin (Sheehan and Tsirka, 2005), fibrinogen (Adams et al., 2007; Ryu et al., 2009a, b) and thrombin (Choi et al., 2003; Hanisch et al., 2004; Möller et al., 2006). Thrombin is strong microglial activating factor that acts not only by pure enzymatic pathways, but also via non enzymatic, possibly receptor-mediated interaction (Hanisch et al., 2004).

Neurotransmitters can modify microglial motility (Fontainhas et al., 2011), morphology (Hung et al., 2010) and cytokine secretion (Noda et al., 2000; Mahe et al., 2005), therefore can be considered as 'activating' stimuli. Both physiological (Rochefort et al., 2002; Hung et al., 2010; Fontainhas et al., 2011) and pathological CNS events such as seizures (Rizzi et al., 2003; Ravizza et al., 2005; Foresti et al., 2009; Johnson and Kan, 2010; Longo et al., 2010; Akin et al., 2011; Jung et al., 2011; Yeo et al., 2011) and spreading depressions (Grinberg et al., 2011) have been associated with different 'stages' of microglial activation, eventually proportional to the degree of neuronal activity (Ravizza et al., 2005; Hung et al., 2010; Fontainhas et al., 2011).

1.3. MICROGLIAL TURNOVER

The microglial cell population comprises at least two subpopulations with individual turnover kinetics in a dynamic relationship: the inherent/resident microglia population, with potential for local self-renewal throughout life (Ajami et al., 2007), and the blood-borne population, which is renewed by circulating bone marrow precursors that invade the CNS (Lawson et al., 1992; Streit, 1993; Streit and Graeber, 1993; Bechmann et al., 2001; Priller et al., 2001; Wirenfeldt et al., 2007, 2011; Hinze et al., 2011). Lacking a discrimination marker, their relative contribution has been investigated in animal models of bone marrow chimeras (Kennedy and Abkowitz, 1997; Priller et al., 2001; Wirenfeldt et al., 2005, 2007) and donor-vector parabiosis (Massengale et al., 2005; Ajami et al., 2007). In bone marrow chimeras, the hematopoietic lineage is depleted by total body irradiation and replenished with labeled transplants, which allow for visualization of the brain (re)population by peripheral progenitor cells. On the other hand, in parabiosis experiments an animal with labeled hematopoietic lineage (donor) is 'co-joint' to a non-labeled vector with a vascular bridge. Parabiosis has the advantage of preventing the irradiation-induced blood-brain barrier damage that may contaminate the physiological progenitor invasion pattern (Perry, 2010).

Under physiological conditions, the invasion of blood-borne macrophages is estimated to contribute by 30% to the annual population turnover. However, only perivascular and leptomeningeal microglia are replaced by blood borne macrophages, whereas parenchymal microglia are considered a self-renewable population (Kennedy and Abkowitz, 1997). After ischemic or traumatic CNS insults resident microglial proliferation predominates the blood-borne cell invasion, which contributes with delayed kinetics and a maximum rate of 40% around the 7^{th} post-lesional day (Schilling et al., 2003, 2009; Wirenfeldt et al., 2005).

1.4. MICROGLIA – NEURON INTERACTIONS

Microglial cells establish a dynamic relationship with neurons, in which they can sense and modify neuronal signaling (Streit, 1993; Biber et al., 2007). The so-called 'neuronal-microglial cross-talk' is a novel research topic with relevance to physiological and pathological conditions, such as aging, stress and inflammation (Jurgens et al., 2010).

1.4.1. NEURON-TO-MICROGLIA SIGNALING

Based on the notion that immune functions are repressed in the healthy brain, the current opinion in neuron-to-microglia communication is that the latter reside under constant repression by neurons (Neumann, 2001; Polazzi et al., 2002; Biber et al., 2007; Ransohoff et al., 2010). Blockade of action potentials with the voltage-gated sodium channel blocker tetrodotoxin suffices to increase MHC-II expression by microglia (Neumann et al., 1996), thus rehearsing their antigen presenting capacity. Moreover, neuronal seeding in primary microglial cultures attenuates their proinflammatory response to bacterial endotoxin (Chang et al., 2001).

The expanding list of neuronal-microglial signaling mediators varies from cell-adhesion molecules (Chang et al., 2000; Burgess et al., 2009) to facultative soluble factors (Harrison et al., 1998; Nishiyori et al., 1998) and neurotransmitters (Pocock et al., 2007) (Figure 2).

1.4.1.1. CONTACT DEPENDENT CROSS-TALK

Microglia, like other cells of the myeloid lineage, can sense the local environment via transmembrane protein-mediated, contact-dependent interactions, which convey more local information compared to soluble factors. Two well-recognized ligand-receptor pairs mediating neuronal-microglial communication are the CD47-CD172α (or SIRPα) and CD200/CD200R (Barclay et al., 2002; Wright et al., 2003; Hatherley et al., 2004).

Both neurons and microglia express CD47 and CD172α (Barclay et al., 2002). Ligation of the microglial CD172α by CD47 downregulates the phagocytic activity (Gitik et al., 2011), and decreased CD47 expression has been associated with exacerbation of multiple sclerosis lesions, probably due to release of microglia from the neuronal inhibitory control (Koning et al., 2007, 2009; Junker et al., 2009).

On the other hand, the membrane-bound glycoprotein CD200 is exclusively found in neurons (Webb and Barcley, 1984; Barclay et al., 2002; Minas and Liversidge, 2006) and the expression of its receptor, CD200R, is restricted to microglia (Hoek et al., 2000; Broderick et al., 2002; Wright et al., 2003). CD200R occupation is a strong suppressive signal for microglia (Hoeket al., 2000; Gorczynski, 2005; Jenmalm et al., 2006). The CD200R-mediated dampening of microglial response to activating stimuli has been considered as a functional part of the CNS immune privilege (Nathan and Müller 2001).

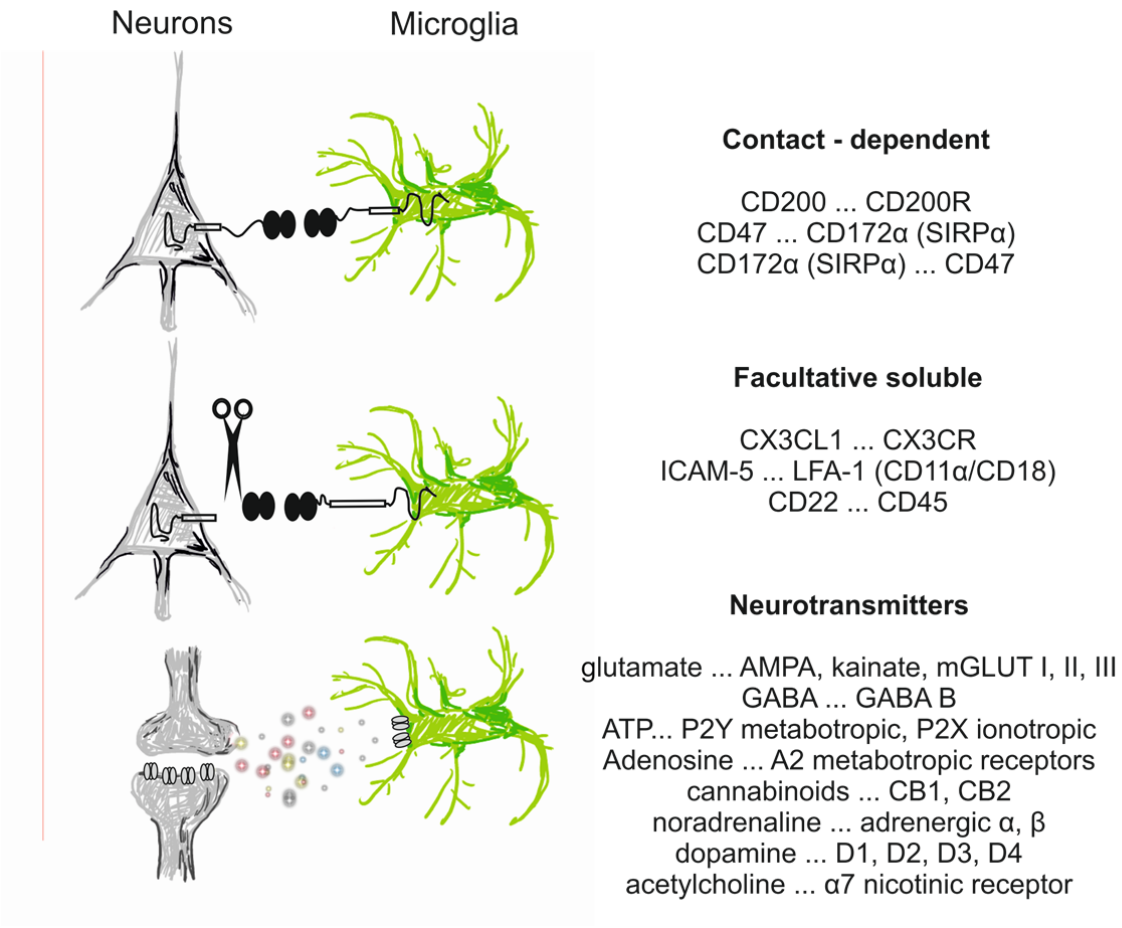

FIGURE 2: MICROGLIA-NEURON CROSS-TALK

Neurons and microglia constitutively express molecules that serve reciprocal signaling and suppress microglial immune functions in the physiological CNS. Some of them require physical contact between neurons and microglia and others are facultative soluble. Microglia sense synaptic activity by expressing a broad list of neurotransmitter receptors.

1.4.1.2. FACULTATIVE SOLUBLE NEURON-TO-MICROGLIA SIGNALING MEDIATORS

The intercellular adhesive molecule 5 (ICAM-5), or telencephalin (Oka et al., 1990; Gahmberg et al., 2008; Yang, 2012) is constitutively expressed by telencephalic neurons as membrane-bound and cleaved glycoprotein (Tian et al., 2008). ICAM-5 is a ligand for the lymphocyte

function–associated antigen 1 (LFA-1) integrin, which is in turn expressed on microglia and tunes chemotaxis (Dalmau et al., 1997; Watanabe and Fan, 1998; Mizuno et al., 1999).

The transmembrane tyrosine phosphatase CD45 (Irie-Sasaki et al., 2001; Penninger et al., 2001; Sasaki et al., 2001) is expressed by microglial cells as membrane bound and cleaved isoform (Mott et al., 2004) and downregulates their activation process (Tan et al., 2000a, 2000b) upon interaction with the neuronal sialoprotein CD22 (Stamenkovic et al., 1991; Aruffo et al., 1992; Sgroi and Stamenkovic, 1994; Tedder et al., 1997; Walker et al., 2007; Nitschke, 2009).

The chemokine CX3CL1 (fractalkine) and its receptor CX3C-R1 (Harrison et al., 1998; Clark, 2011) are also expressed with a polarized pattern: fractalkine is located in neurons and astrocytes (Harrison et al., 1998; Maciejewski-Lenoir, 1999; Hatori et al., 2002), whereas microglia express the fractalkine receptor CX3CR1 (Zujovic et al., 2000; Hatori et al., 2002). Receptor occupation with either membrane bound or soluble fractalkine (Harrison et al., 1998; Hundhausen et al., 2003; Clark et al., 2009), attenuates microglial activation (Harrison et al., 1998; Wynne et al., 2010). Engineering of the fractalkine knockout mouse (Cardona et al., 2006) demonstrated that fractalkine ablation renders microglia permissive to protracted activation (Corona et al., 2011). Thus, endogenous fractalkine acts as a tonic anti-inflammatory chemokine (Zujovic et al., 2000) and as an intrinsic inhibitor against neurotoxicity (Mizuno et al., 2003). Recently, disruption of the fractalkine/CX(3)CR1 signaling was shown to decrease survival and proliferation of neural progenitor cells in young rodents (Bachstetter et al., 2011) and lead to insufficient synaptogenesis and synaptic maturation (Paolicelli et al., 2011). These findings underlined the importance of neuronal-microglia communication for the healthy CNS maturation and function.

1.4.1.3. NEUROTRANSMITTERS MEDIATING NEURON-TO-MICROGLIA SIGNALING

Microglial cells can sense synaptic activity by expressing a broad range of neurotransmitter receptors, coupled to either repressive or activating intracellular cascades.

Ionotropic AMPA-kainate (Noda et al., 2000; Yamada et al., 2006) and metabotropic glutamate receptors of the group II (Taylor et al., 2002, 2005) and III (Taylor et al., 2003) on microglia sense glutamatergic activity by spill over (Okubo et al., 2011). Glutamatergic signaling has a

dual effect: ionotropic and group II metabotropic glutamate receptors prompt, whereas group III metabotropic receptors attenuate the proinflammatory response.

$GABA_B$ receptors on microglial cells (Charles et al., 2003; Kuhn et al., 2004) attenuate the LPS–triggered proinflammatory response by influencing the intracellular calcium-signaling properties (Kuhn et al., 2004).

The growing list of neurotransmitter receptors recognized on microglia includes currently receptors for (endo) cannabinoids (Klegeris et al., 2003; Walter et al., 2003; Ramirez et al., 2005; Stella, 2009), noradrenaline (Tomozawa et al.,1995; Blandino et al., 2006), dopamine (Färber et al., 2005; Tanaka et al., 2008; Mastroeni et al., 2009), acetylcholine (Zhang et al., 1998; Shytle et al., 2004; De Simone et al., 2005; Hwang et al., 2008a, 2008b; Moon et al., 2008; Nizri et al., 2008) and ATP (Honda et al., 2001; Davalos et al., 2005; Haynes et al., 2006). Hence, neuronal activity exerts a multidimensional effect on microglial physiology by tuning migratory behavior, inflammatory response and toxicity.

1.4.2. MODIFICATION OF NEURONAL FUNCTION BY MICROGLIA

Microglia actively respond to and modify neuronal signaling by multiple mechanisms such as (a) secreted factors, such as cytokines, NO and neurotrophins, (b) modifications of the extracellular matrix that affect axonal growth and guidance and (c) structural shaping of synapses and modulation of the presynaptic membrane´s lipid composition.

1.4.2.1. CYTOKINES AND NITRIC OXIDE

The primary evidence for potentiation of the NMDA receptor-mediated response by “heat- and protease-labile molecules released from microglia” (Moriguchi et al., 2003) has triggered the hypothesis that cytokines can directly modify synaptic transmission. Indeed, increasing experimental evidence supports that cytokines are versatile modulators of neuronal excitability and synaptic transmission (Viviani et al., 2007).

The proinflammatory cytokine tumor necrosis factor alpha (TNF-α) has been proposed to regulate the excitatory synaptic strength (Stellwagen and Malenka, 2006) by promoting NMDA (Wheeler et al., 2009) and AMPA receptor trafficking (Beattie et al., 2002; Leonoudakis et al., 2004; Ferguson et al., 2008; Santello et al., 2011), enhancing the NMDA-operated postsynaptic calcium entrance (Frey et al., 2010) and downregulating the expression of ionotropic GABA

receptors (Stellwagen et al., 2005). However, TNF-α can also exert inhibitory effects by enhancing the hyperpolarizing outward potassium currents (Dolga et al., 2008; Panama et al., 2011).

Interleukin-1 beta (IL-1β) is another proinflammatory cytokine with dual impact on neuronal activity. On the one hand, it increases neuronal excitability by blocking the calcium-activated outward potassium currents (Zhang et al., 2008a, 2008c, 2008d, 2010), enhancing NMDA receptor activity via phosphorylation of the NR-1 subunit (Viviani et al., 2003) and blocking of $GABA_A$-mediated inhibitory currents (Wang et al., 2000). Nevertheless, suppression of neuronal excitability by voltage gated calcium channels blockade has also been attested to IL-1β (Plata-Salaman et al., 1992, 1994).

Nitric oxide (NO) is constitutively synthesized in the brain by the neuronal and endothelial nitric oxide synthases (NOS), but also in activated microglia by the inducible NOS isoform (iNOS) (Amitai, 2010). NO, known as a factor for neurovascular coupling and cytotoxic activity (in high concentrations), has also been shown to participate in the establishment of long-term synaptic plasticity (Haley et al., 1992 a, b), synaptic remodeling (Sunico et al., 2005) and regulation of hyperpolarizing potassium current kinetics (Steinert et al., 2011).

The examples of TNF-α, IL-1β and NO demonstrate that microglia and neurons can mutually affect each other in a way that does not necessarily imply toxicity.

1.4.2.2. NEUROTROPHINS

Neurotrophins such as the neural growth factor (NGF), neurotrophin 3 (NT-3) and brain-derived neurotrophic factor (BDNF) are produced by microglia *in vivo* (Elkabes et al., 1996) and *in vitro* (Nakajima et al., 2001). BDNF of microglial origin was shown to invert the polarity of GABA-mediated chloride currents from hyper- to depolarizing during development but also under pathological conditions (Coull et al., 2005).

1.4.2.3. EXTRACELLULAR MATRIX MODIFICATION

The extracellular matrix composition, which provides the structural scaffolding for neurite outgrowth, is remodeled by microglial-secreted structural proteins and proteases. *Thrombospondin*, for instance, is an extracellular matrix protein that guides neurite outgrowth during development and traumatic recovery (Chamak et al., 1994, 1995; Möller et al., 1996).

Tissue plasminogen activator (tPA), an extracellular space protease (Iyer et al., 2010), activates the G-protein-coupled protease activated receptors on neurons, thereby modulating the NMDA receptor-mediated neuronal responses (Tomimatsu et al., 2002).

1.4.2.4. SYNAPTIC 'STRIPPING' AND 'PRUNING'

Morphological changes in synapses and dendritic spines have been correlated with functional synaptic plasticity, thus termed 'experience dependent structural plasticity' (Trachtenberg et al., 2002; Majewska et al., 2006; Harms et al., 2007; Holtmaat et al., 2008, 2009; Knott and Holtmaat, 2008; Bhatt et al., 2009; Fu et al., 2011).

Microglial cells residing proximal to synapses are believed to participate in this plastic remodeling. Synaptic apoptosis describes the local activation of apoptotic biochemical cascades in synapses and dendrites, and microglia are suggested to execute the removal of 'apoptotic' synapses (Mattson et al., 1998). Moreover, microglia selectively remove synapses based on their activity, a process termed synaptic 'stripping' and 'pruning' (Tremblay et al., 2011; Tremblay and Majewska, 2011). During synaptic stripping, as described in motor neurons (Blinzinger et al., 1968; Kreutzberg, 1996; Thamset al., 2008), in the cortex (Trapp et al., 2007) and in the denervated facial nucleus of rodents (Graeber et al., 1993; Thams et al., 2008), microglia mediate the dissociation between pre- and postsynaptic termini. Synaptic pruning, on the other hand, is the phagocytosis of 'apoptotic' synaptic elements that takes place without dissociation of the pre- and postsynaptic elements (Svensson et al., 1993; Tremblay et al., 2011). Both synaptic stripping and pruning are necessary for the physiological development and synaptic maturation in the CNS (Paolicelli et al., 2011).

Recent evidence supports that microglia may shape synaptic morphology not only by removing tagged synapses, but also by interfering with the presynaptic membrane´s lipid composition. Microvesicles comprising lipid rafts are secreted my microglia and incorporated in the presynaptic terminus, in this way possibly modifying the presynaptic vesicles´ release probability (Antonucci et al., 2012).

1.5. HYPOTHESIS, AIMS AND OBJECTIVES

HYPOTHESIS

Microglial activation is correlated with neuronal death and/or dysfunction in many neurodegenerative diseases, such as Alzheimer´s disease (Lim et al., 2011a, 2011b; Liu et al., 2012; Mrak, 2012), multiple sclerosis (Henderson et al., 2009; Amor et al., 2010; Howell et al., 2010; Almolda et al., 2011; Gao and Tsirka, 2011; Sriram, 2011; van Noort et al., 2012) and epilepsy (Järvelä et al., 2011; Maroso et al., 2011a and 2011b; Najjar et al., 2011; Pernot et al., 2011; Yeo et al., 2011; Zattoni et al., 2011; Zurolo et al., 2011). Moreover, psychiatric disorders such as schizophrenia (Juckel et al., 2011; Kato et al., 2011;Monji et al., 2011; Blank and Prinz, 2012; Liaury et al., 2012; Madhusudan et al., 2012; Müller et al., 2012) and autismus (Blaylock and Strunecka, 2009; Morgan et al., 2010; Buehler, 2011; Heo et al., 2011; Young et al., 2011; Derecki et al., 2012; Maezawa et al., 2012; Tetreault et al., 2012;) have recently been correlated with chronic neuroinflammation and distorted immunity. However, it remains controversial whether activation itself is neurotoxic (Streit, 2002, 2005; Neumann et al., 2006; Polazzi et al., 2010). Since the term comprises a variety of distinct physiological reactions, its potential cytotoxicity might be dependent on the pathophysiological context.

AIMS

In the present work we investigated whether and to which extent microglial activation affects the viability and function of a neuronal network. We aimed to:

1. Induce and adequately characterize the ‘activation’ process

2. Assess its effect on neuronal viability and function

OBJECTIVES

In order to address our questions *in vitro* we use organotypic hippocampal slice cultures exposed to the Gram (-) bacterial endotoxin, lipopolysaccharide (LPS). The activation status of microglia and the degree of neurodegeneration are characterized by molecular and morphological methods.

- The culture supernatant is assayed for proinflammatory cytokines (IL-6, TNF-α) and for nitric oxide (NO) metabolites.

- Microglial proliferation and morphological changes are quantified using Iba1 immunostaining, stereology and digital analysis of Neurolucida®-based cell reconstructions.
- Neurodegeneration is evaluated morphologically using the fluorescent marker FluoroJade® B

The integrity of neuronal function is tested by extracellular electrophysiological recordings of the spontaneous and evoked activity in the CA1 hippocampal subregion, focusing on the

- input – output (I-O) and
- short-term plasticity properties

Furthermore, we employ ion sensitive microelectrodes to investigate the

- amplitude and
- kinetics of electrically evoked extracellular potassium transients ($[K^+]_o$),

which convey information on the integrity of not only neuronal but also astrocytic networks.

Thus, by combining morphology, electrophysiology and molecular biology we approach microglial activation and its consequences on neuronal function from several different aspects.

2. MATERIALS AND METHODS

2.1. ETHICS FOR ANIMAL EXPERIMENTS

In line with the reduction, replacement and refinement policy of the European Union for animal experiments, we sought to establish our methods *in vitro,* with the perspective to select and transfer the most important findings *in vivo*.

All procedures were carried out in accordance with the European Community Council Directive 2010/63/EU, the Animal welfare act of 25th Mai 1998 and the local legislation for the protection of animals (Tierschutzgesetz, Bek. v. 18.5.2006 I 1206, 1313; modified after Art. 20 G v. 9.12.2010 I 1934). All experiments were approved by the local committee for ethics in animal research (Landesamt für Gesundheit und Soziales Berlin, LaGeSo, T0032/08).

2.2. ORGANOTYPIC HIPPOCAMPAL SLICE CULTURES

The present study was conducted in organotypic hippocampal slice cultures, prepared from 5-7 day-old male Wistar rats, according to the interface method (Stoppini et al., 1991; De Simoni et al., 2006; Kovacs et al., 2009; Kann, 2011; Kann et al., 2011; Opitz-Araya et al., 2011).

Preparation, medium exchanges and pharmacologic exposures were performed with sterile equipment under a carefully cleaned hood (HERAsafe, Kendro Laboratory products GmbH, Hanau, Germany). This strategy allowed for utilization of antibiotic-free media, a policy aiming to avoid previously reported antibiotic 'artifacts' on neuronal activity, synaptic transmission and susceptibility to seizures (Dimpfel et al., 1996; DeSarro et al., 1999; Rothstein et al., 2005; González et al., 2007; Lee et al., 2007).

Organotypic slices were randomly prepared on a weekly basis from three different animals. After decapitation, the hippocampus was isolated and transversely sliced in 400 µm-thick-slices with a McIllwain tissue chopper (Mickle Laboratory Engineering Co.Ltd., Surrey, UK). Then the slices were transferred in ice-cold dissection medium (Table 1), rigorously bubbled with a gas mixture of 95% oxygen (O_2) and 5% carbon dioxide (CO_2) and pair-wise affixed on Millicell®-CM, 0.4 µm porous membrane inserts (Millipore GmbH, Schwalbach/Ts, Germany). Each insert was immersed in 1 ml of incubation medium (Table 1), which was exchanged the first day after preparation and then on a three-times-weekly basis, unless otherwise indicated.

The slices were incubated with 5% carbogen dioxide (CO_2) and 80% humidity (UniEquip GmbH, Munich, Germany) at 37 °C.

2.2.1. IN VITRO ACTIVATION OF MICROGLIA CELLS USING LIPOPOLYSACCHARIDE

The Gram (-) bacterial endotoxin (lipopolysaccharide, LPS) was selected for triggering microglial cells due to its affinity for the toll-like receptor 4 (TLR4), a pattern-recognition receptor mainly expressed in cells of the macrophage and lymphoid lineage (Heine et al., 2001).

In the CNS, LPS is suggested to selectively target microglia (Lehnardt et al., 2002, 2003) and mediate their activation primarily via TLR4 ligation (Kawai and Akira, 2009). Apart from the TLR4, more LPS-binding sites have been recognized, such as the CD11b/CD18 complex (CR1) (Perera et al., 2001; Park et al., 2004) and the scavenger receptor A (SRA) (Chen et al., 2010). However, the contribution of these sites is considered secondary, since LPS exposure fails to trigger an inflammatory response in TLR4 knockout mice (Chowdhury et al., 2006).

We exposed organotypic slices to purified LPS from *E. coli*, serotype R515 (Re) (ALEXIS biochemicals, Enzo Life Sciences AG, Lausen, Switzerland) according to the protocol summarized in Figure 3. Ten (10) μg/ml LPS were added to the freshly exchanged incubation medium at the 8th day *in vitro* (DIV8) and incubated for 72 consecutive hours without any medium exchange. Cultures from the same preparation served as controls. The incubation medium from control and LPS-exposed slices was harvested and stored at -20 ^{o}C for further determination of sequestered cytokines and nitrite.

2.2.2. GLUTAMATE EXCITOTOXICITY

In order to compare the potential neurodegenerative impact of LPS with a well-established positive control of cell death, we implemented the glutamate excitotoxicity model. Glutamate excitotoxicity is the phenomenon of neuronal apoptosis and necrosis due to excessive activation of glutamatergic N-methyl-D-aspartate (NMDA) and non-NMDA receptors. Neuronal death occurs due to massive calcium entry into the cytosol (Choi et al., 1987; Frandsen et al., 1989), which triggers secondary calcium release from the endoplasmic reticulum (Ruiz et al., 2009),

ER-stress, protein misfolding (Doyle et al., 2011; Walter and Ron, 2011) and, importantly, mitochondrial dysfunction (Nicholls, 2004).

Table 1
Media composition for preparation and maintenance of organotypic cultures

Medium	Component	Company	Concentration in Medium
Dissection Medium	Minimum Essential Medium (MEM)	Gibco, Grand island, New York, USA	1.6% w/v
	Trisbase	Sigma-Aldrich, Chemie GmbH, Steinheim, Germany	Trisbase 0.1M in distilled water for pH buffering to 7.35
Incubation Medium	Hanks Balanced Salt Solution (HBSS)	Sigma-Aldrich	reconstructed in sterile distilled water, 25% v/v
	Minimum Essential Medium (MEM)	Gibco	1.06 % w/v
	Fetal Calf Serum (FCS) *	Gibco	25 % v/v
	L-glutamine 200 mM	Gibco	1 % v/v
	Sodium Bicarbonate ($NaHCO_3$)	Sigma-Aldrich	58 ‰ w/v
	Trisbase 7-9	Sigma-Aldrich	Trisbase 0.1M in sterile distilled water for pH buffering to 7.35
	* FCS was inactivated by swirling at 56ºC for 30 min		
	** all solutions were prepared under the hood and filtered with 0.2 µm pore diameter sterile filters		

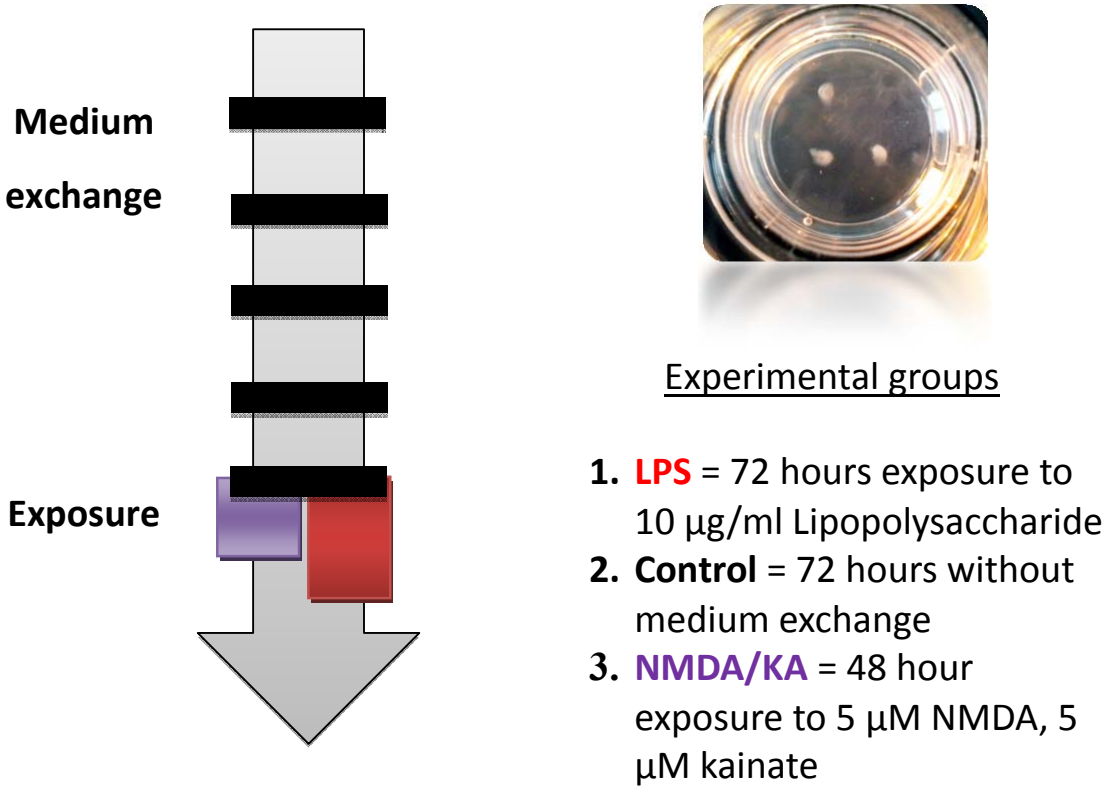

FIGURE 3: ORGANOTYPIC HIPPOCAMPAL CULTURES: MAINTENANCE AND PHARMACOLOGICAL MANIPULATIONS

Organotypic hippocampal slice cultures were incubated on semipermeable membranes for 8 days with medium exchange on the first day after preparation and then every second day. On DIV8 in the freshly-exchanged medium we added (a) 10 µg/ml LPS for 72 hours or (b) 5 µM NMDA and 5 µM KA for 48 hours. Organotypic slices with no medium exchange for 72 hours served as controls.

Excitotoxicity can be experimentally induced *in vitro* and *in vivo* using glutamatergic agonists with higher affinity to ionotropic glutamate receptors than glutamate itself, such as N-methyl-D-aspartate (NMDA) (Bruce et al., 1995; Vornov, 1995) and kainate (KA) (Wang et al., 2005; Zhang and Zhu 2011; Zheng et al., 2011).

Not only neurons, but also astrocytes (Seifert and Steinhäuser, 2001) and microglia (Yamada et al., 2006) express KA-receptors. KA-exposure has been proven lethal for astrocytes *in vitro* (David et al., 1996), whereas microglia respond to KA challenge *in vitro* (Zheng et al., 2010; Zhu et al., 2010) in a neurotoxic way.

The excitotoxic effect of NMDA predominates in the CA1, whereas KA has been shown to induce neuronal loss mostly in the CA3 subregion of organotypic hippocampal slice cultures (Casaccia-Bonnefil et al., 1993a, 1993b; Heppner et al., 1998; Zimmer et al., 2000; Kristensen et al., 2001). We used a combination of 5 μM NMDA and 5 μM KA to expose DIV 8 organotypic cultures for 48 hours (Figure 3). These cultures were processed for morphological quantification of neurodegeneration and microglial activation, using Fluoro-Jade B and anti-Iba1 immunohistochemistry, correspondingly.

2.2.3. IMMUNOHISTOCHEMISTRY

Organotypic hippocampal cultures were fixed in 4% paraformadehyde and 0.05% glutaradehyde in 0.1M phosphate buffered saline (PBS, pH 6.8) overnight. Incubation in 30% sucrose in PBS 0.1M for 2-3 hours preceded the embedding in Jung® freezing medium (Leica Microsystems GmbH, Nussloch, Germany) and slicing with a Jung CM1800® cryostat (Leica Microsystems) in 25 μm thick sections. Consecutive sections were harvested in PBS 0.1M and processed free-floating in wells.

Unspecific immunoglobulin binding was blocked with 10% normal goat serum (Gibco) for 30 min. Primary antibodies (Table 2) were diluted in 0.03% tritonated (Triton™ X-100, Sigma-Aldrich) PBS 0.1M with 10 % normal goat serum (Gibco), 0.1% sodium azide (Sigma-Aldrich) and 0.01% thimerosal (Sigma-Aldrich). Secondary antibodies were diluted in 0.03% tritonated PBS 0.1M with 1% normal goat serum. Both primary and secondary antibodies were incubated overnight at 4 ºC.

The biotin-conjugated secondary antibodies were visualized with a standard avidin-biotin complex kit (Vector Laboratories Inc., CA, USA) diluted 1:200 in 0.2% bovine serum albuminin PBS. The reaction substrate was 0.05% diaminobenzidine and 0.3% ammonium nickel sulphate in 0.05 M Trisbase 7-9 ®(Sigma-Aldrich), buffered at pH 6.8 with 1N HCl, catalysed by 0.003% hydrogen peroxide (H_2O_2).

Table 2
Primary and secondary antibodies used for immunohistochemistry

Primary antibodies	Host; type	Company	Dilution for brightfield microscopy
anti-iba1	rabbit, polyclonal	WAKO	1/1000
anti-S100b	rabbit polyclonal	Vector	1/500
anti-NeuN	mouse monoclonal	Millipore	
Secondary antibodies, reporters	**Host; type**	**Company**	**Dilution for brightfield microscopy**
anti-rabbit, biotin	goat	Sigma-Aldrich	1/2000
anti-rabbit, atto-488	goat	Sigma-Aldrich	
anti-mouse, biotin	goat	Vector	1/1000
anti-mouse, atto-633	goat	Sigma-Aldrich	

2.2.4. DESIGN-BASED STEREOLOGY

The stereological and morphometric analysis of microglia cells was conducted using Stereoinvestigator® and Neurolucida® (MicroBrightField, Inc., Williston, VT, USA). The imaging setup consisted of a brightfield microscope Axioskop® 40 (Carl Zeiss AG, Oberkochen, Germany), a Microfire® TM A/R camera (Optronics, California, USA) and an x-y-z galvo-table (Carl Zeiss). Cell tracing and counting was done with a Plan-Neofluar® 40x, dry type objective lens with NA 0.75 (Carl Zeiss).

Design-based stereology was implemented for the estimation of total microglia cell numbers. This quantitative morphological method is based on uniform random sampling, which means that a predetermined regular sampling pattern (uniform design) is repeatedly applied in random configurations. The method is not limited by assumptions on shape and particle randomness and could be successfully applied in the organotypic hippocampal cultures, as previously

reported (Oorschot et al, 1991). The prediction of a value in stereology is termed 'estimator' and designated with a circumflex accent "^" (Table 3).

The fractionator probe (Gundersen, 1986) provides an estimator of the total particle number in a 3-D object by measuring all particles of each sampling region and extrapolating the results to the total estimated volume of the object. The latter is estimated using the Cavalieri method (Gundersen and Jensen, 1987; Howard and Reed, 2005) (Figure 4B). In this study, for the estimation of neuronal number we used the optical fractionator probe (West, 1991, 2002), as already established for cell number estimations in hippocampal slice cultures (Oorschot et al., 1991).

Table 3
Stereological estimators and the optical fractionator probe sampling parameters

Number estimator	N^	
Area estimator	A^	
Volume estimator	V^	
Frame associated area	a/f	50 x 50 µm
Point associated area	a/p	
Fractionator height	h	18 µm
Points count in a region	P	
Slice thickness	d	25
Section distance	T	25
Slice periodicity	T/d	1
Slices per culture		4 to 5

2.2.4.1. AREA ESTIMATION USING THE WEIBEL METHOD

The contour area (*A*) was estimated with the point-counting system (Weibel, 1979) (Figure 4A) by sampling the number of grid points falling into the sampling space when a uniform grid of points was randomly superimposed on the defined contour. Each point corresponded to an area unit, termed point associated area (*a/p*), the size of which was determined by the grid size. The total area was calculated as the product of the total number of points counted in the contour (P) with the point associated area (*a/p*).

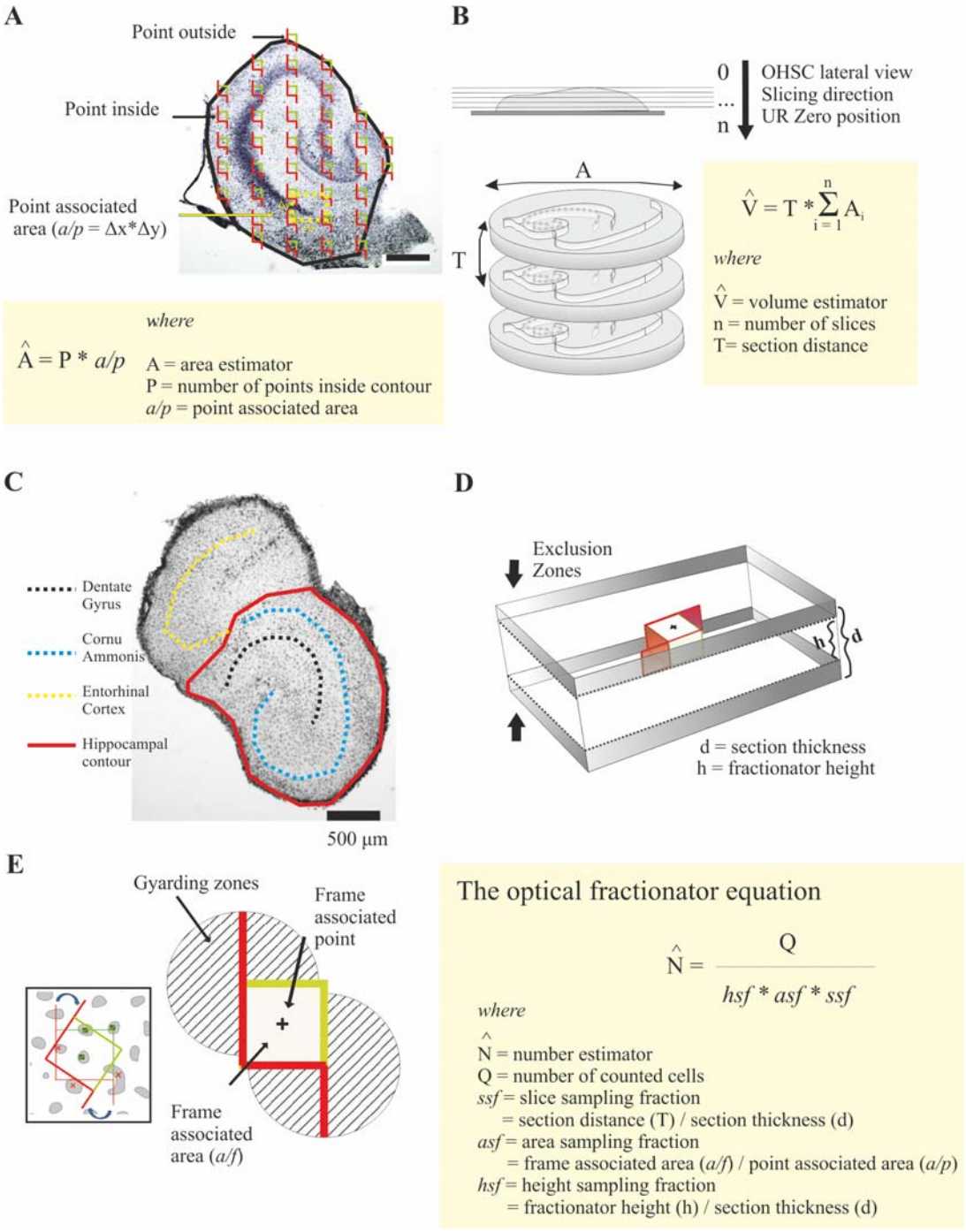

FIGURE 4: STEREOLOGY

Estimation of cell number using the optical fractionator probe.

(A) Organotypic hippocampal slice (DIV 11), 25 µm thick transverse section, stained with toluidine blue. The sampling frames (red and green boxes) are distributed on the region

of interest (ROI, black contour) in a uniform random way; this means that the same pattern of sampling frames could sample the ROI in any possible orientation. The ROI area was estimated according to the Weibel method from the number of frame-associated points (Figure 4E) falling into the contour (*P*). The total area estimator (*A*) is the product of P with the point associated area (*a/p*), averaged over multiple sampling trials. Scale bar = 500 µm.

(B) Volume estimation with the Cavalieri principle. The Cavalieri principle estimates the volume of an object (*V*) as a sum of the volume of its parts ($\Sigma\ T*A$). Organotypic slices are sliced in 25 µm-thick transverse sections. The section distance (*T*) was determined by the section thickness (*d*) divided by the slice sampling periodicity (*T/d*). For the organotypic slices T/d = 1, so the slice thickness (*d*) is equal to the section distance (*T*).

(C) DIV 11 organotypic hippocampal slice, Iba1 immunohistochemistry. Definition of the hippocampal contour (red) as chosen for microglial population size estimation. The neuronal layers of dentate gyrus (DG) and cornu ammonis (CA) are indicated by dotted lines. Scale bar = 500 µm.

(D) The optical fractionator three-dimensional sampling probe. Each sampling frame focuses on the top of the section and then scans the x-y plane towards the z-direction. The z-plane depth, named 'fractionator height' *(h)* is arbitrary set to fit the section thickness (*d*). The upper and lower 2% of the section thickness (exclusion zones) are precluded from sampling, so that the middle part of the section comprises the functional sampling zone. The number estimator (*N*) for the whole specimen is calculated from the total number of sampled cells (*Q*), normalized to the sampled volume fraction.

(E) The size of the sampling frame was 50 x 50 µm in order to fit the size and spatial distribution of microglia cells. It consists of two inclusion (green) and two exclusion (red) edges and two additional guarding exclusion zones, which exclude the rotational bias of sampling. The area included in the sampling square is termed 'frame associated area' (*a/f*) and the geometrical centre of the square 'frame associated point'.

2.2.4.2. VOLUME ESTIMATION USING THE CAVALIERI METHOD

The Cavalieri method (Howard and Reed, 2005; Gundersen and Jensen, 1987) estimates the volume of an object by uniform random sampling of plane sections in standard intervals. The total volume is defined as the sum of volumes between successive sampled areas. The uniform interval between slices *(T)* is the product of slice thickness *(d)* with the section sampling periodicity (Figure 4B, Table 3). The estimators were corrected for the inevitable tissue shrinkage imposed by the staining process by calculating the difference of section thickness between slicing and post-staining mounting.

2.2.4.3. MICROGLIAL POPULATION SIZE ESTIMATION USING THE OPTICAL FRACTIONATOR PROBE

The sampling contour around the hippocampus and the dentate gyrus (DG) was drawn with a low (5x) magnification objective lens, Plan-Neofluar® (0.15 NA) (Carl Zeiss) (Figure 4C).

The optical fractionator was implemented by applying a 3-D geometrical probe within the sampling contour in uniform random configuration and counting the number of points (particles) falling into it. The x-y plane of the 3-D geometrical probe corresponded to the frame associated area (*a/f*) and the z-axis to the height (*h*). The upper and lower 2 μm of the section thickness were excluded from sampling to avoid 'edge artifacts' from ranked tissue surfaces (Figure 4D). The sampling sites were aligned on a uniform grid, which was randomly superimposed on the selected contour. The total slice number per culture, the periodicity of sampling, the characteristics of the grid and the counting frame are summarized in Table 3.

2.2.4.4. COUNTING RULES: GEOMETRICAL PROBE DESIGN, INCLUSION AND EXCLUSION CRITERIA

Rigorous design of the stereological probe is crucial for the precision of the estimator. The counting frame consists of an inclusion (green) and an exclusion (red) line, which defines the frame associated area (*a/f*). Two exclusion guarding lines cover a 270^{o} exclusion zone around the hybrid (inclusion-exclusion line) edges, thus preventing rotational bias of the grid alignment. (Figure 4E). The frame associated point used for the Cavalieri volume estimation is located at the geometrical center of the counting frame.

Cells were sampled as points associated to the centre of the cell soma. For a positive count ('hit') a cell should fulfil the following inclusion criteria:

1. the whole soma being positioned inside the counting frame
2. the soma crossing a green (inclusion) line.

A cell was excluded from counting when:

1. the soma was crossing a red (exclusion) line
2. the soma was crossing a guarding line
3. the soma was positioned outside the counting frame

The optimal size of counting frame and grid spacing was determined with a pilot trial-and-error approach, where sampling parameters were adjusted to achieve a coefficient of sampling error (CE) > 0.9.

2.2.5. MORPHOMETRY AND SHOLL-ANALYSIS

The morphology of microglial cells, as defined by Iba1 immunohistochemistry, was analysed using the Neurolucida ® software for cell tracing and the NeuroExplorer® analysis software for digital processing of cell reconstructions (MicroBrightField).

Microglia cells were classified according to their somatic size and shape, arborisation size and complexity. The morphometric parameters used in this experimental setting were:

1. Area (*A*) and maximum length (*L*) of the soma at the x-y plane.
2. Shape index (*L/A*), deriving from the ratio of the maximum length to the area of the somatic projection. The shape index increased upon deviation from the circular shape (Figure 5A).
3. Microglial cell-process number, length and volume. The main processes (Figure 13A), which emerge directly from the cell soma, were quantified separately from the total process number, where both main and higher order processes were included.
4. Sholl analysis of process number and length with respect to the distance from the soma centre.
5. Microglia domain, defined as the territory occupied by a single cell with its branches (Figure 5C). Here a spherical domain is assumed to encompass the process network (Jinno et al., 2007).

The Sholl analysis model (Sholl, 1953) describes the cell process length and number using a system of homocentric cycles that converge at the geometrical centre of the soma and expand to encompass the cell process tuft. For microglial cells, the Sholl radius step was set at 10 μm, thus the second radial distance corresponded to 20 μm from the soma centre and the second Sholl sector was the area between the 10^{th} and the 20^{th} μm around the soma center. The intersection number of processes with each the homocentric cycle and the total process length in each sector reflected the density and convolution of microglia processes, respectively. (Figure 5B).

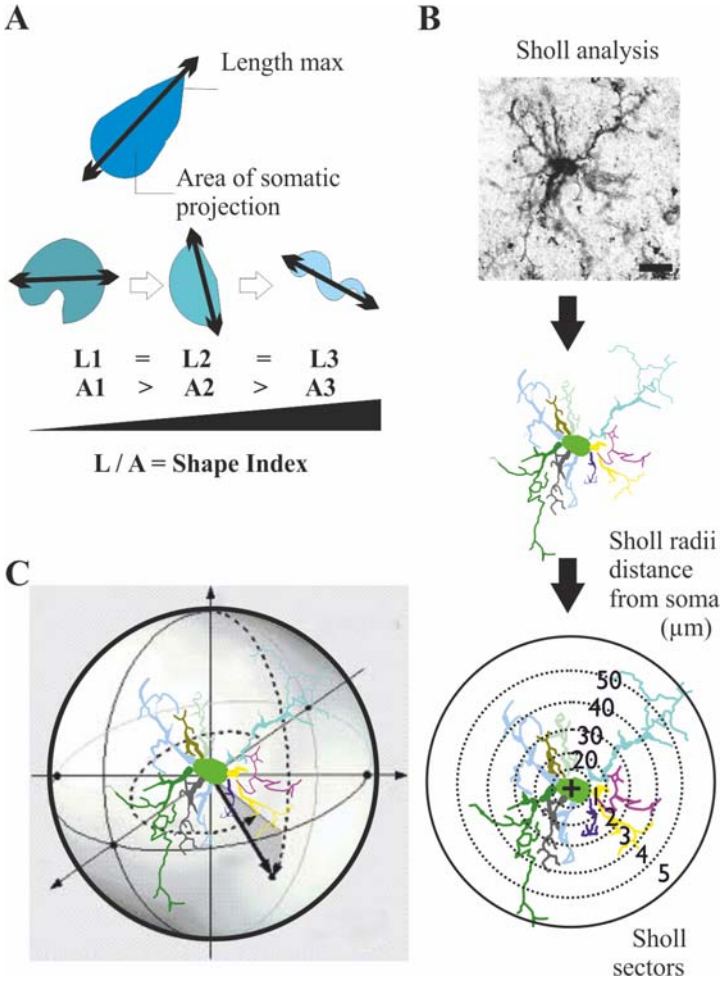

FIGURE 5: MORPHOMETRY

Microglial cells were traced using Neurolucida and analysed for somatic shape and branching pattern using the dedicated Neurolucida Explorer software.

(A) The two-dimensional somatic projection yielded the parameters of maximum somatic length (*L*) and area of somatic projection (*A*). The ratio *L/A* (shape index) provides with information about the somatic shape, since for a given somatic length (*L1 = L2 = L3*) the maximum area corresponds to the circular somatic shape (*A1*). Therefore, the somatic transition from rod-like to round morphology is quantified by the somatic shape index.

(B) Sholl analysis describes a cell´s branching pattern using a grid of homocentric rings with arbitrary (in this case, 10 µm) radial step, which extends to encompass the process tuft. The number of process *intersections* with each ring provides information about the process number, whereas the process *length* within a *sector* (defined by two consecutive rings) infers to the degree of process convolution. Scale bar = 10 µm.

(C) Microglial cell domain: is defined as the spherical region occupied by a cell´s process tuft. The outermost Sholl radius is assumed as the radius of the spherical domain.

2.2.6. ENZYME-LINKED IMMUNOSORBENT ASSAY (ELISA)

To estimate the level of secreted cytokines we assayed the culture supernatant with commercial enzyme-linked immunosorbent assay (ELISA) detection kits for interleukin 6 (IL-6) and tumor necrosis factor alpha (TNF-α) (R&D Systems, Inc., Minneapolis, MN, USA). The assays were carried in 96 well plates with 50 µL solution volume per plate, and the samples were 10-fold diluted in reagent diluent (RD) before testing (Table 4). The optical density was calibrated with known concentrations of the target antigen by construction of standard curves. Eight-point standard curves were constructed from sequential two-fold dilutions of recombinant IL-6 and TNF-α in RD and averaged over 4 repetitions. The highest concentration in the standard curve was 8000 pg/ml for IL-6 and 4000 pg/ml for TNF-α, whereas the lower (8^{th}) position was occupied by fresh culture medium (background).

Capture antibodies (mouse anti-rat IL-6 and mouse anti-rat TNF-α) were diluted in PBS without carrier protein, in working concentration of 4 pg/ml and used for coating the reaction plate at 4 ^{o}C overnight (Table 4). After blocking the plates for 1 hour with RD, samples were incubated for with the capture antibody for 2 hours. Sequentially, the detection antibodies (goat anti-rat IL6 and goat anti-rat TNF-α), diluted at 400 ng/ml and 100 ng/ml in RD, respectively, were incubated for 1.5 hour, washed out and visualized with 100 µL of substrate solution (Table 4). As soon as the standard samples were adequately developed, the reaction was stopped with 50 µL of stop-solution (Table 4) and the optical density (OD) was determined with a micro-plate reader at 540 nm with correction at 450 nm.

The concentration of cytokines in pg/ml was calculated after fitting the standards in a quadratic equation

$$y = y_o + ax^2 + bx$$

where

- y is the cytokine concentration and
- x is the measured OD.

Table 4
ELISA reagents for TNF-α and IL-6 estimation in the culture supernatant

Tradename	Solution	Consistency
	PBS	137 mM NaCl
		2.7 mM KCl
		8.1 mM Na_2HPO_4
		1.5 mM KH_2PO_4
		pH 7.2 - 7.4
	Wash Buffer	0.05 % Tween® 20 in PBS
		pH 7.2 - 7.4
R&D systems, DY995	Reagent Diluent	1% bovine serum albumin in PBS
		pH 7.2 - 7.4
R&D systems, DY999	Substrate Solution	Color Reagent A (H_2O_2)
		Color Reagent B (Tetramethylbenzidine)
R&D systems, DY994	Stop Solution	2 N H_2SO_4

2.2.7. GRIESS REACTION

The amount of secreted nitric oxide (NO) can be estimated from the concentration of its degradation product, nitrite (NO_2). The Griess method (Griess, 1879; Sun et al., 2003) consumes NO_2 in the coupling reaction between the colourless sulfonilamide and N-naphthyl-ethylenediamine, to produce a purple azo-compound with maximum absorption at wavelength $\lambda = 550$ nm.

The Griess assay was carried out in 96-well plates with 100 µL of undiluted medium in each well. Ten-point, two-fold dilution standard curves were constructed in quadruplicate by diluting sodium nitrite (Merck & Co., Darmstadt, Germany) in fresh incubation medium. The high standard sample (80 µM sodium nitrite) was two-fold diluted in fresh incubation medium in eight steps. The 10^{th} standard sample consisted of fresh incubation medium, hence corresponded to zero.

Each well received 100 µL of the Griess reagent mixture (Table 5), and the OD of the established purple color was measured on a microplate-reader at 550 nm, corrected for 450 nm. The molarity of NO (in µM) was calculated after fitting the standards in a linear equation

$$y = y_o + ax$$

where

- y is the NO concentration and
- x is the measured OD.

Table 5
Griess reagents for nitrite detection

Reagent	Chemical, Company, Cat #	Stock solution	Working concentration
Standard Curve:	sodium nitrite (Merck, Cat # 6523)	10 mM in distilled water	80, 40, 20, 10, 5, 2.5, 1.25, 0.625, 0.313 µM
Reagent A:	1-naphthylethylenediamine hydrochloride (Sigma, Cat # N 5889)	0.1% w/v in distilled water	0.05% w/v
Reagent B:	Sulfanilamide (Sigma, Cat # S 9251)	3% w/v in distilled water	0.5% w/v
	Orthophosphoric acid (H_3PO_4) 85% (Sigma, Cat # 438081)	0.06% v/v in distilled water	0.03% v/v
Reagent A is mixed 1:1 with Reagent B before the assay			

2.2.8. FLUORO-JADE B

Fluoro-Jade® B (Chemicon International, Inc., Germany) is a marker for neurodegeneration (Schmued and Hopkins, 2000a, 2000b). Neuronal death occurring in control conditions and as a consequence of LPS exposure was compared to glutamate excitotoxicity with NMDA/KA (Acarin et al., 1996; Bruce-Keller et al., 1999; Lee et al., 2003; Dehghani et al., 2004), which served as positive control for validation of the staining efficacy. Fixed organotypic slice culture sections of 16 µm thickness were mounted on gelatine covered objective glasses and dried overnight at room temperature. For Fluoro-Jade B staining, slices were immersed in alkaline ethanol (1% sodium hydroxide in 80% alcohol) for 5 minutes and then in 70% alcohol for 2 min. After short rinsing in distilled water, slices were transferred in 0.06% aqueous solution of potassium permanganate for 10 minutes and afterwards rinsed in distilled water as previously described. Finally, the slides were incubated for 20 minutes in the staining solution (0.0004% Fluoro-Jade B in 0.1% aqueous solution of acetic acid), rinsed in distilled water, clarified in 100% xylene for three minutes and covered with Entellan®Neu (Merck & Co).

Images of the pyramidal layer the CA1 hippocampal subregion were acquired using a Leica DM 2500 single photon upright confocal microscope optimized for fixed samples, with an oil immersion objective lens (20x), dry condenser (NA 0.9) and a z-galvo- / xy-mechano-stage. All parts of the microscope were purchased from Leica Microsystems. A solid-state LASER at 488 nm was used for excitation and the acquisition band was defined between 500 – 550 nm (centered at the Fluoro-Jade B emission peak of 525 nm).

Images were analyzed in ImageJ® (Wayne Rasband, NIH, USA). Neuronal death is expressed as Fluoro-Jade B-positive cell number counted in standard 322.58 x 322.58 μm frames, centered at the pyramidal cell layer.

2.3. ELECTROPHYSIOLOGY

For assessing the influence of activated microglial cells on the neuronal activity we recorded the extracellular potential in the CA1 hippocampal subregion after stimulating the Schaffer collateral (SC) projection.

2.3.1. THE INTERFACE CHAMBER

A custom-made interface recording chamber was designed to hold the whole membrane insert (Figure 6). In this way, we avoided culture isolation from the membrane insert minimized traumatic manipulations that may contaminate the experimental outcome (Duport et al., 2005; Wang et al., 2010).

In interface chamber conditions the tissue is supplied with nutrients and oxygen from a liquid and a gaseous phase, respectively. The chamber was perfused with artificial cerebrospinal fluid (aCSF, Table 6) at steady flow rate of 1.5 ml/min and gassed with 95% O2 / 5% CO2 at 1 L/ min. The gaseous phase was humidified and warmed via a bath of distilled water at 34 ^{o}C. All recording parts of the setup were fixed on a grounded active vibration isolation table (Series 20© AutoMate Scientific Inc., Berkeley, California, USA) and shielded in a custom-made Faraday cage.

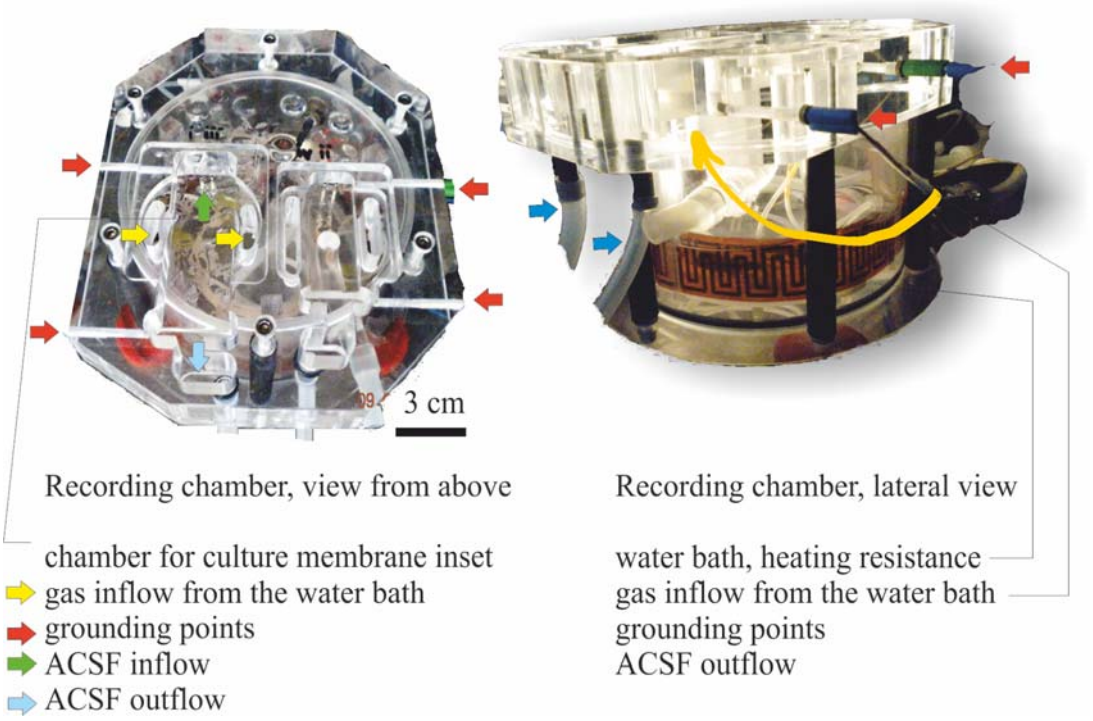

FIGURE 6: ELECTROPHYSIOLOGY, INTERFACE CHAMBER

A custom-made interface chamber was used for extracellular recordings. (left panel) *Viewed from above*, two chambers designed for hosting membrane inserts (left) and acute brain slices (right) allowed inflow and outflow of ACSF (green and blue arrows), as well as gas inflow from the sides (yellow arrows). (right panel) *Viewed from the side*, the gas stream was warmed up and humidified in a distilled water bath below the recording chambers. Each chamber was individually connected with a central grounding (red arrows).

Table 6
Artificial Cerebrospinal Fluid (aCSF)

Chemical	mM
NaCl	129
$NaH_2PO_4*H_2O$	1.25
D-Glucose	10
$MgSO_4$	1.8
KCl	3
$CaCl_2*2H_2O$	1.6
$NaHCO_3$	21
* all chemicals purchased from Sigma	

2.3.2. SIGNAL AMPLIFICATION AND DIGITATION

The voltage signal was amplified using two serially connected, custom-made amplifiers, equipped with dual channel input and negative capacitance compensation. The field potential was recorded with an analogue 3 kHz low pass filter and digitized at 10 kHz, whereas the potassium sensitive channel was low-pass filtered at 0.3 kHz and digitized at 3 kHz using a CED Micro 1401-III® data acquisition unit with Spike2® software (Cambridge Electronic Design Ltd., Cambridge, UK).

2.3.3. STIMULATION AND RECORDING ELECTRODES

Stimulation protocols were programmed on a Master8® pulse stimulator (A.M.P.I., Jerusalem, Israel) and delivered with an Iso-flex® battery isolator (A.M.P.I.) (Figure 7). Custom-made bipolar stimulation electrodes were manufactured with 50 μm diameter tungsten or 25 μm diameter platinum wires, electrically isolated in theta glass capillaries. The distance between wires was adjusted at 200 μm under microscopic observation.

Field potentials were recorded with aCSF-filled glass micropipettes of 3-4 μm tip diameter, pulled from GB150F-8P borosilicate glass with filament (Science Products GmbH, Hofheim, Germany) with a PC-10 vertical micropipette puller (Narishige International Ltd., London, UK). Silver wire rods of 0.45 μm diameter were chlorided by short immersion in heat-molten silver chloride (Sigma).

2.3.4. EXTRACELLULAR ELECTROPHYSIOLOGICAL RECORDINGS

In the present work we monitored the neuronal and field activity with extracellular voltage recordings. Extracellular voltage changes evolve from the spatiotemporal summation of ionic currents occurring in a range of up to several millimeters (Mitzdorf, 1985; Cohen and Miles, 2000; Kajikawa and Schroeder, 2011; Buzsaki et al., 2012). Therefore, the recorded signal is affected not only by the amplitude and the distance of the current source from the recording electrode, but also by the conductive properties of the tissue, namely the properties of (polarized), neuronal and glial cell membranes and extracellular matrix. The contributing

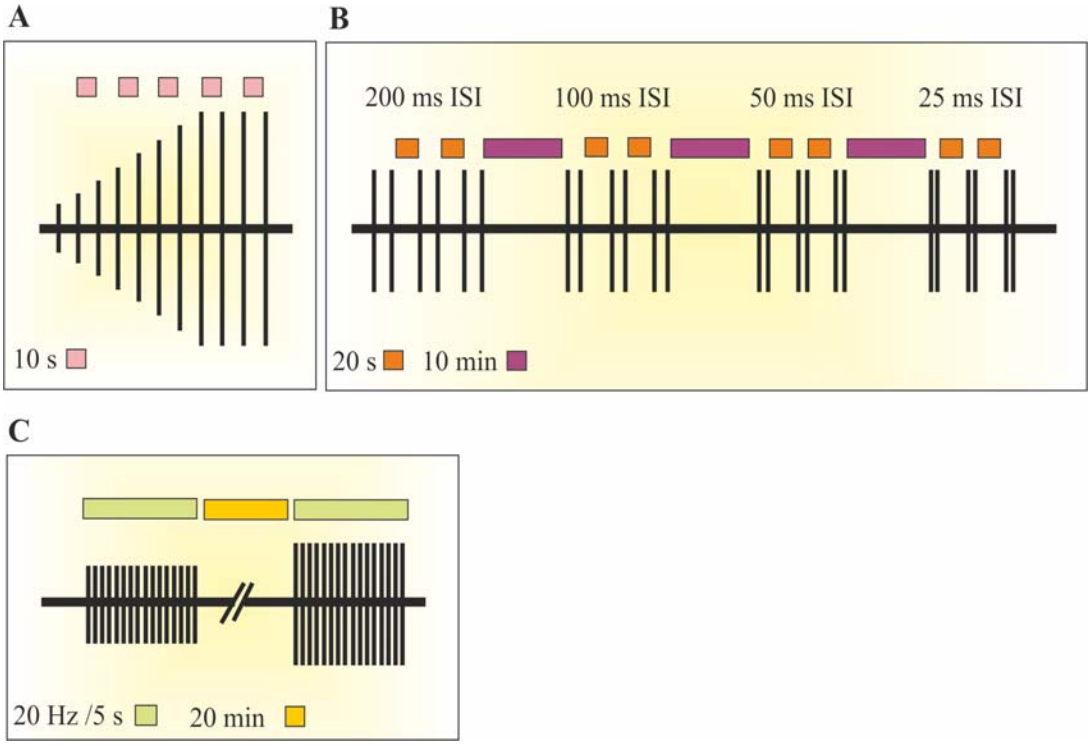

FIGURE 7: STIMULATION PROTOCOLS

Schematic representation of stimulation protocols.

(A) The I-O curve was constructed with single stimuli of increasing intensity and 10 s ISI.

(B) The paired-pulse protocol for short-term plasticity comprised triplicates of paired-pulses with decreasing ISI. The interval between paired-pulses was 20 s and between triplicates 10 min, without changes over trials.

(C) Extracellular potassium transients were elicited with 20 Hz / 5 s stimulation trains of increasing intensity. A time interval of 20 min was allowed between successive trains.

currents to the extracellular voltage can be of neuronal and glial origin, but the neuronal synaptic activity is considered to be the strongest determinant (Buzsaki et al., 2012).

Spontaneous activity and evoked responses were recorded in the s. pyramidale of the CA1 hippocampal subregion after stimulation of the SC pathway in the stratum radiatum, at the CA3:CA1 transition border (Figure 8A) (Johnston and Amaral, 2003).

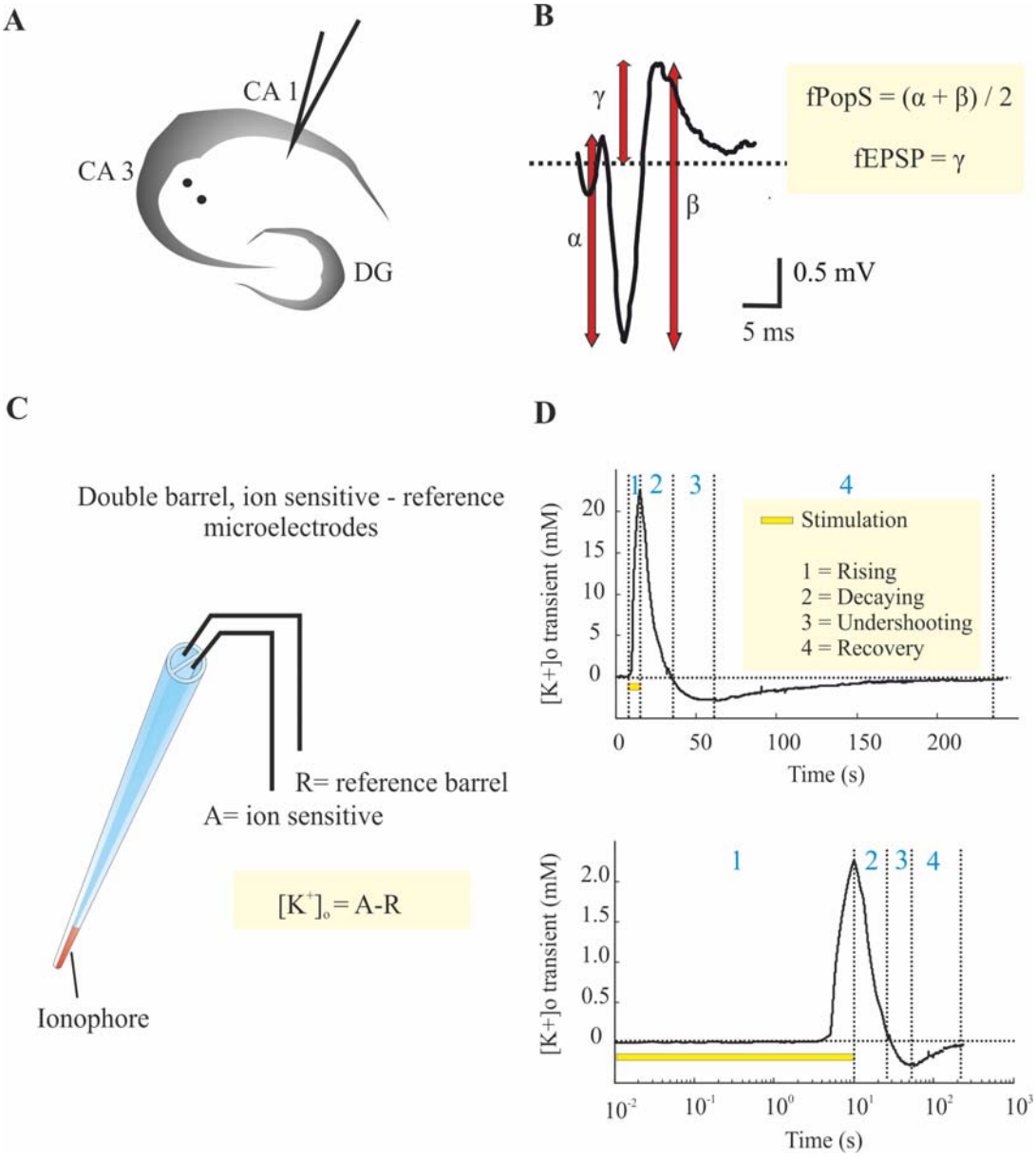

FIGURE 8: ELECTROPHYSIOLOGY: SIGNAL INTERPRETATION

Recording configuration: a single electrode was positioned in the CA1 s. pyramidale. The SC fibers were stimulated in s. radiatum between CA3 and CA1 (double dots) with 100 µs voltage controlled pulses.

(A) The evoked response in CA1 s. pyramidale consisted of the fPopS sink (red), superimposed on a slow, positive source, accounted as the fEPSP return current (black). The fEPSP magnitude is expressed as its maximum amplitude, whereas the fPopS magnitude is the average of its descending *(α)* and ascending *(β)* limbs (both values in mV).

(B) Ion sensitive – reference recording pairs: double-barreled borosilicate glass micropipettes were unilaterally silanized and filled with potassium selective ionophore. The ion sensitive barrel was backfilled with 100 mM KCl and the reference barrel with 150 mM NaCl. The potassium signal $[K^+]_o$ was calculated by subtracting the reference *(R)* from the ion-sensitive *(A)* channel.

(C) The $[K^+]_o$ transients have a rising (increase), a decaying, and undershooting and a recovery phase. The signal is transformed from mV to mM by applying a modified Nernst equation:

$$\log[K^+]_o = \frac{E_m}{S * V} + \log[K^+]_r$$

where

- $[K^+]_o$ is the extracellular potassium activity (*active concentration*) during stimulation,
- E_m is the recorded voltage signal,
- S is the slope of the calibration curve between 3 mM and 30 mM potassium (58±2 mV).
- V is the ion valence of potassium ($v = +1$),
- $[K^+]_r$ is the extracellular potassium concentration at rest, determined at 3 mM by the aCSF.

Note that in the upper panel a 5 s baseline has been included before the stimulation period. In the semi-logarithmic plot (lower panel) the 5 s baseline has been trimmed.

2.3.4.1. ANALYSIS OF THE SPONTANEOUS FIELD ACTIVITY

The extracellularly recorded potential from the CA1 hippocampal subregion was further processed with digital filters to isolate the local field potential (LFP) in the range of 1-200 Hz and the spiking multiunit activity (MUA) between 600 and 2000 Hz.

For the assessment of spontaneous activity we analyzed time lapses of random length (CTL = 13.44 ± 9.75 s, N=20, LPS =15.72 ± 16.41 s, N=33), acquired from electrically and pharmacologically untreated slice cultures, after 10 min of equilibration in the interface setup environment and 5 min after electrode positioning.

The recorded signal, acquired with 3 kHz low-pass analogue filter and digitized at 10 kHz, was processed with the following digital filters (Figure 18A):

a) a 5th order, low-pass Butterworth filter with 200 Hz corner frequency was applied to isolate the LFP

b) an 8th order, band-pass Butterworth filter with corner frequencies at 600 and 2000 Hz defined the range of MUA

The LFP spectrum was extracted with a Discrete Fourier Transformation algorithm implemented in MATLAB (The MathWorks, Inc., Natick, MA, USA), with niquist frequency (n) = 2048 (512*4).

The spiking MUA was filtered out of the background noise with a three standard deviation threshold (Figure 18A), which corresponded to 0.052 ± 0.036 mV for the control and 0.036 ± 0.018 mV for the LPS-exposed cultures (Figure 18A). MUAs were further described regarding their amplitude and occurrence (frequency).

2.3.4.2. FIELD EXCITATORY POSTSYNAPTIC POTENTIAL

The evoked extracellular voltage in s. radiatum, termed as 'field excitatory postsynaptic potential' (fEPSP), reflects the spatiotemporal summation of the local excitatory and inhibitory currents.

The fEPSP expresses the excitatory drive to the local circuitry and conveys information about:

- the number and type (excitatory / inhibitory) of activated synaptic sites
- the amplitude and
- the synchronization of postsynaptic responses

The fEPSP can be recorded either as a voltage 'sink' in s. radiatum, or as voltage 'source' due to return current in s. pyramidale (Johnston and Wu, 1994; Johnston and Amaral, 2003; Buzsaki et al., 2012). In our recordings, the amplitude of fEPSP was inferred by the return current 'deflection' in the CA1 s. pyramidale (Figure 8B).

2.3.4.3. FIELD POPULATION SPIKE

The local field potential recorded in stratum pyramidale (field population spike, fPopS) emerges from the spatiotemporal summation of action potentials (AP). In contrast to the fEPSP signal, the fPopS and reflects the number and synchronization of neurons firing an action potential in response to SC stimulation. Since the generation of an AP is an 'all-or-none' phenomenon, AP-amplitude fluctuations are not considered to be significant determinants of the fPopS (Andersen et al., 1980; but see also Epsztein et al., 2010 for the contribution of 'spikelets').

The amplitude of fPopS was evaluated from the average of its descending and ascending limb (Figure 10D).

2.3.4.4. INPUT–OUTPUT FUNCTION OR EPSP-SPIKING (ES) COUPLING

The 'input – output (I-O) function' or 'EPSP-spiking (E-S) coupling' of a neuron is defined as the correlation of EPSP amplitude with the probability of action potential generation. Extracellular recordings describe the I-O function of the CA1 neuronal population based on the extrapolation of single cell parameters (EPSP and firing probability) to their field correlate (fEPSP and fPopS) (Andersen, 1980; Marder, 2003).

The I-O curves were constructed with 0.1 Hz electrical pulses of subthreshold to maximum response intensity range (Figure 7) and fitted in a sigmoid

$$y = \frac{a}{1 - e^{-\frac{x - EC50}{b}}}$$

where

- α is the ordinate asymptote and corresponded to the maximum fPopS response,
- EC_{50} is the fEPSP that elicited half maximum of the fPopS response
- b is the Hill`s slope (slope at EC_{50}) of the sigmoid

The regression curves had correlation coefficient (R) > 0.95 and coefficient of determination (R^2) > 0.90.

2.3.4.5. SHORT-TERM PLASTICITY AND THE PAIRED PULSE INDEX

The neuronal short-term plasticity properties were tested with the paired-pulse protocol (Zucker and Regehr, 2002; Debanne et al., 2011; Fioravante and Regehr, 2011). The intensity of paired-pulses was adjusted to elicit 50% of the stimulation-response curve maximum. The paired-pulse interstimulus interval (ISI) was gradually decreased from 200 ms to 100, 50 and 25 ms, and each trial was averaged from three repetitions. A 20 s interval was allowed between paired-pulses of the same ISI and a 10 min interval between sequences of different interstimulus intervals (Figure 7).

The paired pulse index (PPI) derived from the ratio of the 2nd to the 1st pulse and the effect was characterized as

- Paired pulse facilitation (PPF) when PPI > 1
- Paired pulse depression (PPD) when PPI < 1
- No effect when PPI = 1

Differences in the paired pulse index were tested for significance within (for different ISIs) and between groups (for corresponding ISIs).

2.3.4.6. EPSP-SPIKE (E-S) PLASTICITY

The plasticity of cell's excitability, termed EPSP-Spike (E-S) plasticity (Andersen, 1980), 'intrinsic plasticity', or 'excitability' (Bliss and Gardner-Medwin, 1973; Bliss and Lomo, 1973; Jester, 1995; Daoudal, 2002, 2003; Marder and Buonomano, 2003; Wang et al., 2003; Zhang and Linden, 2003; Campanac and Debanne, 2008; Campanac et al., 2008) was assessed by extracting the ratio of the PPI in s. radiatum to the PPI in s. pyramidale.

2.3.5. ION SENSITIVE MICROELECTRODES

2.3.5.1. FABRICATION, CALIBRATION AND SIGNAL PROCESSING

Potassium sensitive microelectrodes were manufactured and tested as previously described (Lux and Neher, 1973; Singer et al., 1973; Heinemann and Arens, 1992). Micropipettes from double barreled, theta glass capillaries (Fa. H. Kuglstätter, Garching, Germany) were pulled with a PE-22 vertical micropipette puller (Narishige) and the tip-diameter was shaped to 3 µm. The inner surface of the ion sensitive barrel tip was made lipophilic ('silanized') with aspiration of 5% trimethylchlorosilane solution (Sigma-Aldrich) in dichloromethane (Sigma-Aldrich) under microscopic observation. The silanized tip was aspiration-filled with a 7 µm column of the potassium selective ionophore cocktail A® (Sigma-Aldrich) and backfilled with 100 mM KCl. The reference barrel was backfilled with 150 mM NaCl. A chlorided silver wire was advanced in each barrel and the non-chlorided end was connected to a custom made, dual-channel headstage.

The electrode sensitivity was tested with an oscilloscope using standard solutions of 3 mM and 30 mM KCl (Lux and Neher, 1973; Prince et al., 1973). Potassium sensitive electrodes were screened for a voltage response of 58 ± 2 mV to the transition from 3 mM to 30 mM KCl.

The voltage signal recorded from the reference barrel was subtracted from the ion sensitive barrel signal and the voltage difference was converted to potassium concentration (mM) using a modified Nernst equation in a custom-written script in Matlab 7.0.1 (MathWorks):

$$\log[K^+]_o = \frac{E_m}{S * V} + \log[K^+]_r$$

where

- $[K^+]_o$ is the extracellular potassium activity (active concentration) during stimulation,
- E_m iss the recorded voltage signal,
- S is the slope of the calibration curve between 3 mM and 30 mM potassium in mV, accepted when 58 ± 2 mV.
- V is the ion valence, for potassium v = +1,
- $[K^+]_r$ was the extracellular potassium activity (active concentration) at rest, determined by the aCSF at 3 mM.

2.3.5.2. EXTRACELLULAR POTASSIUM TRANSIENTS

Potassium-sensitive microelectrodes measure the activity of extracellular potassium, which is the concentration of dissociated potassium ions in the solution (Fry and Langley, 2001). Consequently, the ionic activity *(a)* is a fraction of the total ionic concentration *(C)*, determined by the activity coefficient *(γ)* of the particular ion in the particular solution according to the equation:

$$a = \gamma * C$$

For simplicity, the activity of extracellular potassium will be thereafter symbolized as $[K^+]_o$. The total potassium concentration is further determined by the solvent properties, as well as by the activity coefficients of other dissolved ions (Fry and Langley, 2001) and is not a subject of the current study.

Stimulation of CA1 via the SC pathway with 20 Hz for 5 s elicited a transient increase in $[K^+]_o$ (Figure 7, Figure 8D). Paired pulses and potassium transients were randomly induced in different slices in order to avoid possible cross-interference of protocols due to plasticity, such as post-tetanic facilitation (Fioravante et al., 2011). The transient $[K^+]_o$ elevation is followed by a decaying phase, an undershooting phase beyond the baseline activity (Heinemann et al., 1975) and a slow recovering phase back to the baseline (Figure 8D). $[K^+]_o$ transients were induced at different stimulation intensities ranging from subthreshold to maximum response. At high stimulation intensities, $[K^+]_o$ achieves a plateau-response, termed as 'ceiling' (Heinemann and Lux, 1977; Heinemann et al., 1977; Dietzel and Heinemann, 1986).

Fast and slow LFP changes are recorded concomitantly with $[K^+]_o$ transients from the reference barrel of the ion sensitive microelectrode. The fast field potential changes (Figure 24) provide information on the neuronal activity during stimulation. The slow negativity of the local field potential (Figure 25) is correlated with astrocytic potassium reuptake (Gabriel et al., 1998a, 1998b; Jauch et al., 2002) and conveys information on the integrity of astrocytic networks.

2.4. STATISTICS

The statistical analysis was performed in Σplot ® (Systat Software, Inc., Chicago, IL, USA), Matlab® (MathWorks) and Microsoft office Excel® (Microsoft Deutschland GmbH, Munich, Germany). Data distribution was first tested for normality using the Kolmogorov-Smirnoff test.

Intragroup comparisons were done with paired t test or with Wilcoxon signed rank test when normality was not satisfied. Intergroup comparisons were done with unpaired t test or with Mann Whitney rank sum test when normality was not satisfied. For multiple comparisons of a normally distributes single parameter we applied one-way ANOVA with pairwise Bonferroni's post-hoc test. When normality was not satisfied, the same set of data was compared with Kruskal Wallis ANOVA on ranks with Dunn's pairwise post-hoc test. For comparison of two simultaneously changing parameters we applied 2-way ANOVA with replication, and for evaluating the correlation between two parameters we used the Pearson correlation test. Sigmoid regression curves, as applied for the E-S coupling, were accepted if $R > 0.95$ and $R^2 > 0.90$.

Data are uniformly reported in the text as mean ± SEM, values are rounded at the 2^{nd} decimal place and the confidence interval for all tests was set at 0.95. Box plots represent the median with inner quartiles and the error bars encompass the 10^{th} – 90^{th} percentile.

3. RESULTS

3.1. MICROGLIAL ACTIVATION IN ORGANOTYPIC HIPPOCAMPAL SLICE CULTURES

3.1.1. MICROGLIAL CELLS IN THE ORGANOTYPIC HIPPOCAMPAL SLICE CULTURE ATTAIN RAMIFIED MORPHOLOGY

The organotypic hippocampal slice culture (Figure 9A1, D1 for Nissl stain) comprises a preserved cellular network of neurons (Figure 9A2, D2), astrocytes (Figure 9A3., D3) and microglia cells (Figure 9C.1-3 and D.1-3). In this microenvironment the latter attain a higher ramification degree compared with primary and mixed glial cultures (Kettenmann et al., 2011) (Figure 9C1-3 and Figure 9D1-3), therefore provide a sufficient *in vitro* model for studying the surveying and activated status. An additional advantage is that the organotypic condition allows for studying microglial activation in the absence of blood-borne macrophages.

3.1.2. LPS TRIGGERS THE SECRETION OF PROINFLAMMATORY FACTORS: NITRIC OXIDE (NO), TUMOR NECROSIS FACTOR – ALPHA (TNF-A) AND INTERLEUKIN 6 (IL-6)

The proinflammatory response after exposure to 10 µg/ml LPS for 72 hours was quantified by estimating the levels of secreted TNF-α, IL-6 and NO in the culture supernatant.

Cytokine levels were determined with specific anti-rat TNF-α and anti-rat IL-6 monoclonal antibodies using ELISA. Samples of fresh, unused medium collected from all preparations were also assayed for cytokines potentially carried in the serum. TNF-α (Figure 10A) and IL-6 (Figure 10B) in the control culture supernatant did not significantly differ from the unused medium. In contrast, both cytokines (Figure 10A, B) were 20-fold increased in the LPS-exposed culture supernatant.

The nitrite levels, as estimated with the Griess reagent, showed a five-fold increase between LPS-exposed and control cultures (Figure 10C), with the supernatant from control cultures being equal to the unused medium.

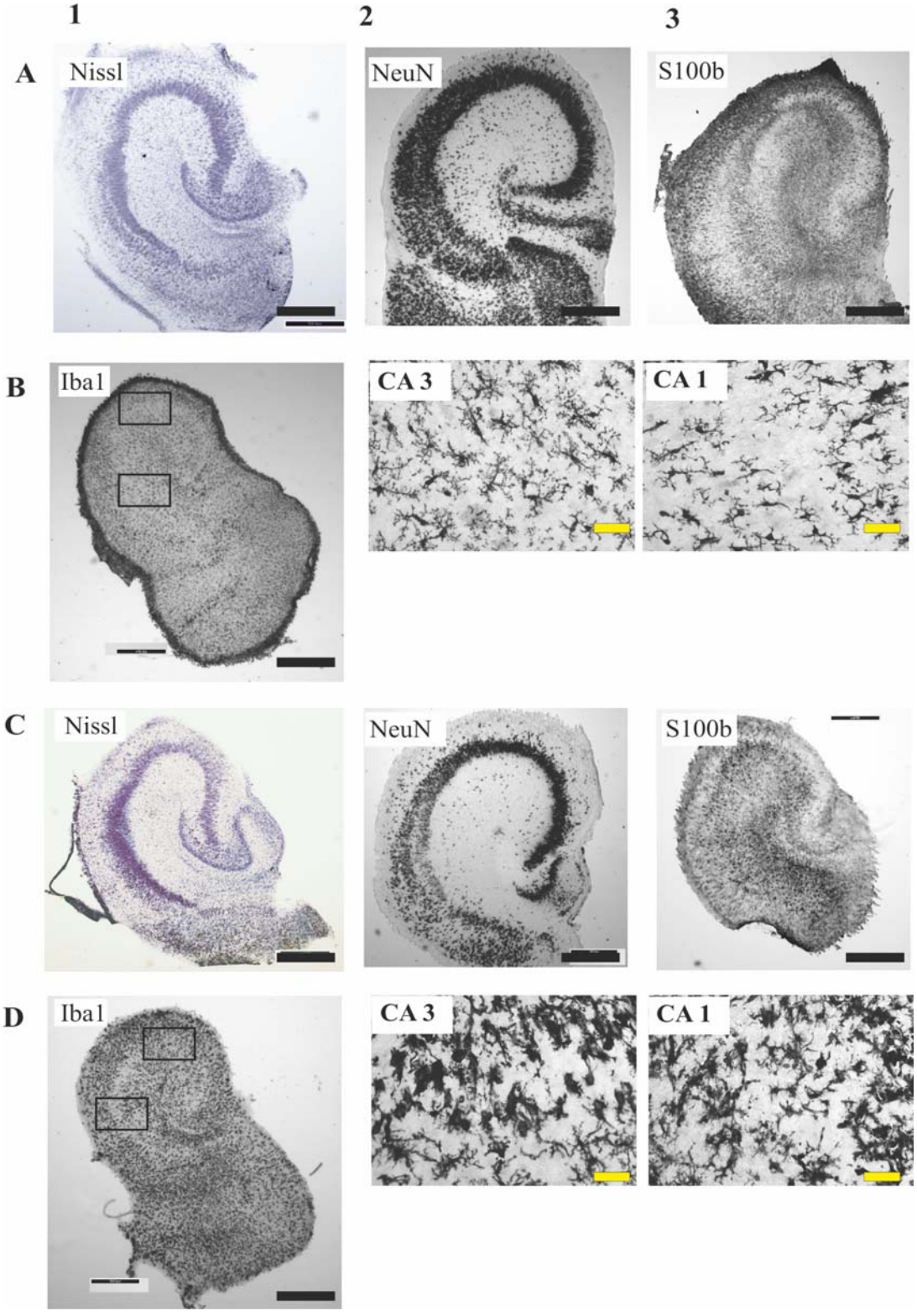
1
2
3
A
Nissl
NeuN
S100b
B
Iba1
CA 3
CA 1
C
Nissl
NeuN
S100b
D
Iba1
CA 3
CA 1

FIGURE 9: MAINTENANCE OF THE HIPPOCAMPAL MORPHOLOGY IN ORGANOTYPIC HIPPOCAMPAL SLICE CULTURES, BEFORE AND AFTER LPS EXPOSURE

Organotypic hippocampal slices (DIV11) stained with toluidine blue and selectively for neuronal (NeuN), astroglial (S100b) and microglial epitopes (Iba1). In both control (A1, 2) and LPS-exposed (C1, 2) cultures the transverse morphology of DG and the CA was comparable to *in vivo*, with the exception of CA1 pyramidal layer dispersion. Astroglial imaging revealed mild astrogliosis in the CA1 subregion of LPS-exposed cultures (C3) but not of controls (A3). Microglia in the middle-transverse level of the cultures were ramified in control (B1, B2 and B3 are CA3 and CA1 insets, respectively), in contrast to LPS exposed conditions (D1, D2 and D3 are CA3 and CA1 insets, respectively), where the anti-Iba1 staining revealed reactive microgliosis. Scale bars: black = 500 µm, yellow = 50 µm.

By conclusion, LPS-exposure triggers microglia activation, confirmed by the sequestration of proinflammatory markers TNF-α, IL-6 and nitrite in the culture supernatant. Importantly, no traces of inflammation were spotted in the supernatant of control cultures, clearly demonstrating the recovery status from the preparation 'trauma' by the time of pharmacological manipulations.

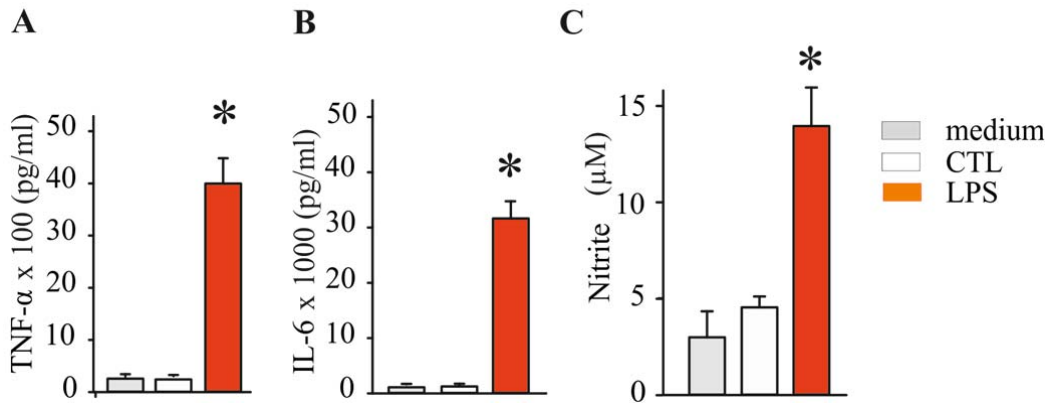

FIGURE 10: CYTOKINES AND NITRIC OXIDE IN CULTURE SUPERNATANT AFTER LPS EXPOSURE.

ELISA and Griess reaction for measuring the secreted cytokines (TNFa, IL6) and nitric oxide by-products (nitrate) in the culture supernatant.
(A) Control culture supernatant had 184.06 ± 44.01 pg/ml TNFα (n = 34 cultures, N = 9 preparations) with 84.22 ± 48.26 pg/ml medium background (n = 23 from N = 8 preparations; $p>0.05$, Mann Whitney U test), whereas the TNF-α concentration in LPS-exposed culture

supernatant was 20-fold increased to 4084.65 ± 661.09 pg/ml TNF-α (n = 28 cultures, N = 8 preparations; $p < 0.01$, Mann-Whitney U test
(B) The concentration of IL-6 in the supernatant from control slices (1371.46 ± 63.01 pg/ml, n = 34 cultures, N = 9 preparations) did not overwhelm the medium background (1217.98 ± 45.33 pg/ml; n = 23 from N = 8 preparations; $p>0.05$, Mann Whitney U test). Equally to TNF-α, the supernatant from LPS-exposed cultures had a 20-fold increase in IL-6 concentration up to 31087.43 ± 5281.93 pg/ml (n = 28 cultures, N = 8 preparations; $p < 0.01$, Mann-Whitney U test).
(C) The supernatant from control cultures contained 2.13 ± 0.32 µM nitrite (n = 34 cultures, N = 9 preparations) and was not significantly different from the medium background of 2.63 ± 0.35 µM nitrite (n = 19 from N_{MED} = 8 preparations). The LPS-exposed supernatant contained 13.39 ± 1.69 µM nitrite (n = 28 cultures, N = 8 preparations; $p < 0.01$, Mann-Whitney U test)

3.1.3. LIPOPOLYSACCHARIDE STIMULATION DOES NOT EXPAND THE MICROGLIAL POPULATION IN ORGANOTYPIC SLICE CULTURES

The volume of organotypic slice cultures was estimated with the Cavalieri stereological method on fixed preparations. The volume of control cultures was 197.9 ± 21.76 * 10^6 μm^3, without significant differences from the LPS-exposed and NMDA/KA-exposed groups (Figure 11A).

Activation of microglia cells with LPS did not cause a significant population expansion, which was achieved only after NMDA/KA excitotoxicity (Figure 11B).

Based on the above, we concluded that even an LPS titer (10 µg/ml) that exceeds the proinflammatory response saturation level (100 ng/ml) by a factor of 100 (Duport et al., 2005; Huuskonen et al., 2005; Regen et al., 2011; but see also Li et al., 2007) is an inadequate stimulus to significantly expand the microglial population. The excitotoxicity-induced population expansion argues for the ability of microglia to proliferate in organotypic slices, as well as for the corresponding sensitivity of the quantification method.

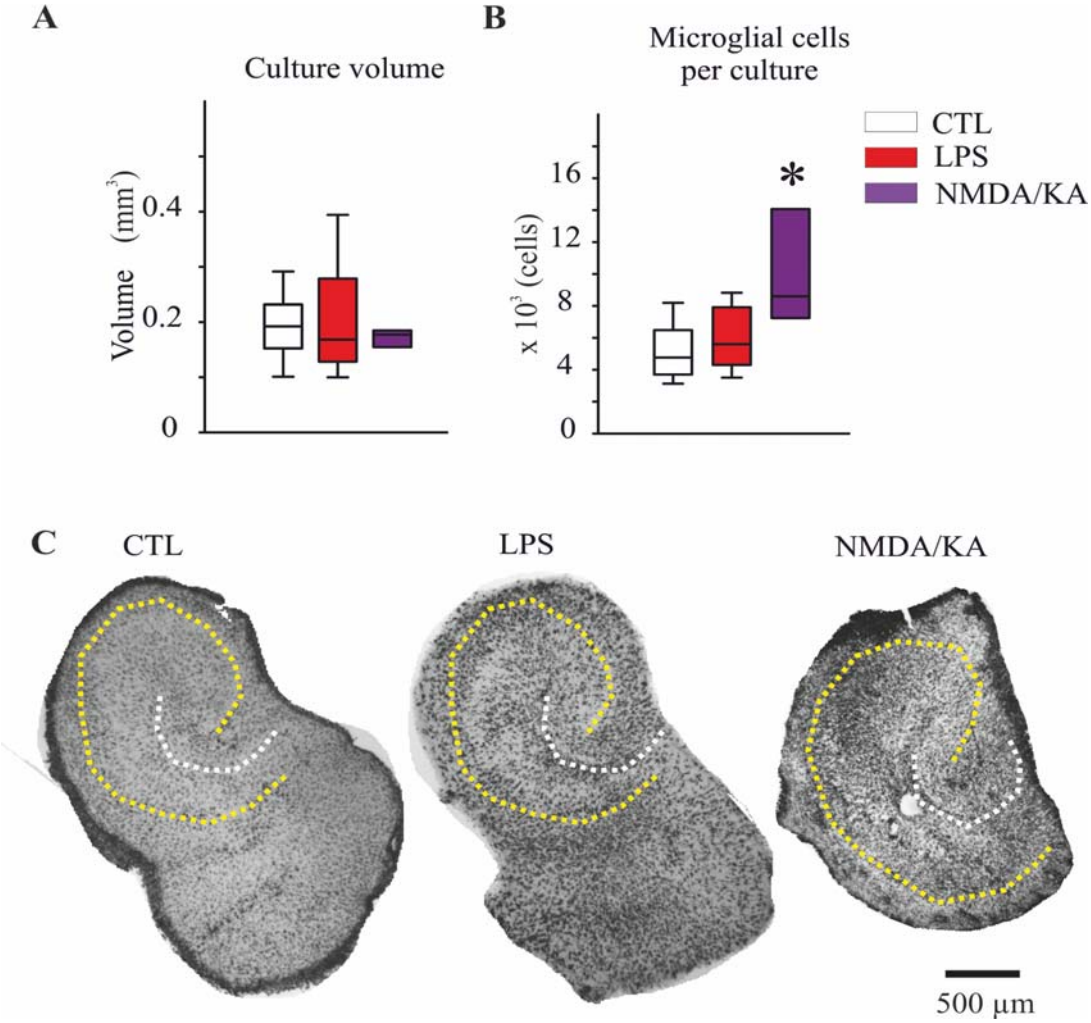

FIGURE 11: THE SIZE OF MICROGLIAL POPULATION IS NOT AFFECTED BY LPS EXPOSURE

(A) Hippocampal slice volume did not differ between control, LPS exposed and NMDA/KA-exposed cultures. Control cultures' volume was 197.9 ± 21.76 * 10^6 µm^3 (n = 17 cultures from N = 12 preparations), which did not differ from the 211.23 ± 21.41 * 10^6 µm^3 of the LPS exposed cultures (n = 23 for N = 12 preparations) and the 173.67 ± 7.77 * 10^6 µm^3 of the NMDA/Kainate exposed ones (n = 6 cultures from N = 4 preparations). Groups were compared with the Kruskal Wallis ANOVA on ranks ($p > 0.05$).

(B) The size of microglial population was not increased in LPS exposed cultures, whereas significant expansion was achieved in NMDA/KA exposed cultures. The number of microglia cells in control organotypic cultures was estimated to 5307.24 ± 583.03 cells per culture (n = 17 cultures from N = 12 preparations), which was not significantly different from the number of microglia cells in LPS exposed cultures (6008.7 ± 412.21 cells per culture, n = 23 for N = 12 preparations; $p > 0.05$, Kruskal-Wallis with pairwise Dunn's post hoc test). In NMDA/KA exposed cultures, which were used as a positive control for excitotoxic cell death, microglia were 2-fold increased up to 10370.17 ±

1862.28 cells per culture, and this was statistically significant to controls (n = 6 cultures from N = 4 preparations; $p < 0.05$, Kruskal-Wallis with pairwise Dunn's post hoc test).

(C) From left to right: Iba1 immunohistochemistry in organotypic slices: control, exposed to LPS or to NMDA/KA. Overview of the microglial population from the middle of the organotypic slice. Dashed lines indicate the neuronal layers of DG (white) and CA (yellow).

3.1.4. MORPHOMETRY OF MICROGLIAL CELLS

3.1.4.1. MICROGLIA IN LIPOPOLYSACCHARIDE EXPOSED ORGANOTYPIC CULTURES HAVE ENLARGED, ROUND-SHAPED SOMATA

The somatic shape of microglial cells in organotypic cultures varied from rod- to round-shaped. The applied morphometric method was based on the fact that activated microglia tend to acquire rounder shape. Accordingly, cell somata were characterized after their maximum length (*L*) and area of their somatic projection (*A*). The somatic shape index, defined as the ratio of the maximum length to the area (*L/A*), indicates the degree of shape transformation and declines as the soma gets round-shaped (see Methods). Both the somatic length and area were increased in LPS-exposed cultures (Figure 12A, B). The decrease of the somatic shape index (*L/A*) indicates somatic shape transition towards rounder somata (Figure 12C).

Hence, the LPS-induced microglia activation in organotypic slice cultures implies changes in somatic size (enlargement) and shape (rounder).

3.1.4.2. LIPOPOLYSACCHARIDE-ACTIVATED MICROGLIA HAVE THICKER PROCESSES BUT MAINTAIN THE TOTAL PROCESS NUMBER AS WELL AS THEIR DOMAIN

Activation of microglia implied changes not only in their soma, but also in the morphology of their process network. Microglial processes were classified as 'main' (first order) and 'higher order' processes (Figure 13A) and quantified using Neurolucida-based cell reconstructions.

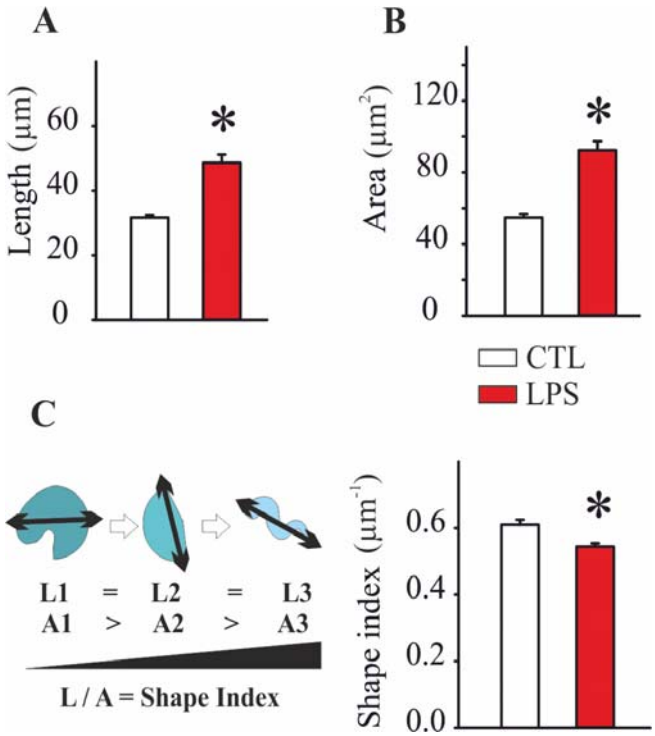

FIGURE 12: LIPOPOLYSACCHARIDE EXPOSED MICROGLIA HAVE LARGER AND ROUND – SHAPED SOMATA

LPS induced changes in both size and shape of microglial somata.

(A) Microglia from LPS-exposed cultures had significantly longer somata compared with controls. The maximum somatic length was 31.63 ± 0.79 µm in control versus 48.61 ± 2.53 µm in LPS exposed cultures ($p < 0.001$, Mann-Whitney U-test).

(B) The area of microglial somata was also increased, from 54.71 ± 2.04 μm^2 in control to 92.36 ± 5.02 μm^2 in LPS-exposed cultures ($p < 0.001$, Mann Whitney U test).

(C) The somatic shape index *L/A* was reduced in LPS exposed compared with control microglia, from 0.61 ± 0.02 μm^{-1} in control to 0.55 ± 0.01 μm^{-1} ($p < 0.001$, Mann-Whitney-U-test). This indicates that LPS triggers round-shaped transition.

For A, B, C: control: n = 76 cells; LPS-exposed: n = 94 cells from N = 12 preparations.

The total number of main processes per cell did not differ between control and LPS-exposed cultures (Figure 13A). The total (main and higher order) process number and length per cell were also not significantly changed in LPS-exposed microglia (Figure 13B). Moreover, the occupying domain of microglia was found unaffected (Figure 13C). However, comparison of the process volume revealed that LPS-exposed microglia had 1.5-fold increased total process volume compared to controls (Figure 13D).

Hence, LPS-exposure drives microglia to increase the volume of processes, albeit without significant changes in the total number and length. This indicates process thickening as a plausible mechanism of volume expansion. In addition, occupation of the same domain volume in LPS-exposed and control cultures means that the surveying territory is not subjected to fundamental changes.

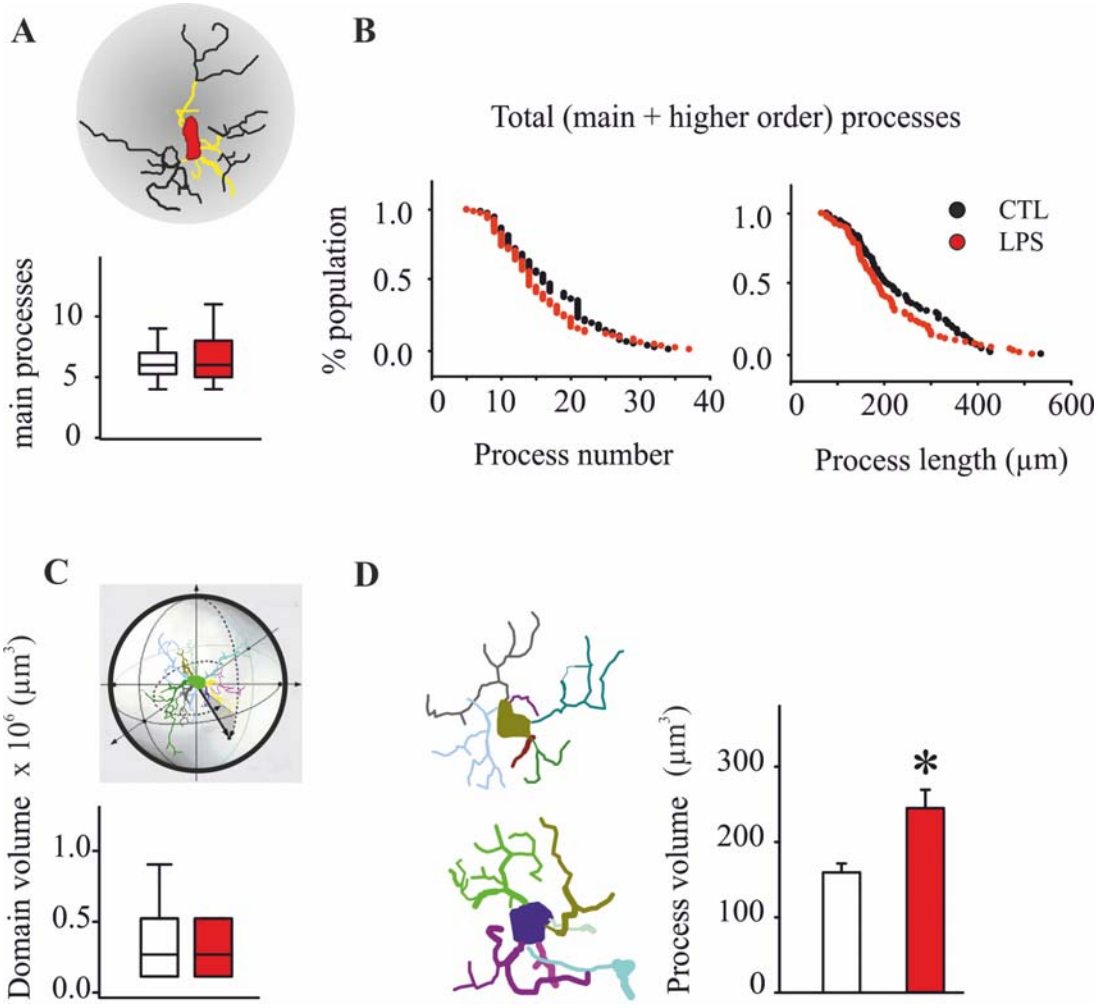

FIGURE 13: LIPOPOLYSACCHARIDE INDUCES THICKENING OF MICROGLIAL PROCESSES, WITHOUT SIGNIFICANTLY AFFECTING THE TOTAL PROCESS NUMBER OR CELL DOMAIN

Changes in microglial ramification are correlated with their activation process. Sholl analysis quantifies the process network in aspects of size and complexity.
(A) (*Upper*) sample trace of microglial cell. Cell body = red, main processes = yellow and higher order processes = black.(*Lower*) LPS-exposed microglia in organotypic slice cultures neither loose nor gain main processes, since their number was identical between control (6.43 ±

0.22 main processes / cell) and LPS exposed cultures (6.87 ± 0.32 main processes / cell; $p > 0.05$, Mann-Whitney U-test).
(B) (*Left panel*) The total number of process intersection with Sholl radii is an index of the total process number per cell. LPS-exposed microglia had 15.65 ± 0.76 total intersections versus 16.97 ± 0.77 in controls, which was not statistically significant ($p > 0.05$, Kolmogorov-Smirnoff test). (*Right Panel*) The total process length per cell was 211.56 ± 11.18 μm per cell in LPS-exposed and 236.48 ± 11.83 μm per cell in control cultures ($p > 0.05$, Kolmogorov-Smirnoff test)
(C) Microglial domain is assumed to occupy a spherical region around the soma, defined by the radius that encompasses the most distal processes. Domain volume was found unchanged between control and LPS-exposed cultures, with 350 ± 36.61 * 10^3 μm^3 in controls and 311.47 ± 28.34 * 10^3 μm^3 in LPS-exposed cultures ($p > 0.05$, Mann Whitney U test).
(D) LPS-exposed microglia had increased total process volume per cell (244.92 ± 24.36 μm^3) versus controls (159.63 ± 11.86 μm^3; $p < 0.05$ Mann-Whitney-U-test). Given that the total process number and length do not significantly change, this indicates thickening of processes.
The morphometric analysis data derived from n = 76 control cells and n = 82 LPS-exposed cells from N = 12 preparations.

3.1.4.3. LIPOPOLYSACCHARIDE INDUCES RETRACTION AND DECONVOLUTION OF PROXIMAL MICROGLIAL PROCESSES

Analysis of process distribution with the model of Sholl homocentric rings (Figure 14A) showed that LPS induced a process number (intersections, Figure 14B) and length (Figure 14C) reduction at the 10 μm radial distance (1st Sholl radius and sector). The total process length in the second Sholl sector (between 10 μm and 20 μm from the soma center) was reduced in LPS-exposed microglia, albeit without a corresponding change in the intersection number.

Therefore, microglia cells respond to LPS exposure with process number and length elimination in the 1st Sholl radius. By contrast, pattern splitting between intersections and length occurred in the 2nd Sholl radius, where the length elimination was not consistent with the intersection number. This discrepancy indicates that the process length deterioration is possibly a result of process deconvolution.

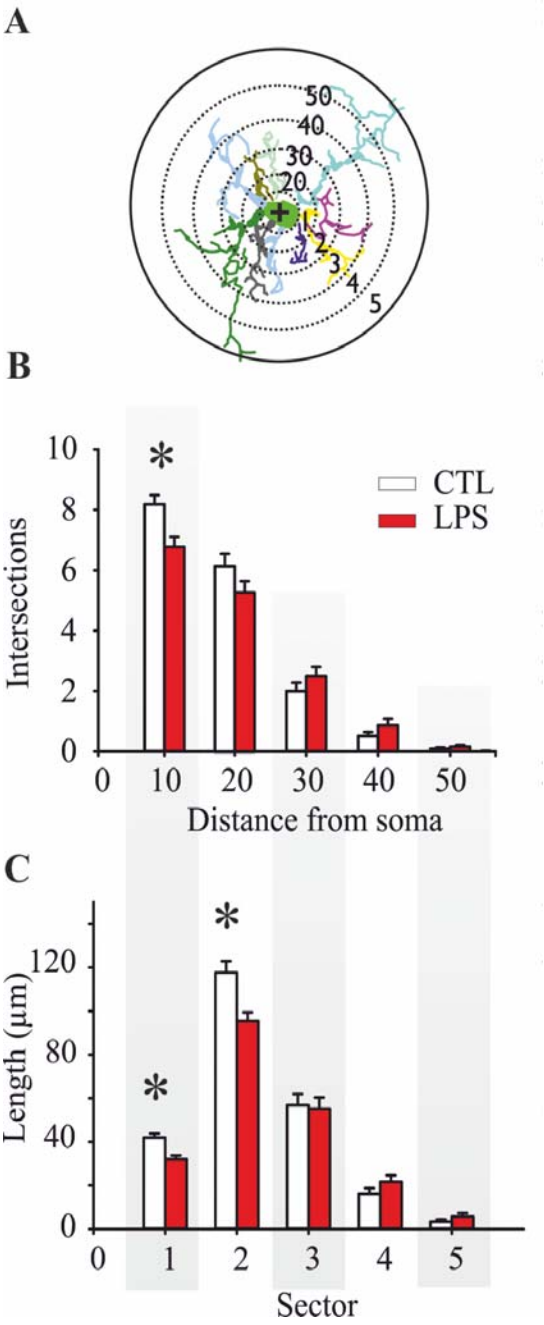

FIGURE 14: LPS INDUCES RETRACTION AND DECONVOLUTION OF PROXIMAL MICROGLIAL PROCESSES

(A) Microglia sample trace and the Sholl analysis model. Cross = geometric centre of the cell soma, homocentric rings starting from the soma centre with 10 µm radial difference. Sholl sectors are defined between two consecutive homocentric rings.

(B) Process intersections with Sholl radii: In control cultures, the intersection number of microglia processes with the 1st Sholl radius was 8.18 ± 0.30 processes, which was significantly reduced in LPS exposed cultures to 6.77 ± 0.33 processes ($p < 0.01$ Mann Whitney U test).

(C) Process length in Sholl sectors. The total process length in the 1st Sholl sector was 41.99 ± 1.84 µm and 32.04 ± 1.68 µm in control and LPS-exposed cultures, correspondingly ($p < 0.01$, Mann Whitney U test). Process length in the 2nd sector was also reduced from 117.69 ± 5.19 µm in controls to 95.42 ± 3.97 µm in LPS-exposed cultures ($p < 0.01$, Mann Whitney U test).

The morphometric analysis data derived from n = 76 control cells and n = 82 LPS-exposed cells from N = 12 preparations.

3.2. LIPOPOLYSACCHARIDE-INDUCED MICROGLIAL ACTIVATION IS NOT ASSOCIATED WITH NEURODEGENERATION IN ORGANOPTYPIC SLICE CULTURES

Microglial activation after LPS exposure, as confirmed by cytokine exposure and morphological criteria, was, surprisingly, not correlated with neurodegeneration. Twelve control, n = 20 LPS-exposed and n = 26 NMDA/KA-exposed cultures deriving from N = 12 preparations were used for quantifying the degree of neuronal damage upon LPS exposure.

Toluidine blue staining (Figure 15A, B, C) was applied for the assessment of neuronal survival. Toluidine blue belongs to the Nissl dye group of acidophilic chromophores with high affinity to nucleic acids, introduced by F. Nissl at 1894 (Geisler et al., 2002). Therefore, toluidine blue stains the rough endoplasmic reticulum (Nissl bodies), the cell nucleus (heterochromatin) and nucleolus, as well as other basophilic cytoplasmic elements. Neuronal cells are recognized due to their enriched in rough endoplasmic reticulum cytoplasm and their light-stained (euchromatic) nuclei with a centrally defined nucleolus. Glial cells are recognized from their dispersed rough endoplasmic reticulum, thus lighter stained cytoplasm and clearly identifiable nuclei.

In LPS-exposed cultures (Figure 15B) the structure of the neuronal cell layer was similar to controls (Figure 15A), with the dentate gyrus and the cornu ammonis preserved in terms of shape and thickness. By contrast, toluidine blue staining in NMDA/KA-exposed cultures indicated massive neuronal death (Figure15C).

The neurodegeneration marker Fluoro-Jade B binds selectively to anionic proteins expressed in apoptotic / necrotic neurons like putrescine, spermine and spermidine (Schmued et al., 1997; 2000a, 2000b, 2005). The number of positive cells in ROIs of predefined size was counted using the ImageJ software (Wayne Rasband, NIH, USA). In line with the tolouidine blue-based observation, LPS exposure had no neurotoxic impact (Figure 15G), and this was in sharp contrast to NMDA/KA exposure, which massively increased the number of Fluoro-Jade B positive cells (Noraberg et al., 1999; Kristensen et al., 2001; Figures 15F, G).

Conclusively, despite the high (10 μg/ml) and long-term (72 hours) LPS exposure and the high titer of cytokines accumulated in the supernatant, microglial activation was not associated with neuronal death.

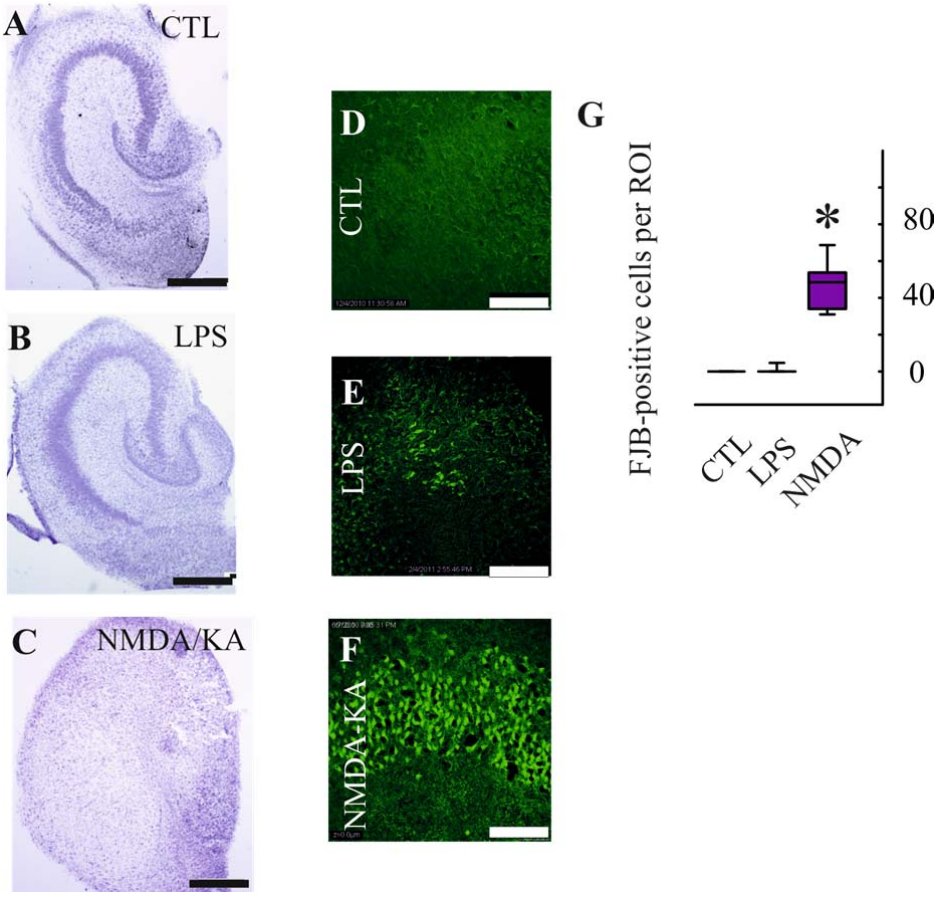

FIGURE 15: LPS-INDUCED MICROGLIAL ACTIVATION IS NOT ASSOCIATED WITH NEURODEGENERATION IN ORGANOTYPIC HIPPOCAMPAL CULTURES

The degree of neuronal death in organotypic hippocampal slices was estimated using Nissl (tolouidine blue, A-C) and Fluoro-Jade B staining (D-F) in fixed samples.
(A-C) Nissl stain revealed no qualitative changes between the control (A) and the LPS treated group of cultures (B). On the other hand, massive neuronal loss was observed in the NMDA/KA exposed group (C). Scale bars = 500 µm.
(D-F) Fluoro-Jade B images from the CA1 subregion of control (D), LPS (E) and NMDA/KA exposed cultures (F) revealed minimal neuronal death in the LPS- and massive neuronal death in the NMDA/KA-exposed group. Scale bars = 100 µm.
(G) The Fluoro-Jade B-positive neuronal number per ROI in the CA1 subregion was zero in n = 16 control cultures, 1.27 ± 0.87 in n = 20 LPS exposed cultures and 15.89 ± 6.42 in the CA3 subregion of n = 26 NMDA/KA exposed cultures. The NMDA/KA group was significantly increased compared to controls and to LPS-exposed cultures ($p < 0.01$, Mann Whitney U test).

3.3. ELECTROPHYSIOLOGICAL ASSESSMENT OF NEURONAL FUNCTION

The assessment of neuronal survival with tolouidine blue and FluoroJade B stainings excluded necrosis and apoptosis, nevertheless without providing any evidence about the functional status of the surviving neurons. Using electrophysiological recordings of the extracellular activity we described not only the single neuron activity status, but also the global effect of LPS exposure on the organotypic network.

Analysis of the spontaneous (local field potentials, multiunit activity) and the evoked activity revealed no fundamental changes in LPS-exposed organotypic cultures, arguing not only against neuronal death, but also for preservation of healthy and metabolically competent neurons.

The spontaneous activity of CA1 s. pyramidale was digitally filtered for two frequency spectra, known to enclose information on different neuronal functions (Johnston and Wu, 1994; Cohen and Miles, 2000; Rasch et al., 2008, 2009; Burns et al., 2010a, 2010b; Denker et al., 2011; Kajikawa and Schroeder, 2011; Linden et al., 2011; Buzsaki et al., 2012): the local field potential (LFP) in the range of 0-200 Hz and the multiunit activity (MUA) spectrum in the range of 600-2000 Hz (Figure 16A).

3.3.1. LOCAL FIELD POTENTIAL

The LFP spectrum, which mainly comprises postsynaptic currents, was decomposed with a discrete Fourier transformation algorithm. Spontaneously occurring oscillations were not observed in any of the groups, and the power spectrum did not reveal any significant difference. However, the spectral range in LPS-exposed cultures had smaller variance than controls, as illustrated with 1σ-thick shadowed zones in the averaged power spectrum graph (Figure 16 B).

3.3.2. SPIKING MULTIUNIT ACTIVITY

The MUA events were identified and isolated with a signal-to-noise threshold of 3 standard deviations (σ) (Figure 16A), and subsequently characterized in term of amplitude and occurrence in time. The frequency of MUA was calculated by dividing their total number by the duration of the sampled time-lapse, therefore it does not provide any information about

regularity. The latter is additionally illustrated in a raster plot. The MUA frequency was identical in control and LPS-exposed slices, with median values of 2.76 Hz and 2.44 Hz,

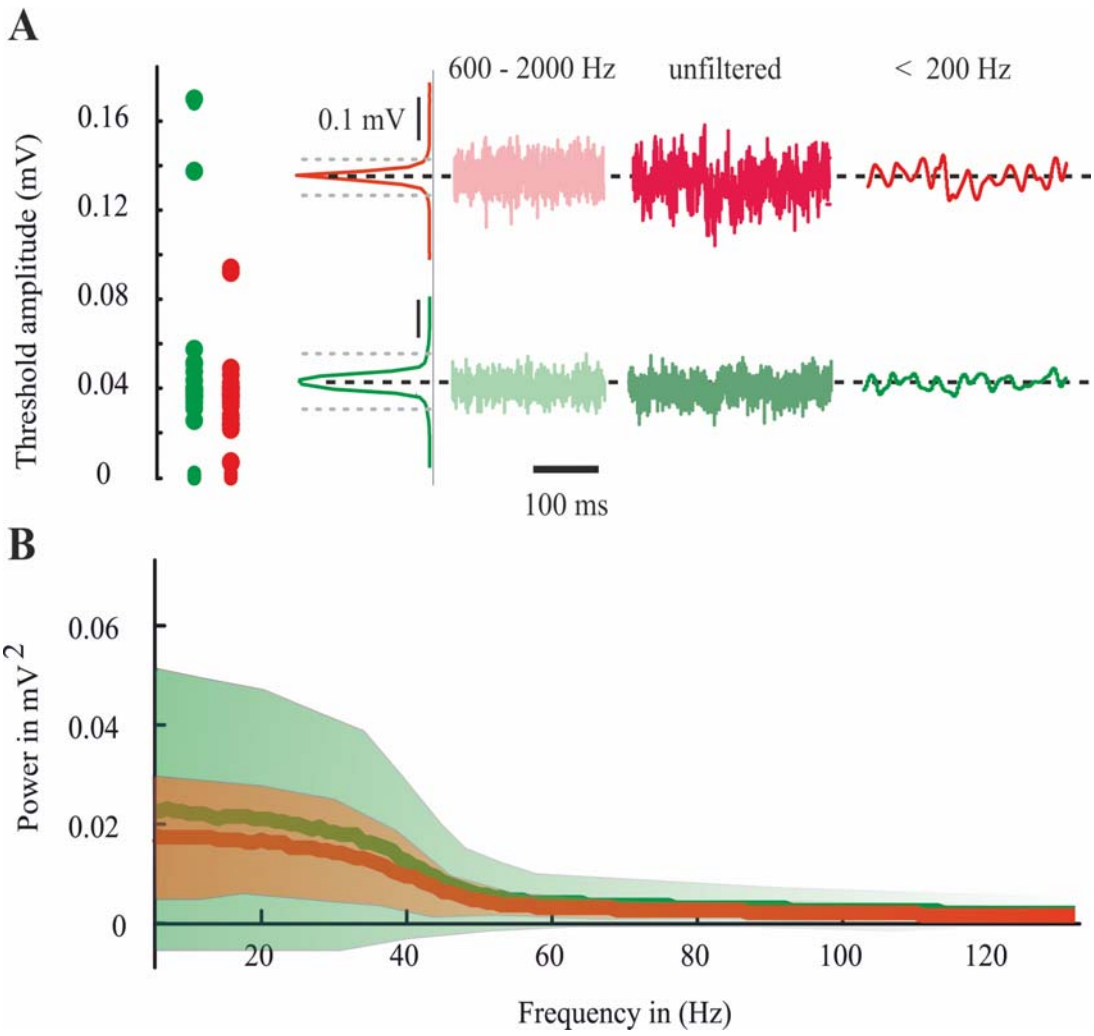

FIGURE 16: EXTRACELLULAR RECORDINGS, LOCAL FIELD POTENTIAL

(A) The spontaneous activity was digitally filtered at low (< 200 Hz) and high (600-2000 Hz) frequencies. The spiking multiunit activity (MUA) events were isolated from the high frequency band by setting the signal-to-noise threshold at 3 standard deviations (3*σ) from the mean activity level (grey dashed lines). This corresponded to an absolute MUA-discrimination threshold of 0.052 ± 0.036 mV in control and 0.036±0.018 in LPS-exposed cultures (mean ± σ).
(B) Spectral analysis of the LFP (frequency band 0-200 Hz), thick lines represent the mean and shadowed regions one standard deviation (σ) from the mean.

correspondingly (Figure 17A). By contrast, LPS-exposure significantly reduced the amplitude of MUA events, from 0.053 mV to 0.03 mV ($p < 0.001$, Mann-Whitney U test) (Figure 17B).

In summary, the LFP spectrum as well as the frequency of spiking MUA in the CA1 subregion of the organotypic cultures were not modified by LPS exposure. However, the MUA amplitude was significantly reduced in the LPS-exposed cultures.

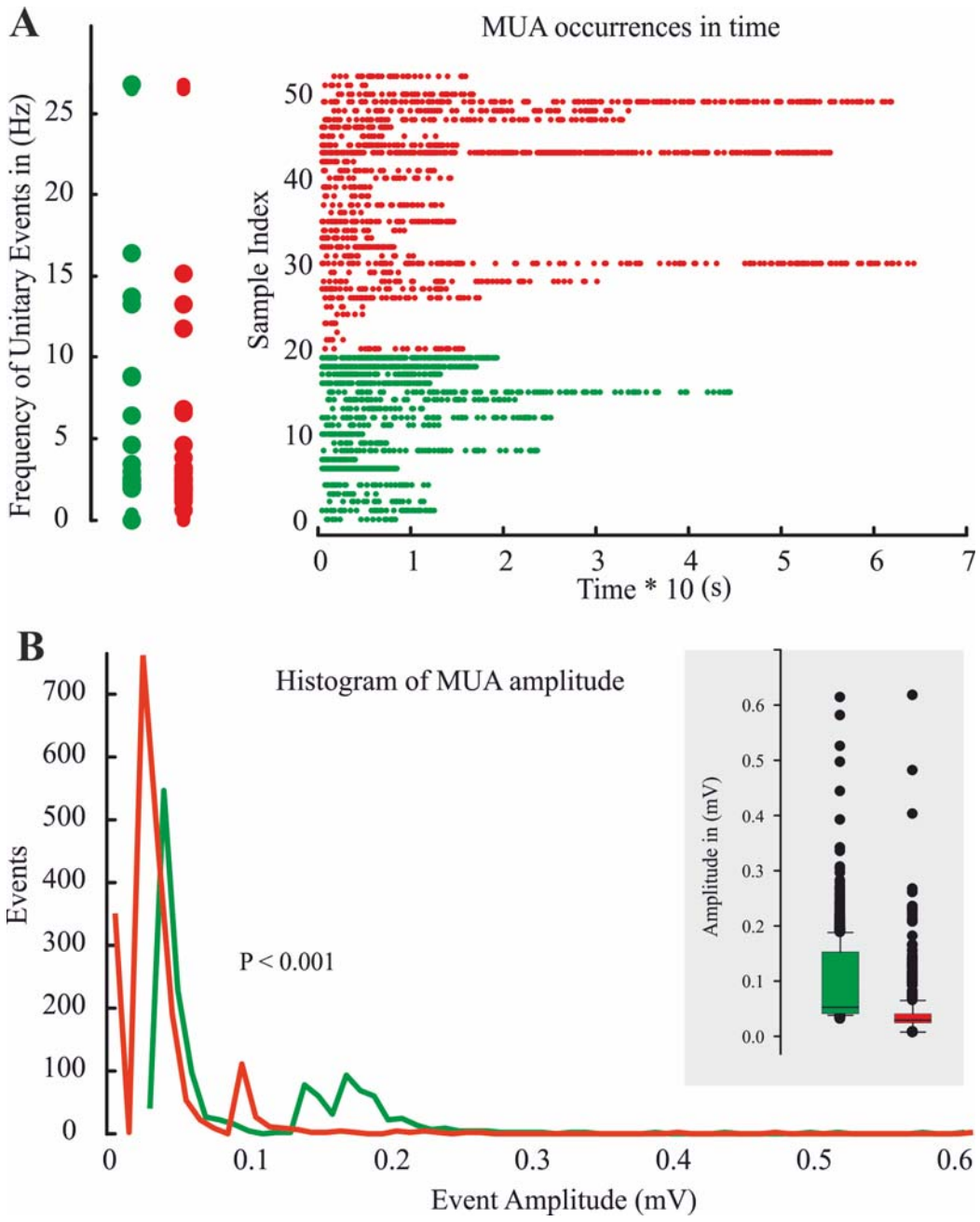

FIGURE 17: MULTIUNIT ACTIVITY

(**A**) Frequency of spiking (MUA) (CTL = 2.76 Hz, n = 20 and LPS = 2.44 Hz, n = 33, $p > 0.05$ Mann Whitney U test; data reported as median values ± inner quartiles). The temporal distribution of MUA occurrences in time-lapses is illustrated with a raster plot (right). Sample indexes 1-20 correspond to controls and 21-53 to LPS-exposed cultures.
(**B**) Histogram of spiking MUA amplitude. The MUA amplitude was significantly reduced on LPS-exposed cultures (insert: CTL = 0.053 mV and LPS-exposed 0.029 mV, $p < 0.01$ Mann Whitney U test; data reported as median values ± inner quartiles).

3.3.3. MICROGLIAL ACTIVATION SUPPRESSES THE INPUT-OUTPUT WITHOUT MODIFYING THE SHORT-TERM PLASTICITY PROPERTIES

The impact of the LPS–induced microglial activation on neuronal excitability was additionally assessed by evoking field potential responses in the CA1 s. pyramidale and studying the short-term plasticity properties.

Stimulation-response curves were assembled by plotting the fEPSP (Figure 18A) and fPopS (Figure 18B) (in mV) as a function of the stimulation intensity (in V).

The fEPSP stimulation-response curve was evenly matched between control and LPS-exposed organotypic hippocampal cultures (Figure 18A), as the mean responses were not significantly different for stimulation intensities between 1 V and 3 V ($p > 0.05$, Mann-Whitney U Test; Table 7A). On the other hand, the fPopS amplitudes were significantly depressed in LPS-exposed cultures (Figure 18B, Table 7B) ($p > 0.05$, Mann-Whitney-U-Test).

Therefore, although the electrically evoked postsynaptic currents remained unaltered after LPS exposure, their AP firing probability was significantly depressed.

The term neuronal excitability describes the probability of a postsynaptic response to elicit an action potential and is schematically represented in the E-S coupling function (Figure 19A). E-S coupling curves were fit into a sigmoid with correlation coefficient $R > 0.98$ and coefficient of determination $R^2 > 0.95$ (Figure 19A, Table 8). The LPS-exposed organotypic cultures had significantly reduced maximum fPopS (Smax) (Figure 19B), and leftwards shifted EC_{50} value compared with controls (Figure 19C). Hill's slope (h), the first derivative of the E-S coupling sigmoid for $x = EC_{50}$ (Reed et al., 1995; Daoudal and Debanne, 2003; Carvalho and Buonomano, 2009) displayed no significant difference between groups (Figure 19D).

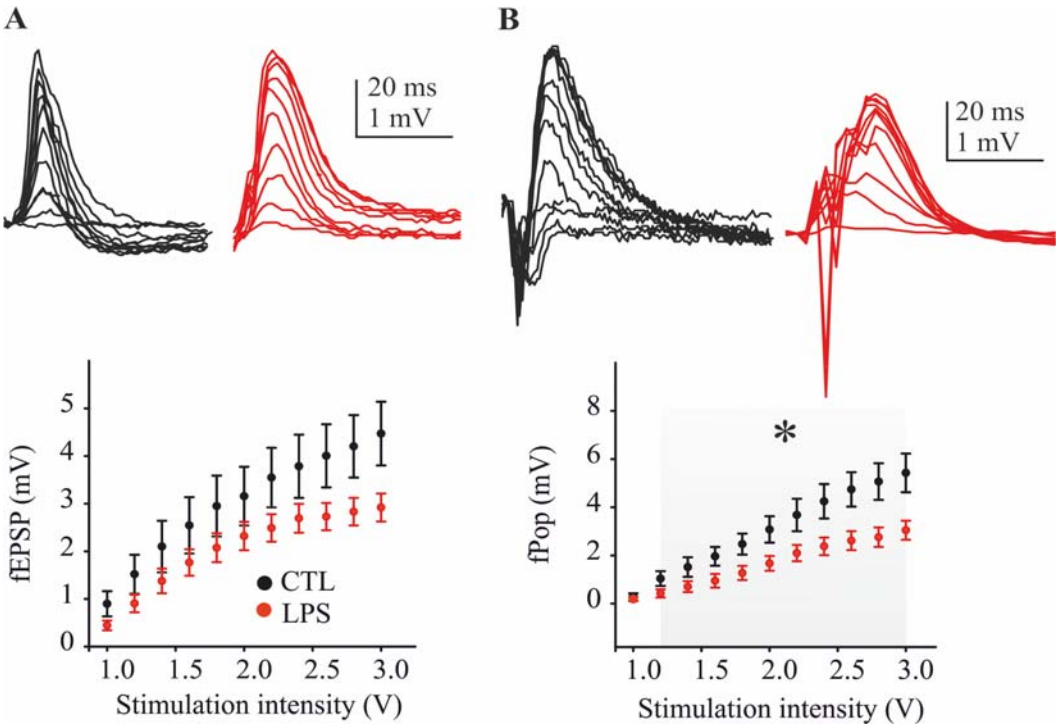

FIGURE 18: EVOKED POTENTIALS IN THE CA1 SUBREGION: MICROGLIAL ACTIVATION SUPPRESSES THE ACTION POTENTIAL FIRING PROBABILITY BUT NOT THE POSTSYNAPTIC CURRENTS

For the construction of stimulation-response (S-R) curves, the SC pathway was stimulated with increasing intensity from 1.0 to 3.0 Volts (also, see Figure 9A for the detailed stimulation protocol).
(*Right panels*) Sample traces of fEPSP and fPopS responses to increasing stimulation intensity.
(A) The fEPSP S-R curve was not significantly different between control and LPS exposed organotypic hippocampal cultures (for all stimulation intensities, $p > 0.05$, Mann Whitney U test).
(B) The fPopS was significantly suppressed in LPS-exposed cultures for almost the whole stimulation intensity spectrum (1.2 V to 3 V, $p > 0.05$, Mann Whitney U test).
n = 15 control, n = 32 LPS exposed cultures, both groups from N = 10 preparations

Thus, although the maximum fPopS response was suppressed, the slope of the E-S coupling sigmoid was unaffected. From these results we conclude that LPS scales down neuronal excitability in terms of maximum efficacy, however without qualitatively modifying the input-output kinetics.

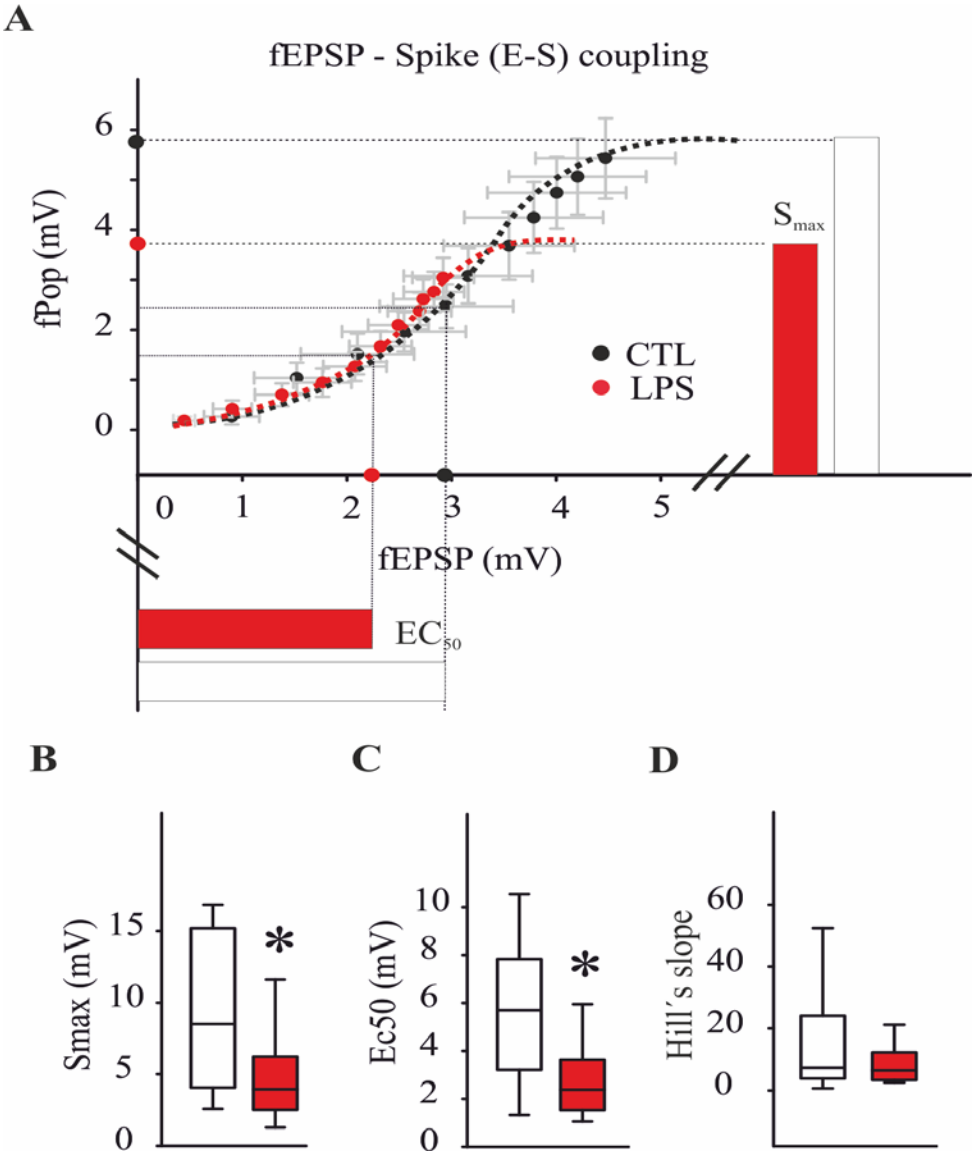

FIGURE 19: CA1 INPUT-OUTPUT PROPERTIES ARE SUPPRESSED BY MICROGLIAL ACTIVATION

The coupling of postsynaptic responses (fEPSP) with the neuronal AP firing (fPopS) in the E-S coupling curve describes the neuronal excitability and the I-O properties of the local circuitry. (A) The E-S coupling: sigmoid fitting with correlation coefficient R_{CTL} = 0.98 ± 0.01 and R_{LPS} = 0.98 ± 0.00, and coefficient of determination R^2_{CTL} = 0.96 ± 0.01 and R^2_{LPS} = 0.95 ± 0.01. The E-S coupling sigmoids were analysed in terms of (i) their maximum asymptote (S_{max}) (ii) the EC_{50} and (iii) the Hill´s slope. In the cross-dot plot the mean ± SEM of the fitted values is illustrated in grey.
(B) Microglial activation suppressed the S_{max} to 5.29 ± 0.85 mV from 9.51 ± 1.58 mV in controls ($p < 0.05$, Mann-Whitney U test).

(C) The EC_{50}, corresponding to the fEPSP value that induces 50% of the S_{max} fPopS , was significantly reduced by 48.78%. $EC_{50\,CTL}$ = 5.72 ± 0.89 mV versus $EC_{50\,LPS}$ = 2.79 ± 0.30 mV ($p < 0.01$, Mann Whitney U test).
(D) The Hill´s slope (h) did not differ between groups: h = 14.74 ± 4.46 in control and h = 10.15 ± 2.22 in LPS exposed cultures ($p > 0.05$, Mann Whitney U test).
n = 15 control and n = 32 LPS exposed cultures deriving from N = 10 preparations

Table 7:
E-S coupling: sigmoid fitting parameters

	Control				LPS exposed		
Column	**Mean**		**SEM**	**Mann Whitney U test**	**Mean**		**SEM**
R	0.979	±	0.01	-	0.976	±	0.00368
Rsqr	0.959	±	0.01	-	0.953	±	0.0071
Smin	0.294	±	0.16	$p > 0.05$	0.0551	±	0.0424
Smax	9.514	±	1.58	$p < 0.05$	5.294	±	0.851
EC50	5.724	±	0.89	$p < 0.01$	2.785	±	0.296
Hill slope	14.737	±	4.46	$p > 0.05$	10.147	±	2.224

Pairs of stimuli were delivered to the SC pathway with ISI progressively declining from 200 to 25 ms, with stimulation intensity adjusted to elicit 50% of the maximum fEPSP response.

The fEPSP paired pulse index (PPI) demonstrated high variance in both control and LPS-exposed organotypic cultures, ranging from facilitation (PPI > 1) to depression (PPI < 1) in all ISIs, as illustrated in the cumulative probability graphs (Figure 20C, D, E, F). However, no significant difference was detected between control and LPS-exposed cultures for all tested ISIs (Figure 20B).

The high variance of PPI (Figure 20C-F) is indicative of heterogeneous responses within the population.

Consequently, we tested whether the fEPSP amplitude influences the paired pulse response. In control organotypic cultures, the fEPSP amplitude was not correlated with the paired pulse index for ISIs of 200, 100 and 50 ms. A negative correlation ($R = -0.36$, $p < 0.05$, Pearson) was confirmed only for ISI as short as 25 ms. In contrast, the fEPSP amplitude was negatively correlated with the PPI in LPS-exposed cultures for all ISIs from 200 ms to 25 ms.

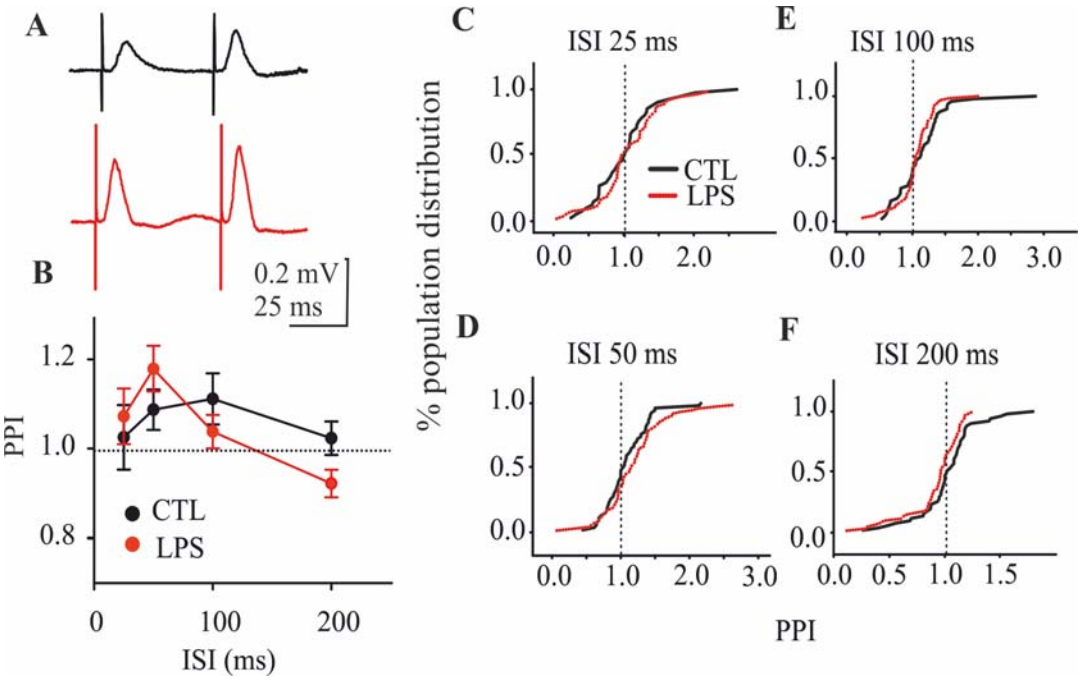

FIGURE 20: SHORT-TERM PLASTICITY OF THE FEPSP

(A) Sample traces of fEPSP paired-pulses, CA1 s. pyramidale, ISI 50 ms. The paired pulse index (PPI) was calculated as the ratio of the second to the first pulse.
(B) The fEPSP paired pulse modulation displayed no significant difference between control and LPS-exposed organotypic slice cultures in any of the tested ISIs (25, 50, 100 and 200 ms).
(C - F) Cumulative distribution of the PPI. Organotypic cultures displayed high variance in paired-pulse modulation, however without differences between control and LPS-exposed group (for all ISIs; $p > 0.05$, Kolmogorov – Smirnoff test).
n = 48 control and n = 65 LPS-exposed cultures from N = 10 preparations.

The effect of the paired stimulation on the fPopS (Figure 21A) varied from facilitation (PPI > 1) to depression (PPI < 1) in both control and LPS-exposed cultures. Similarly to fEPSP, LPS exposure had no significant impact on the fPopS PPI (Figure 21B and Figure 21C-F) for all interstimulus intervals between 200 and 25 ms.

Similarly to the fEPSP, the fPopS PPI was independent from the fPopS amplitude in control cultures, except for ISI as short as 25 ms. By contrast; the fPopS amplitude in LPS-exposed cultures was negatively correlated with the paired pulse index for all ISIs.

Summarizing the above, we demonstrate that LPS exposure induces a qualitative change without depression of the mean PPI. Instead, high fEPSP and fPopS amplitudes are associated

with paired pulse depression in LPS-exposed cultures, whereas in controls the paired pulse index is not dependent the fEPSP amplitude (adjusted to evoke 50% of the maximum response).

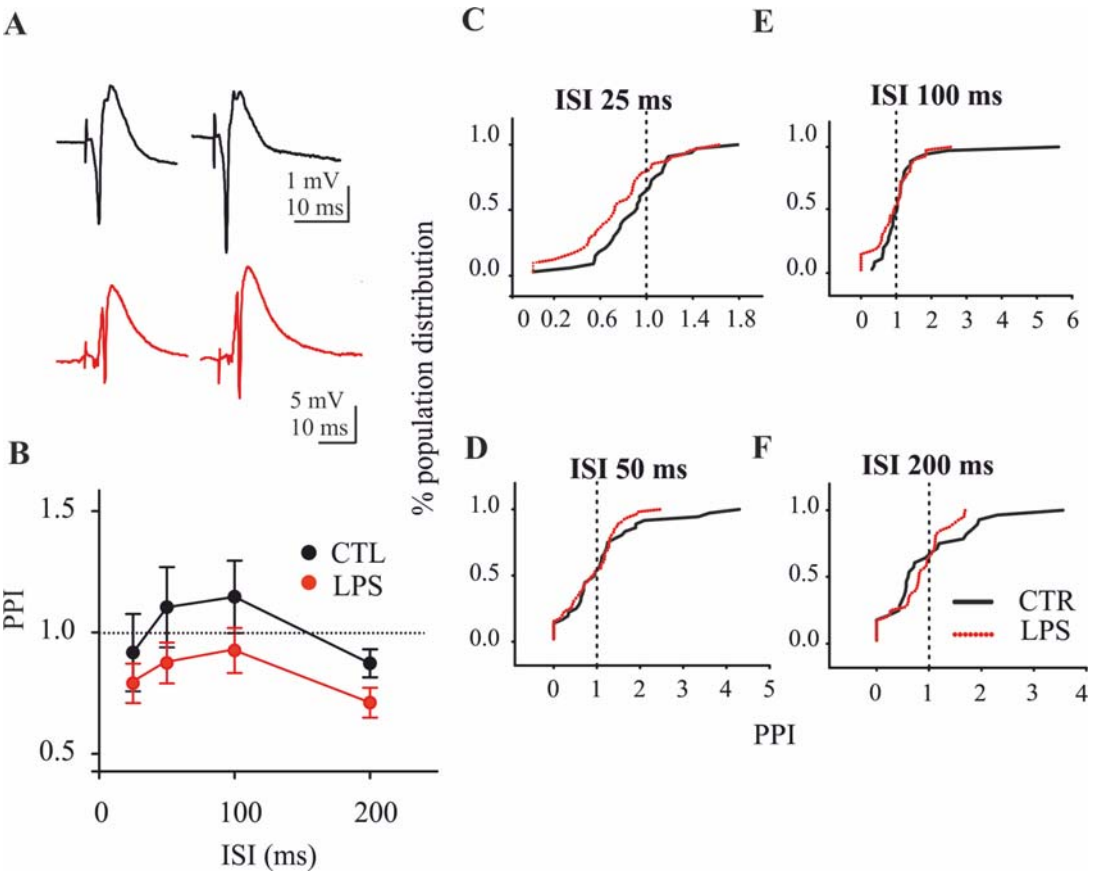

FIGURE 21: SHORT-TERM PLASTICITY OF THE FPOPS

(A) Sample traces, fPopS paired-pulse in CA1 at ISI 50 ms.
(B) The fPopS paired pulse modulation did not differ between control and LPS-exposed cultures in any of the tested ISI (25, 50 100 and 200 ms).
(C - F) Cumulative distribution of the PPI. Organotypic cultures displayed high variance in paired pulse modulation, albeit without difference between control and LPS-exposed group (for all ISIs; $p > 0.05$, Kolmogorov – Smirnoff test).
n = 48 control and n = 65 LPS-exposed cultures from N = 10 preparations.

Whereas the fEPSP PPI reflects synaptic short-term plasticity, the AP firing probability (fPopS) is determined by both the synaptic input (fEPSP) and neuronal excitability. Therefore, the ratio of the fPopS PPI over the fEPSP PPI (E-S ratio) expresses the fEPSP contribution in the fPopS modulation. Deviation of the E-S ratio from the unit means that the postsynaptic short-term

plasticity does not linearly effect the generation of APs. Accordingly, the E-S ratio introduces an additional short-term plasticity component, which is intercalated between the postsynaptic response and the AP generation and shapes the impact of the fEPSP to the fPopS paired-pulse response. This plasticity component is inferred as ‘plasticity of the neuronal excitability’.

In both control and LPS-exposed organotypic slice cultures, the fPopS and fEPSP PPI were not significantly different (Figure 22; for all ISIs $p < 0.01$, Mann-Whitney U test).

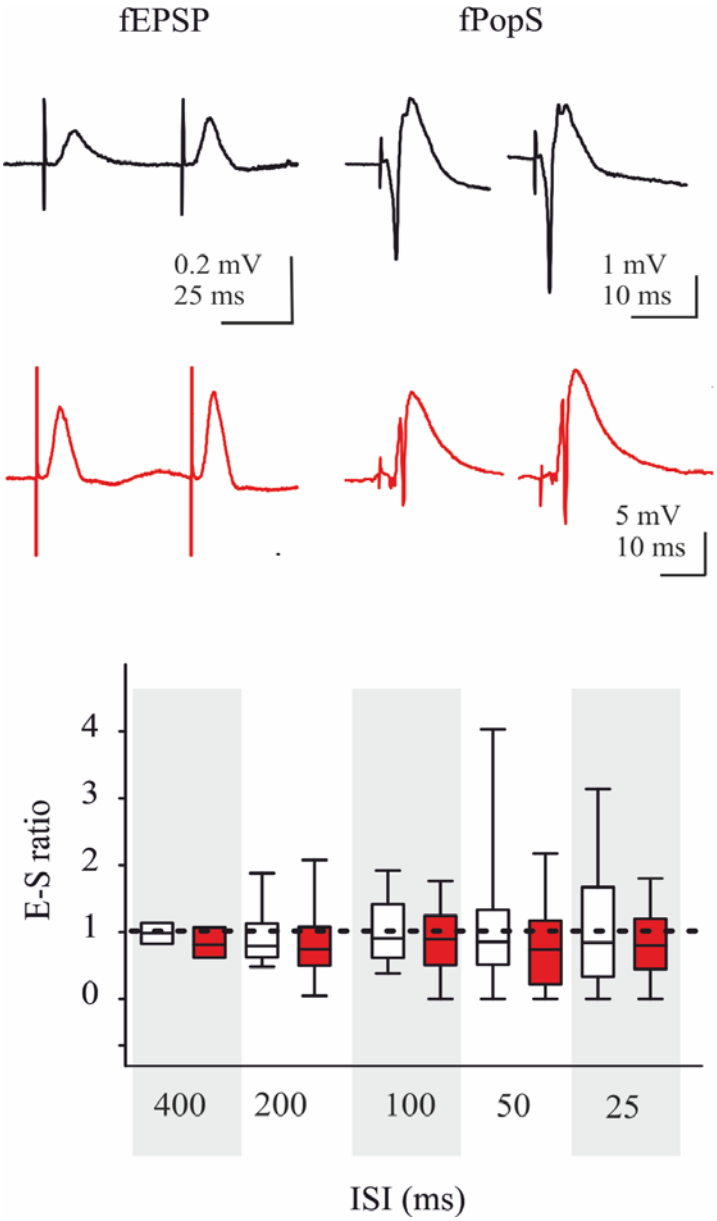

FIGURE 22: SHORT-TERM PLASTICITY OF THE NEURONAL EXCITABILITY

The E-S-ratio (fPopS PPI / fEPSP PPI) detects changes in neuronal excitability that may occur upon paired pulse stimulation. The short-term plasticity properties of neuronal excitability were not affected by microglial activation. For all ISI $p < 0.01$, Mann-Whitney U test; n = 48 control and n = 65 LPS-exposed cultures from N = 10 preparations.

3.3.4. STIMULATION-EVOKED EXTRACELLULAR POTASSIUM ($[K^+]_O$) TRANSIENTS

Membrane de- and re-polarization during neuronal activity is associated with changes in the extracellular potassium concentration. We induced $[K^+]_o$ transients by electrical stimulation (100 pulses at 20 Hz).With ion sensitive – reference pairs we recorded the extracellular potassium activity concomitantly with the local field potentials. This approach allowed for interpretation of the extracellular potassium changes with respect to local neuronal activity. It is important to notice that the applied method measures changes in $[K^+]_o$ and not the absolute $[K^+]_o$ value.

In both control and LPS-exposed cultures, the $[K^+]_o$ transient comprised a rising phase (Figure 23A) followed by a decaying, an undershooting and a slow recovering phase to the baseline. The $[K^+]_o$ rise and undershoot (Figure 23B) amplitudes were measured with progressively increasing stimulation intensity from 1 to 3 V in steps of 0.5 V.

3.3.4.1. THE $[K^+]_O$ RISING AMPLITUDE IS PROPORTIONAL TO THE STIMULATION INTENSITY IN CONTROL AND LPS-EXPOSED CULTURES

$[K^+]_o$ rising amplitude increases with stimulation intensity up to a saturation point (ceiling, $[K^+]_{o\ max}$), which is characteristic for the tissue and shall not be exceeded unless pathological activity takes place

Both control and LPS-exposed organotypic hippocampal slices responded to increasing intensity electrical stimulation with $[K^+]_o$ transients of increasing amplitude ($p < 0.001$, Kruskal Wallis with Dunn's pairwise post hoc test) (Figure 23B).

However, the $[K^+]_o$ ceiling amplitude was achieved with lower stimulation intensity in LPS-exposed cultures. In control cultures, the maximum $[K^+]_o$ increase ($[K^+]_{o\ max}$= 6.58 ± 0.51 mM,

n = 17**)** was achieved with higher stimulation intensity compared to LPS-exposed cultures, where the maximum $[K^+]_o$ increase ($[K^+]_o$max = 5.21 ± 0,52 mM, n = 22**)**. However, the intergroup comparison at corresponding stimulation intensities revealed no significant differences.

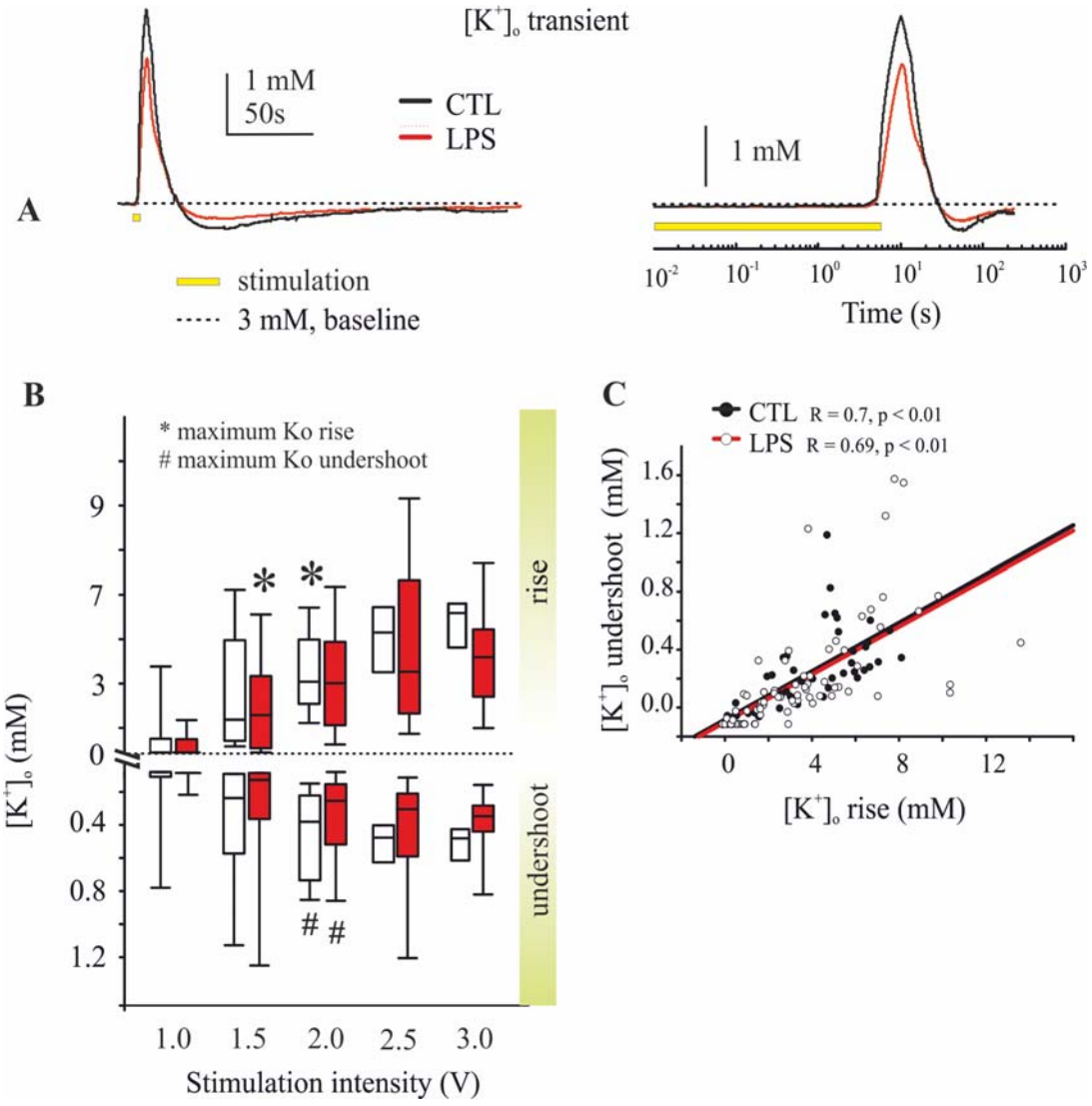

FIGURE 23: MICROGLIAL ACTIVATION DOES NOT AFFECT THE AMPLITUDE OF $[K^+]_O$ TRANSIENTS

(A) Average traces of electrically evoked $[K^+]_o$ transients in the s. pyramidale of CA1 (20 Hz for 5 s at 1.5 V, yellow bar), n = 17 control and n = 22 LPS-exposed cultures form N = 10 preparations. (*Right panel*) semi-logarithmic plot.

(B) The $[K^+]_o$ rising amplitude increased with stimulation intensity: In control cultures, the maximum (ceiling) $[K^+]_o$ rise ($[K^+]_{o\ max}$ = 6.58 ± 0.51 mM) was achieved with 2 V stimulation intensity. In LPS-exposed cultures, the maximum $[K^+]_o$ rise ($[K^+]_{o\ max}$ = 5.21 ± 0.52 mM) was achieved with lower (1.5 V) stimulation intensity (n = 17 control and n = 22, $p < 0.001$, Kruskal Wallis with Dunn's pairwise post hoc test). However, the difference was not significant between groups ($p > 0.05$, Mann-Whitney U test between corresponding stimulation intensities).
The $[K^+]_o$ undershoot increased with stimulation intensity in both control and LPS-exposed slices. The maximum $[K^+]_o$ (0.24 ± 0.08 mM for controls and 0.17 ± 0.08 mM for LPS-exposed cultures) corresponded to 2 V stimulation intensity in both groups ($p < 0.001$, Kruskal Wallis with Dunn's pairwise post hoc test), without significant intergroup difference ($p > 0.05$, Mann Whitney U test).
(C) The activity undershoot was positively correlated with the magnitude of the $[K^+]_o$ activity rise. The correlation coefficient was R = 0.7 for control and R = 0.69 for LPS-exposed cultures; $p < 0.001$, Pearson correlation for n = 17 control and n = 22 LPS-exposed organotypic cultures.

3.3.4.2. THE $[K^+]_O$ UNDERSHOOT IS PROPORTIONAL TO THE $[K^+]_O$ RISE AND OF EQUAL AMPLITUDE IN CONTROL AND LPS-EXPOSED CULTURES

Both neurons and astrocytes compensate for the elevated $[K^+]_o$ by potassium reuptake. Overcompensation beyond the resting baseline generates the $[K^+]_o$ undershoot (Heinemann and Lux, 1975) in both control and LPS-exposed cultures (Figure 23A).

The $[K^+]_o$ undershoot was positively correlated with the magnitude of $[K^+]_o$ rise (Figure 23D), with correlation coefficient R = 0.7 for control and R = 0.69 for LPS-exposed cultures ($p < 0.001$, Pearson correlation for n = 54 control and n = 94 traces from LPS-exposed organotypic cultures, pooled from all stimulation intensities). Accordingly, the $[K^+]_o$ undershoot increased with stimulation intensity in both control and LPS-exposed slices ($p < 0.001$, Kruskal Wallis with Dunn's pairwise post hoc test, Figure 23C). The maximum undershoot, 0.24 ± 0.08 mM $[K^+]_o$ for controls and 0.17 ± 0.08 mM $[K^+]_o$ for LPS-exposed cultures, was reached with 2 V stimulation intensity in both groups without significant intergroup differences for the corresponding stimulation intensities ($p > 0.05$, Mann-Whitney U test).

Despite microglial activation, the $[K^+]_o$ undershoot was quantitatively and qualitatively maintained with minimal changes: the undershoot amplitude increased with stimulation intensity proportionally to the $[K^+]_o$ rise, without significant difference between control and LPS-exposed cultures.

3.3.5. LIPOPOLYSACCHARIDE INDUCES ONLY SLIGHT RETARDATION IN POTASSIUM UPTAKE

3.3.5.1. THE FREQUENCY MODULATION OF FAST POTENTIALS IS NOT AFFECTED BY LIPOPOLYSACCHARIDE-EXPOSURE

The homeastasis of extracellular $[K^+]_o$ is under the control of potassium release (neuronal excitability) and reuptake (neuronal and astrocytic mechanisms). For assessing the relative contribution of neuronal excitability in the $[K^+]_o$ rise, we analyzed the amplitude of the concomitantly recorded fEPSPs (Figure 24A).

The amplitude of fEPSPs during the 100 pulse / 20 Hz stimulation sequence at submaximal intensity (1.5 V) did not significantly differ between LPS-exposed cultures and controls ($p > 0.05$, Mann-Whitney U test for $n = 17$ control and $n = 22$ LPS-exposed cultures from $N = 10$ preparations) (Figure 24B).

Hence, the occurrence of $[K^+]_o$ ceiling amplitude at lower stimulation intensity in LPS-exposed cultures is unlikely attributed to increased neuronal excitability.

The high frequency stimulation interrogates the kinetics of the different presynaptic vesicle pools (Wesseling et al., 2002; Rizzoli and Betz, 2005; Denker and Rizzoli, 2010). Therefore, lack of significant differences in the postsynaptic responses argues against fundamental disruption of the presynaptic neurotransmitter vesicle compartments and their release machinery.

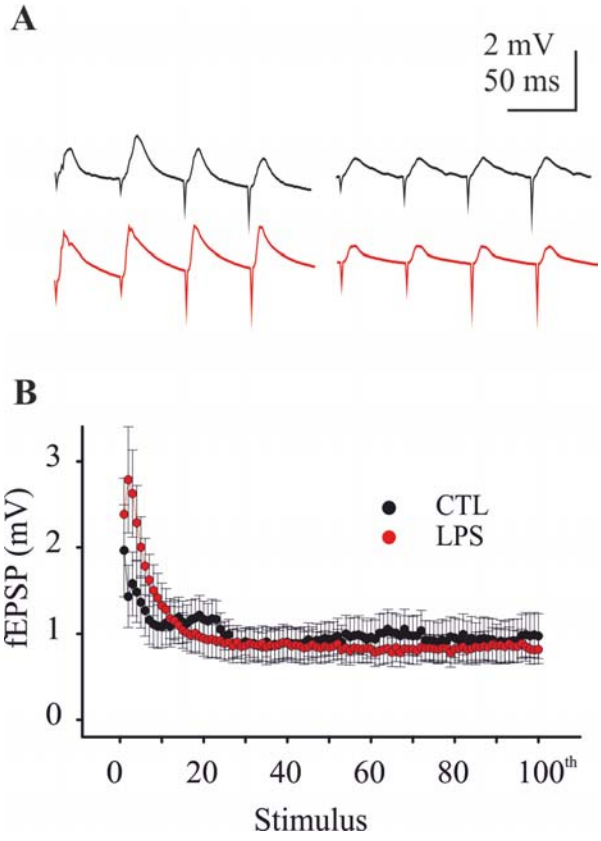

FIGURE 24: FREQUENCY MODULATION OF FAST POTENTIALS

The amplitude of evoked fEPSPs with 20 Hz / 5 s stimulation at 1.5 V was not affected ($p > 0.05$, Mann-Whitney U test for n = 17 control and n = 22 LPS exposed cultures from N = 10 preparations). (*Upper*) Mean traces, from the 1st to the 4th and the 80th to the 84th stimulus.

3.3.5.2. RETARDED KINETICS OF THE SLOW VOLTAGE NEGATIVITY IN LIPOPOLYSACCHARIDE-EXPOSED SLICES

The $[K^+]_o$ rising phase is associated with a simultaneous slow negativity of the local field potential, which is superimposed on the fast events (Figure 25A) (Gabriel et al., 1998a; Heinemann et al., 2000). The slow negativity has been suggested to derive from the local depolarization of glial cells due to the electrochemically driven, inward-rectifying potassium channel (K_{ir}) mediated $[K^+]_o$ uptake (Jauch et al., 2002). Therefore, it partially reflects the integrity of $[K^+]_o$ reuptake mechanisms.

The minimum point of the slow negativity, measured at the end of the stimulation sequence, did not differ between groups (Figure 25B). However, analysis of the slow field potential kinetics during the 5 s /20 Hz stimulation revealed slower kinetics in LPS-exposed cultures compared with controls (Figure 25C).

Consequently, despite the fact that the amplitude of the field potential negativity remains unchanged, delayed kinetics and loss of the correlation between $[K^+]_o$ rise and slow negativity amplitude in the LPS-exposed cultures suggests a defect in the potassium reuptake mechanism.

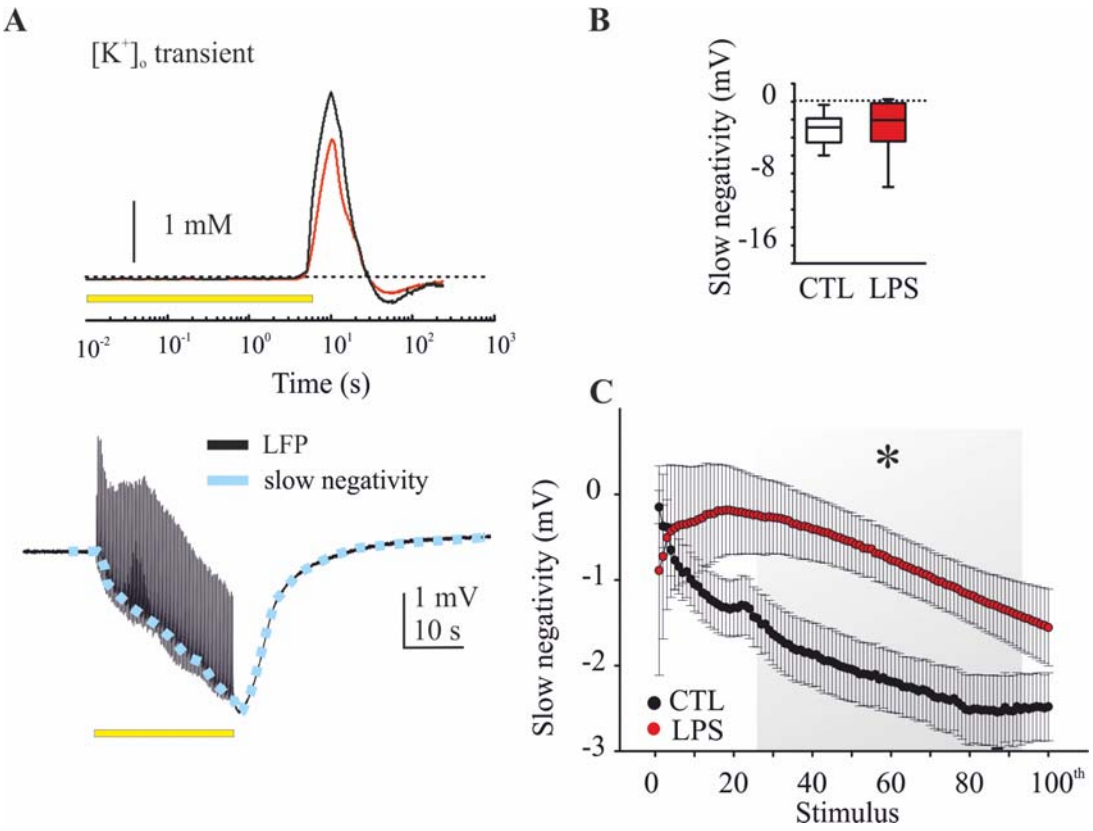

FIGURE 25: THE SLOW FIELD POTENTIAL NEGATIVITY OF THE $[K^+]_O$ TRANSIENTS IS RETARED BY MICROGLIAL ACTIVATION, SUGGESTING DELAYED POTASSIUM REUPTAKE

(A) Average trace of electrically evoked $[K^+]_o$ transients in CA1 s. pyramidale (20 Hz/5 s at 1.5 V). (*Upper panel*) ion sensitive signal and (*lower panel*) reference channel. The LFP comprises a fast (black solid line) and a slow component (blue dotted line).
(B) The slow negativity by the end of 1.5 V stimulation was -2.94 ± 1.04 mV in LPS-exposed cultures, which was not significantly different from the control value of 3.06 ± 0.45 mV (n = 17 control, n = 22 LPS-exposed cultures from N = 10 preparations; $p > 0.05$ Mann Whitney U test).
(C) Microglial activation attenuated slow negativity's kinetics at 1.5 V stimulation (n = 17 control cultures, n = 22 LPS-exposed cultures from N = 10 preparations, $p < 0.05$ for the range between the 25th and the 90th pulse, Mann Whitney U test). This is suggestive of delayed potassium reuptake.

4. DISCUSSION

4.1. ORGANOTYPIC CULTURES AT REST: THE BASELINE MICROGLIAL STATUS

In order to achieve a quantitative description of microglial cell morphology with brightfield microscopic imaging, we combined stereology with Sholl analysis of cell reconstructions.

Organotypic hippocampal slice cultures are well-established for *in vitro* modeling of traumatic brain injury (Wang and Andreasson, 2010), excitotoxicity, non-excitotoxic toxicity (Rossaint et al., 2009; Merz et al., 2010) and neuroprotection (Lee et al., 2010; Su et al., 2011). Disease models such as oxygen glucose deprivation for stroke (Dave et al., 2011) and epilepsy (Gutiérrez et al., 1999; Albus et al., 2008; Wahab et al., 2011) have been developed in organotypic slices, along with an increasing list of physiological neuronal functions such as synaptic plasticity (Bahr,1995; Bahr et al., 1995; Müller et al., 2000; Mellentin et al., 2006), fast oscillations (Huchzermeyer et al., 2008), metabolic demands of neuronal activity (Kann et al., 2003a, 2003b; Kovacs et al., 2009), stem cell physiology (Sarnowska et al., 2009) and development (Wenzel et al., 2007).

Organotypic cultures have been successfully used in microglial research (Huuskonen et al., 2005; Vogt et al., 2008), because they provide a near – physiological parenchymal structure, necessary for achieving ramified microglia (Hailer et al., 1997a). Moreover, they maintain the transverse hippocampal connectivity (Hailer et al., 1996), thus allowing for extracellular recordings that convey information not only on the single neuron activity, but also on the extended neuro-glial network integrity and function (Gähwiler, 1984a, 1984b; Zimmer et al., 1984; Noraberg et al., 2005; Sundstrom et al., 2005).

4.1.1. RECOVERY STATE OF THE CULTURES AT THE TIME OF EXPERIMENTATION (DIV 7-8)

Direct after slice isolation and during the first 3 days *in vitro* microglial cells are activated as a response to the isolation trauma. From DIV3 the tissue starts recovering and by DIV7 hippocampal slices are fully recovered from trauma, as judged by the levels of proinflammatory cytokines in the medium, by the re-establishment of ramified morphology, expression of adhesion molecules, phagocytosis, chemotaxis, and superoxide anion production (Coltman and Ide, 1996; Hailer et al., 1996, 1997a; Jankowsky et al., 2000; Mertsch et al., 2001; Huuskonen

et al., 2005). Our experiments were conducted on organotypic hippocampal slice cultures from P5-P7 Wistar rats, cultivated for 7-8 days before any manipulation took place. With this approach we allowed in vitro recovery from the isolation trauma and established a non-inflammatory baseline for our experimental procedures.

Importantly, microglial cells from the medial transverse plain of the organotypic hippocampal culture were selected for morphologic analysis. Both the upper and lower surface of the explants develop a gliotic scar as an inevitable consequence of the cutting and cultuvation process, therefore microglia from these layers were excluded from morphologic characterization (Coltman and Ide, 1996; Hailer et al., 1996; Mersch et al., 2001).

4.1.2. WHAT IS THE CORRELATION OF MICROGLIAL RAMIFICATION WITH THEIR FUNCTIONAL STATUS?

Ramification is a marker of microglial activation, albeit not a synonym for activation. Microglia *in vivo* (Davis et al., 1994; Wu et al., 1994, 2001; Olah et al., 2011) and *in vitro* (Hailer et al., 1997a; Skibo et al., 2000) exist in variably ramified phenotypes, which do not necessarily correspond to the secreted level of proinflammatory cytokines (Wu et al., 1997; Stern et al., 2000; Rochefort et al., 2002). *In vivo*, microglial cells in active cortical regions are less ramified compared to inactive cortex (Rochefort et al., 2002). *In vitro,* microglia decrease their ramification and increase their motility upon neuronal stimulation (Hung et al., 2010). However, this transition to a less ramified status is not accompanied with proinflammatory cytokine secretion or with phagocytic activity. On the other hand, LPS stimulation *in vivo* (Wu et al., 1997; Stern et al., 2000) and *in vitro* (Nörenberg et al., 1994; Ilschner et al., 1995) induces microglial transition to a less ramified state along with a strong proinflammatory reaction and phagocytic activity.

In vitro studies have shown that astrocytic-conditioned medium and tumor growth factor β (TGFβ) can both 'boost' microglial ramification resulting in morphologically similar populations, nevertheless with different functional properties (Möller et al., 2000a, 2000b; Schilling et al., 2001).

Resting / surveying microglia *in vivo*, in organotypic cultures and monocultures have gradually decreasing ramification level. Despite the reduced ramification level occurring *in vitro* compared to *in vivo*, both organotypic slice cultures and microglial monocultures display low

levels of proinflammatory cytokines and phagocytic activity at their 'resting' state, and maintain the ability to respond to LPS with secretion of proinflammatory cytokines and reversal of the potassium membrane conductance (Kettenmann et al., 1990; Nörenberg et al., 1994; Ilschner et al., 1995).

4.2. THE LIPOPOLYSACCHARIDE MODEL FOR MICROGLIAL ACTIVATION

In response to LPS-exposure, microglial cells displayed morphological changes compatible with activation (Nörenberg et al., 1994; Ilschner et al., 1995; Skibo et al., 2000), along with accumulation of proinflammatory cytokines (TNF-α and IL-6) and nitric oxide products in the culture supernatant. The LPS concentration used in our study was enough to saturate the proinflammatory response, as previously quantified (Huuskonen et al., 2005), and aimed to enhance the phenotypic contrast between resting / surveying and activated microglia (Häusler et al., 2002).

The level of cytokines (Mertsch et al., 2001; Häusler et al., 2002; Huuskonen et al., 2005) and NO detected in the LPS-exposed culture supernatant was comparable with previous reports from primary (Chang et al., 2000a, 2000b) and organotypic slice cultures (Kim et al., 2003; Huuskonen et al., 2005).

4.2.1. LIPOPOLYSACCHARIDE HAS VARIOUS CELLULAR TARGETS, ALBEIT PROBABLY WITH DIFFERENT FUNCTIONS

Among glia cells, LPS has been suggested to selectively target microglia (Lehnardt et al., 2002, 2003). However, growing evidence supports the active contribution of astrocytes in the inflammatory response. TLR4 mRNA is expressed by astrocytes in culture (Bowman et al., 2003), which in turn react to LPS exposure by phagocytosis (Kalmar et al., 2001). LPS sufficiently elicits an inflammatory response in primary astrocytic cultures (Krasowska-Zoladek et al., 2007; Go et al., 2009; Li et al., 2009; Lu et al., 2010; Van Neerven et al., 2010), indicating the functional expression of TLR4 (El-Hage et al., 2011; Okun et al., 2011). Nevertheless, strong evidence for the role of astrocytes is still lacking, partially due to methodological constraints and limitations in the establishment of microglia-free astrocytic cultures (Sola et al., 2002; Saura et al., 2007; Ransohoff and Perry, 2009).

Till recently neurons were considered to be devoid of the LPS target receptor TLR4 (Heine et al., 2001; Lehnardt et al., 2003). However, current data from human cortex (Maroso et al., 2010; Zurolo et al., 2010) and from primary neuronal cultures (Tang et al., 2007) argue for neuronal expression of TLR4 receptor and upregulation in response to immunological stimuli such as interferon gamma (Tang et al., 2007; Dilger and Johnson, 2008) and brain pathologies such as epilepsy (Maroso et al., 2010; Zurolo et al., 2011). However, the role of the neuronal TLR4 remains controversial, since no inflammatory response or neuronal damage is induced in primary neuronal cultures by LPS (Araki et al., 2001). The failure of LPS to elicit an inflammatory response in neuronal monocultures (Weis et al., 2002; Préhaud et al., 2005) occurs unlikely due to limited neuronal proinflammatory potential, since the viral double stranded ribonucleic acid (ds-RNA), which is a ligand for the TLR3 member of the same receptor family, sufficiently elicits the secretion of proinflammatory cytokines by neurons (Préhaud et al., 2005; Lafon et al., 2006). Hence, the expression and physiological significance of TLR4 signaling in neurons remain controversial (Préhaud et al., 2005; Tang et al., 2007, 2008; Okun et al., 2011).

Summarizing the above, the CNS response to immunological challenges (in this case, LPS-exposure) is a product of coordinated responses from different cell subtypes (simplified: microglia, astrocytes and neurons, but also oligendentroglia, endothelial cells and other cell types which are not a topic of the present study), and the phenotype is not a scalar sum of individual cell-type responses as studied in primary cultures. Therefore, the component of the proinflammatory response deriving from a direct LPS interaction with astroglia and neurons should also be taken into account. The refinement of microglial contribution in neuroinflammation defines one of our future goals.

4.3. LIPOPOLYSACCHARIDE EXPOSURE INDUCES MICROGLIAL ACTIVATION WITHOUT NEURODEGENERATION IN ORGANOTYPIC SLICE CULTURES.

The most intriguing finding in the LPS-exposed organotypic cultures is that the massive microglia activation and proinflammatory cytokine accumulation did not induce significant neurodegeneration, as assessed with Nissl (toluidine blue) and Fluoro-Jade B stainings.

4.3.1. METHODOLOGICAL QUALIFICATION OF THE FLUORO-JADE B STAINING

Fluoro-Jade B is a well-established marker for degenerative (necrotic, apoptotic and autophagic) neurons (Schmued et al., 1997; Noraberg et al., 1999, 2000a, 2000b, 2005), with results coherent with the lactate dehydrogenase and propidium iodide-uptake assays (Noraberg et al., 2004).The probability of a methodological failure was eliminated by the fact that the expected excessive neurodegeneration was detected in NMDA/KA-exposed cultures (Lee et al., 2003; Dehghani et al., 2004).

4.3.2. LIPOPOLYSACCHARIDE -INDUCED NEURODEGENERATION: EVIDENCE FROM DIFFERENT MODELS

Injection of LPS *in vivo*, either systemically (by i.p. injection) (Lehnardt et al., 2003; Liu and Bing, 2011) or by *in situ* injection (Kim et al., 2000; Ambrosini et al., 2005; Park et al., 2007; Couch et al., 2011;) is followed by secretion of proinflammatory cytokines (Stern et al., 2000), neurodegeneration and neurological/cognitive deficits (Ambrosini et al., 2005; Williamson et al., 2011).

In vitro incubation of primary neuronal cultures in LPS-microglial conditioned medium induced dose- and time-dependent neuronal death (Li et al., 2007; but see also Kim et al., 2000). The same results were acquired upon co-cultivation of primary microglial and neuronal cultures in transwells (Zujovic and Taupin, 2003), as well as with mixed neuronal-glial cultures (Neher et al., 2011).

In the meanwhile, the reports concerning LPS-induced neurodegeneration in ornanotypic conditions remain contradictive. In agreement with our observation, previous reports using various assays have failed to detect neurodegeneration in LPS-exposed organotypic slice cultures: neuronal survival has been confirmed with visual inspection and electrophysiology (Hellstrom et al., 2005), with lactate dehydrogenase (LDH) assay (Huuskonen et al., 2005) and with propidium iodide uptake (Duport et al., 2005). By contrast, Lee et al. (2003) reported neuronal death detected as increased propidium iodide uptake in LPS-exposed organotypic hippocampal slice cultures, and Johanssonet al. (2005), using the expression of NMDA-R1 as criterion for neuronal viability, detected dose- and time-dependent neuronal damage.

According to the above, the contradictive experimental evidence indicates that LPS in organotypic conditions does not have a clear and devastative neurodegenerative impact and the effect seems to be context-dependent.

In an attempt to list and exclude some factors that may bias towards neuronal survival *in vitro* we questioned the effect of serum –containing media. The addition of serum in the culture medium exposes the parenchyma to substances that *in vivo* access the CNS only after disruption of the blood-brain barrier. Numerous scientific reports argue for deleterious (Friedman et al., 2009; Heinemann et al., 2012; Ralay Ranaivo et al., 2012) and others for beneficial effects of serum (van der Valk et al., 2010). Nevertheless, neurotoxicity has been observed in primary cell cultures with (Zujovic and Taupin, 2003) and without serum in the medium (Li et al., 2007). Similarly, in organotypic cultures LPS exposure did not induce neurotoxicity, independently of the use of serum containing (Hellstrom et al., 2005) or serum free (Huuskonen et al., 2005) medium. Thus, in spite the fact that the existence of serum in the culture medium is an important determinant of the culture quality (Brewer et al., 1993, van der Valk et al., 2010), it does not appear to be a determinant factor of the LPS-induced neurotoxicity.

The two widely used in vitro models for LPS-induced neurotoxicity, incubation of primary neuronal cultures with microglial conditioned medium (Li et al., 2007) and co-cultivation of primary neuronal and microglial cell lines in transwells (Zujovic and Taupin, 2003), are restricted to humoral interactions (secreted and facultative soluble substances) and exclude cell contact-mediated effects, which may be decisive for neuronal survival. However, previous experiments in mixed neuronal – glial cultures (Neher et al., 2011), where cell contact is permitted, support that, in non-organotypic *in vitro* systems, neuronal death occurs despite of glial-neuronal contact.

Another parameter which may underlie the conflicting results between different in vitro models is the dose-dependence of the LPS-mediated neurotoxic effect, described by Li et al. (2007) in a microglial-conditioned medium transfer preparation. Interestigly, the cytokine concentration that defined the toxicity threshold was 2-fold (IL-6) to three-fold (TNFα) higher than those achieved in our and other (Duport et al., 2005; Huuskonen et al., 2005) organotypic models. This is in line with the observation of Duport et al. (2005), that microglia in organotypic cultures become neurotoxic only upon artificial expansion of their population with growth

factors. From the above we deduce that the microglial population in organotypic slice cultures might be quantitatively insufficient for inducing neurotoxicity after LPS stimulation, and either a stimulus that amplifies cytokine secretion or a factor that boosts population expansion is additionally required.

4.4. MICROGLIAL PROLIFERATION AFTER LIPOPOLYSACCHARIDE STIMULATION

Microglial cell number density has been associated with the degree of neurotoxicity *in vitro* and *in vivo***.** However, in vitro data show that microglial proliferation is necessary but not sufficient for neurotoxicity, which occurs only in presence of a proinflammatory stimulus (Duport et al., 2005; Pintado et al., 2011).

Despite the fact that in our experiments a proinflammatory response was evident after LPS-exposure, the microglial population was not significantly increased. However, increased microglial proliferation as a component of reactive gliosis (Streit et al., 1999) cannot be excluded by our data, because Iba1 immunohistochemistry provides no information on the turnover rate.

In vivo experimental data coherently report that LPS triggers microglial proliferation (Bachstetter et al., 2010) and increases microglial numbers (Shankaran et al., 2007). On the other hand, *in vitro* reports have shown that application of LPS on microglial cultures decreases their proliferation rate (Gebicke-Haerter et al., 1989) in a dose – dependent (Ganter et al., 1992) and age-dependent manner (Lee et al., 1994). Accordingly, LPS was reported to reduce microglial cell number without affecting their apoptotic rate *in vitro* (Bianco et al., 2006). Altogether, in sharp contrast to *in vivo* data, LPS exposure suppresses microglial turnover rate (proliferation and apoptosis) in *in vitro* systems. Thus, an equivocal suppression of the population turnover may explain the numerical stationarity over the 72-hours follow-up time frame.

The microglial density in organotypic hippocampal slice cultures is two- to threefold elevated compared to the adult rat hippocampus, probably as a result of the preparation trauma and tissue shrinkage that takes place during cultivation (data not shown, in line with Duport et al., 2005). Despite the higher density, microglia still maintain the potential to proliferate in response to the appropriate stimuli such as glutamate excitotoxicity. Therefore, in line with

previous reports, microglial cell density was increased after NMDA/KA exposure (Hailer et al., 2001; Dehghani et al., 2004). This suggests that the numerical stationarity of the microglial population after LPS-exposure is unlikely a result of 'saturation' of the population expansion capacity.

4.5. MICROGLIAL MORPHOLOGICAL CHANGES AFTER LIPOPOLYSACCHARIDE STIMULATION

The transition from ramified to ameboid phenotype is a morphological correlate of microglial activation (Nakamura et al., 1999; Stence et al., 2001). Microglial cell processes progressively retract and widen, while somata enlarge and acquire a rounder shape (Streit et al., 1999; Soulet and Rivest, 2008a, 2008b; Bilbo and Schwarz, 2009; Kettenmann et al., 2011). However, morphological changes of microglial cells are not a sufficient documentation of the proinflammatory response *per se* and have to be co-evaluated with other inflammatory markers, such as the secretion of cytokines. This is because an ameboid-like microglial phenotype can be triggered by neuronal activity (Hung et al., 2010; Fontainhas et al., 2011), albeit without being accompanied by proinflammatory cytokine secretion.

Indeed, LPS-exposure induced reduction of the microglial process length, enlargement and rounding of microglial somata. In the organotypic slice cultures a small fraction of the microglial population has ameboid morphology under control conditions; the fraction of which, however, does not change upon LPS-exposure (results not shown). This indicates that, although LPS exposure drives activation-like morphological changes, it does not lead to a massive ameboid transformation within the studied time-period of 72 hours.

The morphometric decomposition of microglial traces enabled the evaluation of ramification with respect to their distance from the center of the cell soma. The proximal processes appeared to be selectively retracted after LPS exposure, whereas neither the number nor the length of distal microglial processes, nor the process tuft domain were affected. This novel observation raises the question whether microglial processes are functionally differentiated with respect to their distance from the cell soma.

4.6. INFLUENCE OF MICROGLIAL ACTIVATION ON NEURONAL EXCITABILITY

Microglial cells are surveyors and potent modulators of the neuronal activity (Vélez-Fort et al., 2011; Rosi, 2011). Despite the LPS-induced activation and the elevated levels of proinflammatory cytokines in the neuronal environment, the extracellular electrophysiological recordings argued against any fundamental disruption of the neuronal function.

4.6.1. SPONTANEOUS FIELD ACTIVITY IN ORGANOTYPIC SLICE CULTURES UNDER MICROGLIAL ACTIVATION

The average spontaneous frequency power did not change upon LPS exposure, which indicates that events with slow time constant, such as postsynaptic currents, remained fundamentally unaffected. However, the variance of the LFP power spectrum among controls was considerably bigger than in LPS-exposed cultures. Interestingly, this is in line with the evoked field potential responses, where LPS-exposed cultures were consistently more homogeneous (smaller variance) compared with controls. This indicates that control cultures have a higher variance of activity status, which is restricted upon LPS exposure, however without significant changes in the mean activity.

The amplitude and frequency of MUA events reflect the number and AP-firing frequency of neurons within a distance of 100 – 200 µm around the recording pipette (Holt and Koch, 1999; Gold et al., 2006; see also Hughes et al., 2011; Kajigawa et al., 2011). Since the MUA events are extracellularly recorded, they are affected not only by the distance between the pipette and the AP source, but also by the conductive properties of the intercalated parenchyma.

The frequency of MUA events provides information on AP generation within the recording field, which is a weighted product of the neuronal number and their firing frequency. The fact that LPS exposure did not modify the MUA frequency indicates that the AP-firing pattern in the CA1 s. pyramidale remained unchanged. However, this does not distinguish between the number of active neurons and their AP-firing frequency, i.e. the same MUA frequency pattern could be generated either by a single, high frequency firing neuron, or by more than one, low frequency neurons, firing in interchange.

Analysis of the MUA amplitude enriches the frequency pattern with information on the spatiotemporal summation of spontaneously firing units. The MUA amplitude histogram

comprises two peaks that differ approximately by one order of magnitude. A possible explanation is that the first peak harvests single-neuron MUA events, whereas the second, double in amplitude peak, comprises summated events of two spontaneously occurring APs. The double-peaked amplitude histogram of MUA events is in line with previous observations, arguing that APs from more than 2 units are rarely simultaneously recorded by a single electrode, because neighboring neurons do not tend to fire together (Buzsaki et al., 2012).

In our data, the relative frequency of AP-firing from single neurons and neuronal pairs is the same in CTL and LPS cultures. However, the MUA amplitude histogram of LPS cultures is leftwards shifted, thus causing a small but significant reduction in the average.

Since the amplitude of MUA is a spatiotemporally weighted sum of APs and the unchanged frequency does not argue for modifications of the temporal component, the conductive properties of the intercalated parenchyma and a putatively increased tissue resistivity could provide a possible explanation that would fit to the depression of the evoked potentials as well.

The resistivity of the extra-neuronal space is determined not only by the extracellular matrix, but also (and very importantly) by the resting membrane potential and passive currents of the surrounding glia. Indeed, microglial activation implies expression of inward rectifying potassium channels and membrane hyperpolarization from -20 mV at rest down to -70 mV (Kettenmann et al., 1990; Eder et al., 1995; Kettenmann et al., 2011), which could participate in increasing the parenchymal resistivity and attenuating the propagation of APs (Johnston and Wu, 1994).

4.6.2. LIPOPOLYSACCHARIDE EXPOSURE AND TNF-ALPHA SECRETION MODERATELY SUPRESSES NEURONAL EXCITABILITY

In our model, microglial activation left the CA1 postsynaptic responses almost intact. This was an intriguing finding, because TNF-α, which was profoundly elevated in the culture supernatant, is a homeostatic modulator of the glutamatergic and GABAergic neurotransmission *in vivo* (Leonoudakis et al., 2004; Petrova et al., 2005; Yang, 2005; Serantes et al., 2006; Stellwagen and Malenka, 2006; Ren, 2011; Park and Bower, 2010; Zhang and Sun, 2010).

In sharp contrast to the *in vivo* conditions, the impact of TNF-α on the excitatory neurotransmission was not confirmed in organotypic hippocampal slice cultures, neither from our laboratory nor from a previous study (Hellstrom et al., 2005).

LPS-exposed cultures responded to increasing voltage steps with lower amplitude of fPopS compared with controls. This reflects a reduced or desynchronized AP firing rate of the local neuronal population (Johnston and Wu, 1994; Cohen and Miles, 2000).

According to the morphological markers (Nissl stain, Fluoro-Jade B), the reduced AP-firing rate is not likely attributed to local neurodegeneration. Notably, it cannot be explained as a result of suppressed input, since the fEPSP response remained unaltered.

Presumably, suppression of AP-firing without input changes is suggestive of changes in the neuronal excitability. The spatiotemporal summation profile of excitatory and inhibitory postsynaptic currents as they propagate to the soma and their final contribution to the generation of an AP is determined by the neuronal electrotonic properties (Squire et al., 2003), a change in which could attenuate the propagation to the soma and suppress the generation of action potentials without modifying the peripherally recorded component (Mitchell and Silver, 2003; Carvahlo and Buonomano, 2009; Takahashi and Magee, 2009).

Hellstrom et al (2005) characterized the postsynaptic currents and membrane properties of CA1 neurons in LPS-exposed organotypic slice cultures using patch-clamp recordings. In line with our findings, the action potential firing threshold was found elevated and the AP-firing rate depressed after long-term LPS-exposure. Indeed, independent studies have shown that morphological changes occurring in neurons as a result of LPS-exposure may modify their electrotonic properties (Richwine et al, 2008). Based on the postsynaptic potential kinetics, Hellstrom et al (2005) also speculated a putative contribution of the depolarization-activated potassium conductance (I_A). Further investigation of the resting and voltage activated currents are required to elucidate the underlying mechanisms.

4.7. LPS EXPOSURE DOES NOT AFFECT SHORT-TERM PLASTICITY IN ORGANOTYPIC SLICE CULTURES

4.7.1. FEPSP PAIRED PULSE MODULATION

The paired pulse stimulation protocol interrogates the properties of the readily releasable pool (RRP) of neurotransmitter vesicles (Betz, 1970; Zucker, 1989; Matveev and Wang, 2000a, 2000b; Rizzoli and Betz, 2005; Denker and Rizzoli, 2010). A high release probability (P_r) depletes the RRP, thus diminishing the number of vesicles available on the second stimulation, a phenomenon called 'paired pulse depression'. On the other hand, a presynaptic terminus with low P_r is not prone to RRP exhaustion and the first pulse may even facilitate vesicle release on the second pulse as a result of cumulative calcium kinetics (Dodge and Rahamimoff, 1967a, 1967b; Borst and Sakmann, 1996; Dittman and Regehr, 1996, 1998). Importantly for understanding the extracellular signal dynamics, the same model applies to both excitatory (Zucker, 1989; Dobrunz, 1997) and inhibitory synapses (Kraushaar and Jonas, 2000; Gulyas et al., 2010).

In our experimental setting, long – term LPS exposure did not affect the fEPSP paired pulse modulation properties. Interestingly, LPS has been shown to modulate the fEPSP short-term plasticity in a model- and time-dependent manner. Acute LPS exposure (in the range of hours) does not affect the fEPSP *in vitro* (Cunningham et al., 1996; Jo et al., 2001; Mizuno et al., 2004) but has been reported to block the fEPSP paired pulse facilitation *in vivo* (Commins et al., 2001). Coherently with our findings, long-term *in vivo* LPS exposure did not modify the EPSP short-term plasticity as measured *ex vivo* in acute brain slices (Jakubs et al., 2008).

The stimulation intensity used for paired pulses was adjusted to elicit 50% of the maximum response in order to avoid presynaptic exhaustion, and the amplitude of the first pulse did not affect the PPI in control cultures. By contrast, in LPS-stimulated organotypic slices, the amplitude of the first pulse was negatively correlated with the PPI. This means that high fEPSP response could have been a consequence of high release probability, which in turn rendered the presynaptic termini more prone to exhaustion after long-term LPS exposure. It is, however, interesting to notice that the 20 Hz stimulation sequence failed to demonstrate any differences in frequency modulation. Hence, the biological significance of the paired pulse result should be

cautiously interpreted and verified with single cell recordings that allow for discriminating between excitatory, inhibitory, pre- and postsynaptic elements.

Overall, our data suggest that the presynaptic machinery is only minimally affected after LPS-exposure, and that short-term plasticity properties are surprisingly maintained in the environment of microglia activation.

4.7.2. FPOPS PAIRED PULSE MODULATION AND E-S PLASTICITY

In contrast to the paired pulse modulation of fEPSP, which is mainly determined by presynaptic calcium kinetics, the paired-pulse modulation of fPopS is shaped by both the postsynaptic responses and neuronal excitability. The latter determines the spatiotemporal summation of postsynaptic currents and their integration impact on the generation of APs.

The ratio of the fPopS PPI over the fEPSP PPI reflects the relative contribution of postsynaptic responses to the modulation of neuronal firing probability. An E-S ratio equal to the unit designates that the fPopS modulation is linearly proportional to the fEPSP modulation. Deviation of the E-S ratio from the unit implies a disproportional fEPSP-to-fPopS modulation, termed EPSP-spike (E-S) plasticity or 'plasticity of the cell's excitability' (Bliss and Gardner-Medwin, 1973; Bliss and Lomo, 1973; Andersen, 1980; Jester, 1995; Daoudal, 2002; Daoudal and Debanne, 2003; Marder, 2003; Wang, 2003; Campanac et al., 2008).

The impact of LPS on neuronal excitability, as reported by previous studies, varies with time after exposure. Acute LPS exposure has been reported as proictogenic, deciphering increased neuronal excitability (Akarsu et al., 2006; Rodgers et al., 2009). By contrast, chronic LPS exposure was reported to have anti-ictogenic effect (Mirrione et al., 2010) after 24 hours (Akarsu et al., 2006).In the organotypic culture environment, chronic LPS-exposure does not affect neuronal excitability, as it is represented by the fPopS PPI and the fPopS-to-fEPSP PPI ratio. Nevertheless, the low number of studies in the field jeopardizes the formulation of a rigid statement considering the microglial effect on neuronal excitability.

4.8. IMPACT OF MICROGLIAL ACTIVATION ON EXTRACELLULAR POTASSIUM HOMEOSTASIS

Excitation of CA1 pyramidal neurons by SC fiber stimulation triggers a $[K^+]_o$ transient due to local membrane depolarization (Lux and Neher, 1973; Gabriel et al., 1998a, 1998b). The subsequent uptake of extracellular potassium by neurons and astrocytes occurs via active electrogenic processes (Na+ K+ ATPase; Skou, 1971; Grisar, 1986; Ransom et al., 2000) and facilitated uptake (K-Cl channels; Hertz, 1965, Ballanyi et al., 1987). The astrocyte-mediated uptake is responsible for the redistribution of potassium to remote locations by current loops through a gap junction-coupled syncytium. This process is known as 'spatial buffering' (Orkand, 1966; Holthoff, 2000; Wang et al., 2004) and depends on the extent of astrocytic coupling (Lee et al., 1994; Wallraff et al., 2006).

$[K^+]_o$ monitoring provides an overview of the local membrane depolarization and potassium reuptake mechanisms. We recorded the fluctuations of $[K^+]_o$ using ion sensitive microelectrodes that allowed for concomitant capturing of the local field potentials. Thus, we deciphered the relative contribution of neuronal excitability and $[K^+]_o$ reuptake in shaping the $[K^+]_o$ transient.

In both control and LPS-exposed organotypic slice cultures, the $[K^+]_o$ rise was proportional to the stimulation intensity. The mean ceiling level value in both groups was within the physiological range of 8 mM (Heinemann and Lux, 1977; Heinemann et al., 1983). In the LPS-exposed organotypic cultures the $[K^+]_o$ ceiling level sometimes exceeded 12 mM, but was still below the immature brain ceiling $[K^+]_o$ concentration (Hablitz and Heinemann, 1987, 1989), which can reach 18 mM. Thus, the $[K^+]_o$ transients in organotypic hippocampal cultures are comparable to mature hippocampal responses.

Although the $[K^+]_o$ transient amplitudes did not significantly differ between groups, LPS exposure was associated with increased $[K^+]_o$ rise at lower stimulation intensity compared with controls. This difference could not be attributed to increased excitability of the CA1 neurons, since the amplitudes of local field potentials were not significantly affected. However, LPS-exposed cultures revealed a retarded slow local field potential negativity, which reflects the inward-rectifying potassium channel (K_{IR})-mediated potassium reuptake by astrocytes (Gabriel et al., 1998a, 1998b; Jauch et al., 2002). Consequently, we assume that the increased $[K^+]_o$ rise

under conditions of LPS exposure could be a result of altered potassium reuptake properties. The astrocytic activation putatively underlying this effect may occur either via LPS ligation on astrocytic TLR4 receptors (Krasowska-Zoladek et al., 2007; Lu et al., 2010; van Neerven et al., 2010) or via microglial-operated astrocytic activation. Activated astrocytes downregulate the physiological potassium inward-rectification and switch to an immature phenotype with eliminated inward currents. This alteration has already been inferred as a mechanism of impaired $[K^+]_o$ buffering (Hinterkeuser et al., 2000; Schröder et al., 2000; Bordey et al., 2001). Not only astrocytes, but also activated microglia reverse the 'resting' K_{IR}-phenotype towards a dominating outward rectifying potassium conductance (K_{OR}) (Nörenberg et al., 1992, 1994; Fisher et al., 1995; Visentin et al., 2001; Li et al., 2008; reviewed in Eder, 1995a, 1995b; Kettenmann et al., 2011) but up to now no solid evidence supports a direct microglial role in $[K^+]_o$ reuptake and buffering.

Intriguingly, the $[K^+]_o$ undershoot was not affected by microglial manipulations. $[K^+]_o$ undershoot has been attested to an active potassium reuptake (Heinemann and Lux, 1975) mediated by astrocytic and neuronal Na-K-ATPase electrogenic pump activity (Heinemann and Gutnick, 1979) with different kinetics (Ransom et al., 2000). Thus, the unaffected $[K^+]_o$ undershoot is an index of unperturbed Na-K-ATPase activity, which argues for a metabolically competent parenchyma and excludes radical and devastating changes in neuronal metabolism due to microglial activation.

5. CONCLUSIONS AND FUTURE PERSPECTIVES

Microglial activation has been associated with a broad range of CNS pathologies, however it remains unclear whether and under which conditions it becomes harmful for neurons. The aim of the current study is to elucidate the impact of microglial activation by addressing some debating issues of the *in vitro* neuroinflammation modeling. For this purpose we used organotypic hippocampal slice cultures and assessed neuronal viability and function by means of morphology and electrophysiology.

Our findings demonstrate that microglial activation is not necessarily associated with defects in neuronal function. In contrast to *in vivo* findings, neither neuronal death nor major changes in evoked LFP responses occurred after long-term microglial activation (72 hours) in organotypic hippocampal slice cultures. Taking into account previous experimental evidence, we point out

that microglial activation might be necessary but not sufficient for neurotoxicity. Our perspective studies will focus on factors that perpetuate microglial activation towards neurodegeneration.

The inflammatory response in organotypic hippocampal slice cultures accounts for more than one cell type. Not only microglial cells but also astrocytes, neurons, oligodendrocytes and perhaps endothelial cells from vascular remnants participate in the imprinted phenotype. Hence, we suggest that role discrimination between individual cell compartments could facilitate further understanding of neuroinflammation.

We hope that this study will contribute with scientific knowledge and inspire new approaches in the field.

6. SUMMARY / ZUSAMMENFASSUNG

6.1. SUMMARY

Microglia are the central nervous system´s (CNS) resident macrophages. The myeloid progenitors that determine the microglial lineage colonize the CNS in the early embryonic life and serve thereafter the local innate immunity.

In the immune privileged CNS, microglial innate immune functions are constitutively suppressed ('resting'), whereas interruption of microglial –neuronal contact is permissive to protracted microglial activation. The expanding list of humoral and contact-dependent neuronal-microglial crosstalk pathways as well as the constant scavenging movement of microglial branches have recently introduced the term 'active surveyors' as an alternative to the static 'resting' terminology. Activation of microglial innate immune functions, such as direct cytotoxicity, antigen presentation, sequestration and stimulation of lymphocytes and phagocytosis, has been associated with reduction of the 'resting/surveying' ramified morphology and somatic transition to a round, 'ameboid' shape. Microglial activation is a pathologic hallmark in many CNS diseases and a common finding in *in vitro* neurodegeneration models. However, the causality underlying the correlation between microglial activation and neurodegeneration is currently debated.

In this study we used the organotypic hippocampal slice culture as a model to investigate the impact of microglial activation on neuronal function and survival.

After exposure of organotypic slices to the purified bacterial endotoxin lipopolysaccharide (LPS), for 72 hours, the microglial activation was quantified by assaying the supernatant for nitrite production, as well as for the proinflammatory cytokines interleukin 6 (IL-6) and tumor necrosis factor α (TNF-α). By applying anti-Iba1 immunohistochemistry and quantitative morphological methods (stereology and Neurolucida® tracings) we additionally described the microglial population in terms of size and ramification pattern. Standard histochemical and immunohistochemical staining (toluidine blue, NeuN) in combination with the specific neurodegeneration marker Fluoro-Jade B® were used to quantify neurodegeneration.

The impact of microglial activation on neuronal function was assessed in the CA1 hippocampal subregion by extracellular electrophysiological measurements of the spontaneous (multiunit activity and local field potential) and evoked field activity (input-output properties and short-

term plasticity). Moreover, by studying stimulation-evoked potassium ($[K^+]_o$) transients with ion-sensitive microelectrodes we probed the homeostatic capacity of the local neuro-glial network.

Our results show that the LPS-triggered microglial activation did not result to neurodegeneration. Furthermore, minimal changes in the electrophysiological field activity and $[K^+]_o$ transients argue against a fundamental perturbation of the neuronal and astroglial function.

The absence of neuronal death after LPS exposure in organotypic slice cultures, in sharp contrast to the severe degeneration occurring *in vivo* and in primary cultures, suggests that microglial activation is not necessarily neurotoxic and toxicity may occur in a context-dependent manner. With the present study we have established a model to further investigate the factors that may link microglial activation with neurotoxicity.

6.2. ZUSAMMENFASSUNG

Die Aufgaben von Makrophagen werden im zentralen Nervensystem von Mikroglia-Zellen übernommen. Deren Myeloid Vorläuferzellen wandern während der frühen Embryogenese in das zentrale Nervensystem (ZNS) ein und vermitteln dort die lokale, angeborene Immunität.

Die angeborene Immunität ist im ZNS unter normalen Bedingungen konstitutiv unterdrückt, demzufolge befinden sich die Mikrogliazellen in einem „Ruhezustand“. Störungen im Kontakt zwischen Mirgrogliazellen und Neuronen führen zu einer lang anhaltenden Aktivierung dieser Zellen. Für die Kommunikation zwischen Neuronen und Mikroglia ist eine stetig wachsende Anzahl von humoralen und kontaktabhängigen Botenstoffen und Signaltransduktionswegen verantwortlich. Auch legen neuere Forschungsergebnisse nahe, dass die „ruhenden“ Mikrogliazellen sich in einem Zustand der aktiven Überwachung ihrer Umgebung befinden, manifestiert u.a. durch permanente Mobilität ihrer Auswüchse, die der Überprüfung des umgebenden Milieus dient. Aus diesen Gründen ist der Begriff „aktive beobachtenden“ dem der „ruhenden“ Mikrogliazell vorzuziehen.

Der Übergang zum aktiven Status der Mikrogliazellen, ausgelöst z.B. durch Zelltoxizität, Antigenpräsentation, Lymphozytenstimulation oder Phagozytose führt zu einer bemerkenswerten Veränderung der Zellmorphologie: Die weitverzweigte Erscheinung der ruhenden/beobachtenden Zellen wird durch ein eher „amöboides“ Erscheinungsbild des Zellkörpers ersetzt.

Dieser Aktivierungsprozess ist nicht nur ein auffälliges Erscheinungsbild vieler pathologischer Zustände des ZNS, sondern lässt sich auch in diversen *in vitro* Modellen neurodegenerativer Krankheiten beobachten. Dies legt einen kausalen Zusammenhang zwischen Aktivierung und pathologischer Manifestation nahe, ohne dass diese allerdings zweifelsfrei nachgewiesen werden konnte.

Zu diesem Zweck wurde in der vorliegenden Arbeit der Einfluss von Mikrogliazellenaktivierung auf neuronale Zellen und ihr Überleben untersucht.

Inkubation mit dem bakteriellen Endotoxin LPS für 72 Stunden führte zu einer verlässlichen und reproduzierbaren Aktivierung der Mikrogliazellen. Dies konnte durch Quantifizierung des Nitritgehalts im Überstand, der entzündungsfördernden Interleukine IL-6 und des Tumor-necrosis factors α (TNF-α) belegt werden. Eine detaillierte Analyse der Mikroglia- Morphologie wurde durch immunohistochemische und stereologische Methoden durchgeführt, mit einem Schwerpunkt auf Zellkörpergröße und Verzweigungsgrad. Diese Parameter, die den Aktivierungsgrad der Mikrogliazellen charakterisieren, wurden mit verschiedenen, histo- und immunzytochemischen Markern (toluidine blue, NeuN) des Zellüberlebens und solchen spezifisch für Neurodegeneration (Fluoro-Jade B®) korreliert.

Unabhängig vom Überleben der Nervenzellen, wurde auch deren Funktion nach Mikrogliaaktivierung untersucht. Dazu wurden in der hippokampalen CA1 Region extrazelluläre elektrophysiologische Ableitungen durchgeführt, die Aufschlüsse über spontanes und evoziertes Verhalten (multiunit activity, evoked and spontaneous local field potential, Kurzzeitplastizität) geben. Darüber hinaus wurde auch die Dynamik und homeostatische Regulation der extrazellulären Kaliumkonzentration mit ionensensitiven Elektroden charakterisiert.

In dieser Studie wurden neurodegenerative Vorgänge nicht von LPS-induzierter Mikrogliaaktivierung beeinflusst. Darüber hinaus wiesen auch die elektrophysiologischen und ionensensitiven Messungen nicht auf eine grundlegende Veränderung der neuronalen und astrogliären Funktionen hin, sondern enthüllten nur geringfügige Veränderungen.

Diese Resultate sind in scharfem Kontrast/widersprechen bisherigen Erkenntnissen aus *in vivo* und Primärkulturexperimenten. Eine mögliche Interpretation der Daten stellte daher keinen zwangsläufigen kausalen Zusammenhang zwischen Mikrogliazellenaktivierung und Neurotoxizität her; ein solcher Zusammenhang könnte aber im hohen Maße kontextabhängig und

nicht kanonisch sein. Um solche kontextabhängigen Zusammenhänge aufzuklären, ist das in dieser Arbeit etablierte experimentelle Modell hervorragend geeignet.

7. REFERENCE LIST

EMAP eMouse Atlas Project.1-6-2012. (Accessed 13-7-2012 at http://www.emouseatlas.org.)

Acarin L, Gonzalez B, Castellano B, Castro AJ. Microglial response to N-methyl-D-aspartate-mediated excitotoxicity in the immature rat brain. J Comp Neurol 1996;367:361-374.

Adams RA, Bauer J, Flick MJ et al. The fibrin-derived gamma377-395 peptide inhibits microglia activation and suppresses relapsing paralysis in central nervous system autoimmune disease. J Exp Med 2007;204:571-582.

Ajami B, Bennett JL, Krieger C, Tetzlaff W, Rossi FM. Local self-renewal can sustain CNS microglia maintenance and function throughout adult life. Nat Neurosci 2007;10:1538-1543.

Akarsu ES, Ozdayi S, Algan E, Ulupinar F. The neuronal excitability time-dependently changes after lipopolysaccharide administration in mice: possible role of cyclooxygenase-2 induction. Epilepsy Res 2006;71:181-187.

Akin D, Ravizza T, Maroso M et al. IL-1beta is induced in reactive astrocytes in the somatosensory cortex of rats with genetic absence epilepsy at the onset of spike-and-wave discharges, and contributes to their occurrence. Neurobiol Dis 2011;44:259-269.

Albus K, Wahab A, Heinemann U. Standard antiepileptic drugs fail to block epileptiform activity in rat organotypic hippocampal slice cultures. Br J Pharmacol 2008;154:709-724.

Almolda B, Gonzalez B, Castellano B. Antigen presentation in EAE: role of microglia, macrophages and dendritic cells. Front Biosci 2011;16:1157-1171.

Ambrosini A, Louin G, Croci N, Plotkine M, Jafarian-Tehrani M. Characterization of a rat model to study acute neuroinflammation on histopathological, biochemical and functional outcomes. J Neurosci Methods 2005;144:183-191.

Amitai Y. Physiologic role for "inducible" nitric oxide synthase: a new form of astrocytic-neuronal interface. Glia 2010;58:1775-1781.

Amor S, Puentes F, Baker D, van der Valk J. Inflammation in neurodegenerative diseases. Immunology 2010;129:154-169.

Andersen P, Sundberg SH, Sveen O, Swann JW, Wigstrom H. Possible mechanisms for long-lasting potentiation of synaptic transmission in hippocampal slices from guinea-pigs. J Physiol 1980;302:463-482.

Antonucci F, Turola E, Riganti L et al. Microvesicles released from microglia stimulate synaptic activity via enhanced sphingolipid metabolism. EMBO J 2012;31:1231-1240.

Araki E, Forster C, Dubinsky JM, Ross ME, Iadecola C. Cyclooxygenase-2 inhibitor ns-398 protects neuronal cultures from lipopolysaccharide-induced neurotoxicity. Stroke 2001;32:2370-2375.

Aruffo A, Kanner SB, Sgroi D, Ledbetter JA, Stamenkovic I. CD22-mediated stimulation of T cells regulates T-cell receptor/CD3-induced signaling. Proc Natl Acad Sci U S A 1992;89:10242-10246.

Austin SA, Floden AM, Murphy EJ, Combs CK. Alpha-synuclein expression modulates microglial activation phenotype. J Neurosci 2006;26:10558-10563.

Avignone E, Ulmann L, Levavasseur F, Rassendren F, Audinat E. Status epilepticus induces a particular microglial activation state characterized by enhanced purinergic signaling. J Neurosci 2008;28:9133-9144.

Bachstetter AD, Jernberg J, Schlunk A et al. Spirulina promotes stem cell genesis and protects against LPS induced declines in neural stem cell proliferation. PLoS One 2010;5:e10496.

Bachstetter AD, Morganti JM, Jernberg J et al. Fractalkine and CX 3 CR1 regulate hippocampal neurogenesis in adult and aged rats. Neurobiol Aging 2011;32:2030-2044.

Bahr BA. Long-term hippocampal slices: a model system for investigating synaptic mechanisms and pathologic processes. J Neurosci Res 1995;42:294-305.

Bahr BA, Kessler M, Rivera S et al. Stable maintenance of glutamate receptors and other synaptic components in long-term hippocampal slices. Hippocampus 1995;5:425-439.

Ballanyi K, Grafe P, ten Bruggencate G. Ion activities and potassium uptake mechanisms of glial cells in guinea-pig olfactory cortex slices. J Physiol 1987;382:159-174.

Banchereau J, Briere F, Caux C et al. Immunobiology of dendritic cells. Annu Rev Immunol 2000;18:767-811.

Barclay AN, Wright GJ, Brooke G, Brown MH. CD200 and membrane protein interactions in the control of myeloid cells. Trends Immunol 2002;23:285-290.

Beattie EC, Stellwagen D, Morishita W et al. Control of synaptic strength by glial TNFalpha. Science 2002;295:2282-2285.

Bechmann I, Priller J, Kovac A et al. Immune surveillance of mouse brain perivascular spaces by blood-borne macrophages. Eur J Neurosci 2001;14:1651-1658.

Betz WJ. Depression of transmitter release at the neuromuscular junction of the frog. J Physiol 1970;206:629-644.

Beyer M, Gimsa U, Eyupoglu IY, Hailer NP, Nitsch R. Phagocytosis of neuronal or glial debris by microglial cells: upregulation of MHC class II expression and multinuclear giant cell formation in vitro. Glia 2000;31:262-266.

Bhatt DH, Zhang S, Gan WB. Dendritic spine dynamics. Annu Rev Physiol 2009;71:261-282.

Bianco F, Ceruti S, Colombo A et al. A role for P2X7 in microglial proliferation. J Neurochem 2006;99:745-758.

Biber K, Neumann H, Inoue K, Boddeke HW. Neuronal 'On' and 'Off' signals control microglia. Trends Neurosci 2007;30:596-602.

Bilbo SD, Schwarz JM. Early-life programming of later-life brain and behavior: a critical role for the immune system. Front Behav Neurosci 2009;3:14.

Blandino P, Jr., Barnum CJ, Deak T. The involvement of norepinephrine and microglia in hypothalamic and splenic IL-1beta responses to stress. J Neuroimmunol 2006;173:87-95.

Blank T, Prinz M. Microglia as modulators of cognition and neuropsychiatric disorders. Glia 2012; doi: 10.1002/glia.22372 [Epub ahead of print].

Blaylock RL, Strunecka A. Immune-glutamatergic dysfunction as a central mechanism of the autism spectrum disorders. Curr Med Chem 2009;16:157-170.

Blinzinger K, Kreutzberg G. Displacement of synaptic terminals from regenerating motoneurons by microglial cells. Z Zellforsch Mikrosk Anat 1968;85:145-157.

Bliss TV, Gardner-Medwin AR. Long-lasting potentiation of synaptic transmission in the dentate area of the unanaestetized rabbit following stimulation of the perforant path. J Physiol 1973;232:357-374.

Bliss TV, Lomo T. Long-lasting potentiation of synaptic transmission in the dentate area of the anaesthetized rabbit following stimulation of the perforant path. J Physiol 1973;232:331-356.

Block ML, Wu X, Pei Z et al. Nanometer size diesel exhaust particles are selectively toxic to dopaminergic neurons: the role of microglia, phagocytosis, and NADPH oxidase. FASEB J 2004;18:1618-1620.

Bordey A, Lyons SA, Hablitz JJ, Sontheimer H. Electrophysiological characteristics of reactive astrocytes in experimental cortical dysplasia. J Neurophysiol 2001;85:1719-1731.

Borst JG, Sakmann B. Calcium influx and transmitter release in a fast CNS synapse. Nature 1996;383:431-434.

Boucsein C, Kettenmann H, Nolte C. Electrophysiological properties of microglial cells in normal and pathologic rat brain slices. Eur J Neurosci 2000;12:2049-2058.

Bowman CC, Rasley A, Tranguch SL, Marriott I. Cultured astrocytes express toll-like receptors for bacterial products. Glia 2003;43:281-291.

Brewer GJ, Torricelli JR, Evege EK, Price PJ. Optimized survival of hippocampal neurons in B27-supplemented Neurobasal, a new serum-free medium combination. J Neurosci Res 1993;35:567-576.

Brockhaus J, Ilschner S, Banati RB, Kettenmann H. Membrane properties of ameboid microglial cells in the corpus callosum slice from early postnatal mice. J Neurosci 1993;13:4412-4421.

Brockhaus J, Möller T, Kettenmann H. Phagocytozing ameboid microglial cells studied in a mouse corpus callosum slice preparation. Glia 1996;16:81-90.

Broderick C, Hoek RM, Forrester JV et al. Constitutive retinal CD200 expression regulates resident microglia and activation state of inflammatory cells during experimental autoimmune uveoretinitis. Am J Pathol 2002;161:1669-1677.

Bruce-Keller AJ, Geddes JW, Knapp PE et al. Anti-death properties of TNF against metabolic poisoning: mitochondrial stabilization by MnSOD. J Neuroimmunol 1999;93:53-71.

Bruce AJ, Sakhi S, Schreiber SS, Baudry M. Development of kainic acid and N-methyl-D-aspartic acid toxicity in organotypic hippocampal cultures. Exp Neurol 1995;132:209-219.

Bsibsi M, Ravid R, Gveric D, van Noort JM. Broad expression of Toll-like receptors in the human central nervous system. J Neuropathol Exp Neurol 2002;61:1013-1021.

Buehler MR. A proposed mechanism for autism: an aberrant neuroimmune response manifested as a psychiatric disorder. Med Hypotheses 2011;76:863-870.

Burgess A, Saini S, Weng YQ, Aubert I. Stimulation of choline acetyltransferase by C3d, a neural cell adhesion molecule ligand. J Neurosci Res 2009;87:609-616.

Burns SP, Xing D, Shapley RM. Comparisons of the dynamics of local field potential and multiunit activity signals in macaque visual cortex. J Neurosci 2010;30:13739-13749.

Burns SP, Xing D, Shelley MJ, Shapley RM. Searching for autocoherence in the cortical network with a time-frequency analysis of the local field potential. J Neurosci 2010;30:4033-4047.

Buzsaki G, Anastassiou CA, Koch C. The origin of extracellular fields and currents--EEG, ECoG, LFP and spikes. Nat Rev Neurosci 2012;13:407-420.

Campanac E, Daoudal G, Ankri N, Debanne D. Downregulation of dendritic I(h) in CA1 pyramidal neurons after LTP. J Neurosci 2008;28:8635-8643.

Campanac E, Debanne D. Spike timing-dependent plasticity: a learning rule for dendritic integration in rat CA1 pyramidal neurons. J Physiol 2008;586:779-793.

Cardona AE, Pioro EP, Sasse ME et al. Control of microglial neurotoxicity by the fractalkine receptor. Nat Neurosci 2006;9:917-924.

Carson MJ, Reilly CR, Sutcliffe JG, Lo D. Mature microglia resemble immature antigen-presenting cells. Glia 1998;22:72-85.

Carvalho TP, Buonomano DV. Differential effects of excitatory and inhibitory plasticity on synaptically driven neuronal input-output functions. Neuron 2009;61:774-785.

Casaccia-Bonnefil P, Benedikz E, Shen H et al. Localized gene transfer into organotypic hippocampal slice cultures and acute hippocampal slices. J Neurosci Methods 1993;50:341-351.

Casaccia-Bonnefil P, Benedikz E, Rai R, Bergold PJ. Excitatory and inhibitory pathways modulate kainate excitotoxicity in hippocampal slice cultures. Neurosci Lett 1993;154:5-8.

Chamak B, Morandi V, Mallat M. Brain macrophages stimulate neurite growth and regeneration by secreting thrombospondin. J Neurosci Res 1994;38:221-233.

Chamak B, Dobbertin A, Mallat M. Immunohistochemical detection of thrombospondin in microglia in the developing rat brain. Neuroscience 1995;69:177-187.

Chan WY, Kohsaka S, Rezaie P. The origin and cell lineage of microglia: new concepts. Brain Res Rev 2007;53:344-354.

Chang JY, Liu LZ. Catecholamines inhibit microglial nitric oxide production. Brain Res Bull 2000;52:525-530.

Chang JY, Liu LZ. Inhibition of microglial nitric oxide production by hydrocortisone and glucocorticoid precursors. Neurochem Res 2000;25:903-908.

Chang RC, Hudson P, Wilson B, Haddon L, Hong JS. Influence of neurons on lipopolysaccharide-stimulated production of nitric oxide and tumor necrosis factor-alpha by cultured glia. Brain Res 2000;853:236-244.

Chang RC, Chen W, Hudson P et al. Neurons reduce glial responses to lipopolysaccharide (LPS) and prevent injury of microglial cells from over-activation by LPS. J Neurochem 2001;76:1042-1049.

Charles KJ, Deuchars J, Davies CH, Pangalos MN. GABA B receptor subunit expression in glia. Mol Cell Neurosci 2003;24:214-223.

Chen Y, Wermeling F, Sundqvist J et al. A regulatory role for macrophage class A scavenger receptors in TLR4-mediated LPS responses. Eur J Immunol 2010;40:1451-1460.

Choi DW. Ionic dependence of glutamate neurotoxicity. J Neurosci 1987;7:369-379.

Choi SH, Joe EH, Kim SU, Jin BK. Thrombin-induced microglial activation produces degeneration of nigral dopaminergic neurons in vivo. J Neurosci 2003;23:5877-5886.

Chowdhury P, Sacks SH, Sheerin NS. Toll-like receptors TLR2 and TLR4 initiate the innate immune response of the renal tubular epithelium to bacterial products. Clin Exp Immunol 2006;145:346-356.

Ciesielski-Treska J, Ulrich G, Taupenot L et al. Chromogranin A induces a neurotoxic phenotype in brain microglial cells. J Biol Chem 1998;273:14339-14346.

Clancy B, Finlay BL, Darlington RB, Anand KJ. Extrapolating brain development from experimental species to humans. Neurotoxicology 2007;28:931-937.

Clancy B, Kersh B, Hyde J et al. Web-based method for translating neurodevelopment from laboratory species to humans. Neuroinformatics 2007;5:79-94.

Clark AK, Yip PK, Malcangio M. The liberation of fractalkine in the dorsal horn requires microglial cathepsin S. J Neurosci 2009;29:6945-6954.

Cohen I, Miles R. Contributions of intrinsic and synaptic activities to the generation of neuronal discharges in in vitro hippocampus. J Physiol 2000;524 Pt 2:485-502.

Coltman BW, Ide CF. Temporal characterization of microglia, IL-1 beta-like immunoreactivity and astrocytes in the dentate gyrus of hippocampal organotypic slice cultures. Int J Dev Neurosci 1996;14:707-719.

Commins S, O'Neill LA, O'Mara SM. The effects of the bacterial endotoxin lipopolysaccharide on synaptic transmission and plasticity in the CA1-subiculum pathway in vivo. Neuroscience 2001;102:273-280.

Corona AW, Fenn AM, Godbout JP. Cognitive and behavioral consequences of impaired immunoregulation in aging. J Neuroimmune Pharmacol 2012;7:7-23.

Couch Y, Alvarez-Erviti L, Sibson NR, Wood MJ, Anthony DC. The acute inflammatory response to intranigral alpha-synuclein differs significantly from intranigral lipopolysaccharide and is exacerbated by peripheral inflammation. J Neuroinflammation 2011;8:166.

Coull JA, Beggs S, Boudreau D et al. BDNF from microglia causes the shift in neuronal anion gradient underlying neuropathic pain. Nature 2005;438:1017-1021.

Cross AK, Woodroofe MN. Chemokine modulation of matrix metalloproteinase and TIMP production in adult rat brain microglia and a human microglial cell line in vitro. Glia 1999;28:183-189.

Cuadros MA, Navascues J. The origin and differentiation of microglial cells during development. Prog Neurobiol 1998;56:173-189.

Cunningham AJ, Murray CA, O'Neill LA, Lynch MA, O'Connor JJ. Interleukin-1 beta (IL-1 beta) and tumour necrosis factor (TNF) inhibit long-term potentiation in the rat dentate gyrus in vitro. Neurosci Lett 1996;203:17-20.

Dalmau I, Vela JM, Gonzalez B, Castellano B. Expression of LFA-1alpha and ICAM-1 in the developing rat brain: a potential mechanism for the recruitment of microglial cell precursors. Brain Res Dev Brain Res 1997;103:163-170.

Daoudal G, Hanada Y, Debanne D. Bidirectional plasticity of excitatory postsynaptic potential (EPSP)-spike coupling in CA1 hippocampal pyramidal neurons. Proc Natl Acad Sci U S A 2002;99:14512-14517.

Daoudal G, Debanne D. Long-term plasticity of intrinsic excitability: learning rules and mechanisms. Learn Mem 2003;10:456-465.

Davalos D, Grutzendler J, Yang G et al. ATP mediates rapid microglial response to local brain injury in vivo. Nat Neurosci 2005;8:752-758.

Dave KR, Pileggi A, Raval AP. Recurrent hypoglycemia increases oxygen glucose deprivation-induced damage in hippocampal organotypic slices. Neurosci Lett 2011;496:25-29.

David JC, Yamada KA, Bagwe MR, Goldberg MP. AMPA receptor activation is rapidly toxic to cortical astrocytes when desensitization is blocked. J Neurosci 1996;16:200-209.

Davis EJ, Foster TD, Thomas WE. Cellular forms and functions of brain microglia. Brain Res Bull 1994;34:73-78.

De SA, Cecchetti V, Fravolini V et al. Effects of novel 6-desfluoroquinolones and classic quinolones on pentylenetetrazole-induced seizures in mice. Antimicrob Agents Chemother 1999;43:1729-1736.

De SR, Ajmone-Cat MA, Carnevale D, Minghetti L. Activation of alpha7 nicotinic acetylcholine receptor by nicotine selectively up-regulates cyclooxygenase-2 and prostaglandin E2 in rat microglial cultures. J Neuroinflammation 2005;2:4.

De SA, Yu LM. Preparation of organotypic hippocampal slice cultures: interface method. Nat Protoc 2006;1:1439-1445.

Debanne D, Campanac E, Bialowas A, Carlier E, Alcaraz G. Axon physiology. Physiol Rev 2011;91:555-602.

Dehghani F, Conrad A, Kohl A, Korf HW, Hailer NP. Clodronate inhibits the secretion of proinflammatory cytokines and NO by isolated microglial cells and reduces the number of proliferating glial cells in excitotoxically injured organotypic hippocampal slice cultures. Exp Neurol 2004;189:241-251.

Denker A, Rizzoli SO. Synaptic vesicle pools: an update. Front Synaptic Neurosci 2010;2:135.

Denker M, Roux S, Linden H et al. The local field potential reflects surplus spike synchrony. Cereb Cortex 2011;21:2681-2695.

Derecki NC, Cronk JC, Lu Z et al. Wild-type microglia arrest pathology in a mouse model of Rett syndrome. Nature 2012;484:105-109.

Dietzel I, Heinemann U. Dynamic variations of the brain cell microenvironment in relation to neuronal hyperactivity. Ann N Y Acad Sci 1986;481:72-86.

Dilger RN, Johnson RW. Aging, microglial cell priming, and the discordant central inflammatory response to signals from the peripheral immune system. J Leukoc Biol 2008;84:932-939.

Dimpfel W, Dalhoff A, von KE. In vitro modulation of hippocampal pyramidal cell response by quinolones: effects of HA 966 and gamma-hydroxybutyric acid. Antimicrob Agents Chemother 1996;40:2573-2576.

Dittman JS, Regehr WG. Contributions of calcium-dependent and calcium-independent mechanisms to presynaptic inhibition at a cerebellar synapse. J Neurosci 1996;16:1623-1633.

Dittman JS, Regehr WG. Calcium dependence and recovery kinetics of presynaptic depression at the climbing fiber to Purkinje cell synapse. J Neurosci 1998;18:6147-6162.

Dobrunz LE, Stevens CF. Heterogeneity of release probability, facilitation, and depletion at central synapses. Neuron 1997;18:995-1008.

Dodge FA, Jr., Rahamimoff R. Co-operative action a calcium ions in transmitter release at the neuromuscular junction. J Physiol 1967;193:419-432.

Dodge FA, Jr., Rahamimoff R. On the relationship between calcium concentration and the amplitude of the end-plate potential. J Physiol 1967;189:90P-92P.

Dolga AM, Granic I, Blank T et al. TNF-alpha-mediates neuroprotection against glutamate-induced excitotoxicity via NF-kappaB-dependent up-regulation of K2.2 channels. J Neurochem 2008;107:1158-1167.

Doyle KM, Kennedy D, Gorman AM et al. Unfolded proteins and endoplasmic reticulum stress in neurodegenerative disorders. J Cell Mol Med 2011;15:2025-2039.

Dringen R. Oxidative and antioxidative potential of brain microglial cells. Antioxid Redox Signal 2005;7:1223-1233.

Duport S, Garthwaite J. Pathological consequences of inducible nitric oxide synthase expression in hippocampal slice cultures. Neuroscience 2005;135:1155-1166.

Eder C, Fischer HG, Hadding U, Heinemann U. Properties of voltage-gated potassium currents of microglia differentiated with granulocyte/macrophage colony-stimulating factor. J Membr Biol 1995;147:137-146.

El-Hage N, Podhaizer EM, Sturgill J, Hauser KF. Toll-like receptor expression and activation in astroglia: differential regulation by HIV-1 Tat, gp120, and morphine. Immunol Invest 2011;40:498-522.

Elkabes S, DiCicco-Bloom EM, Black IB. Brain microglia/macrophages express neurotrophins that selectively regulate microglial proliferation and function. J Neurosci 1996;16:2508-2521.

Enzo Life Sciences I. LPS from *E. coli*, Serotype R515 (Re) (TLR *grade* Ô).5-7-2012. (Accessed 26-7-2012 at http://www.enzolifesciences.com/fileadmin/reports/els_fe738950cb.pdf.)

Epsztein J, Lee AK, Chorev E, Brecht M. Impact of spikelets on hippocampal CA1 pyramidal cell activity during spatial exploration. Science 2010;327:474-477.

European Parliament and Council. Directive on the protection of animals used for scientific purposes. Official Journal of the European Union 2010;L 276:33-76.

Farber K, Pannasch U, Kettenmann H. Dopamine and noradrenaline control distinct functions in rodent microglial cells. Mol Cell Neurosci 2005;29:128-138.

Ferguson AR, Christensen RN, Gensel JC et al. Cell death after spinal cord injury is exacerbated by rapid TNF alpha-induced trafficking of GluR2-lacking AMPARs to the plasma membrane. J Neurosci 2008;28:11391-11400.

Fioravante D, Regehr WG. Short-term forms of presynaptic plasticity. Curr Opin Neurobiol 2011;21:269-274.

Fischer HG, Eder C. Voltage-gated K+ currents of mouse dendritic cells. FEBS Lett 1995;373:127-130.

Fischer HG, Eder C, Hadding U, Heinemann U. Cytokine-dependent K+ channel profile of microglia at immunologically defined functional states. Neuroscience 1995;64:183-191.

Fisher SN, Vanguri P, Shin HS, Shin ML. Regulatory mechanisms of MuRantes and CRG-2 chemokine gene induction in central nervous system glial cells by virus. Brain Behav Immun 1995;9:331-344.

Fontainhas AM, Wang M, Liang KJ et al. Microglial morphology and dynamic behavior is regulated by ionotropic glutamatergic and GABAergic neurotransmission. PLoS One 2011;6:e15973.

Foresti ML, Arisi GM, Katki K et al. Chemokine CCL2 and its receptor CCR2 are increased in the hippocampus following pilocarpine-induced status epilepticus. J Neuroinflammation 2009;6:40.

Frandsen A, Drejer J, Schousboe A. Direct evidence that excitotoxicity in cultured neurons is mediated via N-methyl-D-aspartate (NMDA) as well as non-NMDA receptors. J Neurochem 1989;53:297-299.

Frey JU. Continuous blockade of GABA-ergic inhibition induces novel forms of long-lasting plastic changes in apical dendrites of the hippocampal cornu ammonis 1 (CA1) in vitro. Neuroscience 2010;165:188-197.

Friedman A, Kaufer D, Heinemann U. Blood-brain barrier breakdown-inducing astrocytic transformation: novel targets for the prevention of epilepsy. Epilepsy Res 2009;85:142-149.

Fry CH, Langley SEM. Ion-selective electrodes for biological systems. Amsterdam, The Netherlands: Harwood Academic Publishers, 2001.

Fu M, Zuo Y. Experience-dependent structural plasticity in the cortex. Trends Neurosci 2011;34:177-187.

Gabriel S, Kivi A, Eilers A, Kovacs R, Heinemann U. Effects of barium on stimulus-induced rises in [K+]o in juvenile rat hippocampal area CA1. Neuroreport 1998;9:2583-2587.

Gabriel S, Kivi A, Kovacs R et al. Effects of barium on stimulus-induced changes in [K+]o and field potentials in dentate gyrus and area CA1 of human epileptic hippocampus. Neurosci Lett 1998;249:91-94.

Gahmberg CG, Tian L, Ning L, Nyman-Huttunen H. ICAM-5--a novel two-facetted adhesion molecule in the mammalian brain. Immunol Lett 2008;117:131-135.

Gähwiler BH. Development of the hippocampus in vitro: cell types, synapses and receptors. Neuroscience 1984;11:751-760.

Gähwiler BH. Slice cultures of cerebellar, hippocampal and hypothalamic tissue. Experientia 1984;40:235-243.

Ganter S, Northoff H, Mannel D, Gebicke-Harter PJ. Growth control of cultured microglia. J Neurosci Res 1992;33:218-230.

Gao Z, Tsirka SE. Animal Models of MS Reveal Multiple Roles of Microglia in Disease Pathogenesis. Neurol Res Int 2011;2011:383087.

Garcao P, Oliveira CR, Agostinho P. Comparative study of microglia activation induced by amyloid-beta and prion peptides: role in neurodegeneration. J Neurosci Res 2006;84:182-193.

Gebicke-Haerter PJ, Bauer J, Schobert A, Northoff H. Lipopolysaccharide-free conditions in primary astrocyte cultures allow growth and isolation of microglial cells. J Neurosci 1989;9:183-194.

Geisler S, Heilmann H, Veh RW. An optimized method for simultaneous demonstration of neurons and myelinated fiber tracts for delineation of individual trunco- and palliothalamic nuclei in the mammalian brain. Histochem Cell Biol 2002;117:69-79.

Ginhoux F, Greter M, Leboeuf M et al. Fate mapping analysis reveals that adult microglia derive from primitive macrophages. Science 2010;330:841-845.

Gitik M, Liraz-Zaltsman S, Oldenborg PA, Reichert F, Rotshenker S. Myelin down-regulates myelin phagocytosis by microglia and macrophages through interactions between CD47 on myelin and SIRPalpha (signal regulatory protein-alpha) on phagocytes. J Neuroinflammation 2011;8:24.

Go HS, Shin CY, Lee SH et al. Increased proliferation and gliogenesis of cultured rat neural progenitor cells by lipopolysaccharide-stimulated astrocytes. Neuroimmunomodulation 2009;16:365-376.

Gold C, Henze DA, Koch C, Buzsaki G. On the origin of the extracellular action potential waveform: A modeling study. J Neurophysiol 2006;95:3113-3128.

Gonzalez JC, Egea J, Del Carmen GM et al. Neuroprotectant minocycline depresses glutamatergic neurotransmission and Ca(2+) signalling in hippocampal neurons. Eur J Neurosci 2007;26:2481-2495.

Gorczynski RM. CD200 and its receptors as targets for immunoregulation. Curr Opin Investig Drugs 2005;6:483-488.

Gottschall PE, Yu X, Bing B. Increased production of gelatinase B (matrix metalloproteinase-9) and interleukin-6 by activated rat microglia in culture. J Neurosci Res 1995;42:335-342.

Gottschall PE, Yu X. Cytokines regulate gelatinase A and B (matrix metalloproteinase 2 and 9) activity in cultured rat astrocytes. J Neurochem 1995;64:1513-1520.

Graeber MB, Bise K, Mehraein P. Synaptic stripping in the human facial nucleus. Acta Neuropathol 1993;86:179-181.

Griess, P. Bemerkungen zu der Abhandlung der HH. Weselsky und Benedikt: Über einige Azoverbindungen. Ber deutsch chem Gesellsch 1879;12:426-428.

Grinberg YY, Milton JG, Kraig RP. Spreading depression sends microglia on Levy flights. PLoS One 2011;6:e19294.

Grisar T, Delgado-Escueta AV. Astroglial contribution in human temporal lobe epilepsy: K+ activation of Na+,K+-ATPase in bulk isolated glial cells and synaptosomes. Brain Res 1986;364:1-11.

Gulyas AI, Szabo GG, Ulbert I et al. Parvalbumin-containing fast-spiking basket cells generate the field potential oscillations induced by cholinergic receptor activation in the hippocampus. J Neurosci 2010;30:15134-15145.

Gundersen HJ. Stereology of arbitrary particles. A review of unbiased number and size estimators and the presentation of some new ones, in memory of William R. Thompson. J Microsc 1986;143:3-45.

Gundersen HJ, Jensen EB. The efficiency of systematic sampling in stereology and its prediction. J Microsc 1987;147:229-263.

Gutierrez R, Armand V, Schuchmann S, Heinemann U. Epileptiform activity induced by low Mg2+ in cultured rat hippocampal slices. Brain Res 1999;815:294-303.

Gyoneva S, Orr AG, Traynelis SF. Differential regulation of microglial motility by ATP/ADP and adenosine. Parkinsonism Relat Disord 2009;15 Suppl 3:S195-S199.

Hablitz JJ, Heinemann U. Extracellular K+ and Ca2+ changes during epileptiform discharges in the immature rat neocortex. Brain Res 1987;433:299-303.

Hablitz JJ, Heinemann U. Alterations in the microenvironment during spreading depression associated with epileptiform activity in the immature neocortex. Brain Res Dev Brain Res 1989;46:243-252.

Hailer NP, Jarhult JD, Nitsch R. Resting microglial cells in vitro: analysis of morphology and adhesion molecule expression in organotypic hippocampal slice cultures. Glia 1996;18:319-331.

Hailer NP, Heppner FL, Haas D, Nitsch R. Fluorescent dye prelabelled microglial cells migrate into organotypic hippocampal slice cultures and ramify. Eur J Neurosci 1997;9:863-866.

Hailer NP, Bechmann I, Heizmann S, Nitsch R. Adhesion molecule expression on phagocytic microglial cells following anterograde degeneration of perforant path axons. Hippocampus 1997;7:341-349.

Hailer NP, Wirjatijasa F, Roser N et al. Astrocytic factors protect neuronal integrity and reduce microglial activation in an in vitro model of N-methyl-D-aspartate-induced excitotoxic injury in organotypic hippocampal slice cultures. Eur J Neurosci 2001;14:315-326.

Haley JE, Dickenson AH, Schachter M. Electrophysiological evidence for a role of nitric oxide in prolonged chemical nociception in the rat. Neuropharmacology 1992;31:251-258.

Haley JE, Wilcox GL, Chapman PF. The role of nitric oxide in hippocampal long-term potentiation. Neuron 1992;8:211-216.

Hanisch UK, van RD, Xie Y et al. The microglia-activating potential of thrombin: the protease is not involved in the induction of proinflammatory cytokines and chemokines. J Biol Chem 2004;279:51880-51887.

Hanisch UK, Kettenmann H. Microglia: active sensor and versatile effector cells in the normal and pathologic brain. Nat Neurosci 2007;10:1387-1394.

Harms KJ, Dunaevsky A. Dendritic spine plasticity: looking beyond development. Brain Res 2007;1184:65-71.

Harrison JK, Jiang Y, Chen S et al. Role for neuronally derived fractalkine in mediating interactions between neurons and CX3CR1-expressing microglia. Proc Natl Acad Sci U S A 1998;95:10896-10901.

Hartlage-Rubsamen M, Lemke R, Schliebs R. Interleukin-1beta, inducible nitric oxide synthase, and nuclear factor-kappaB are induced in morphologically distinct microglia after rat hippocampal lipopolysaccharide/interferon-gamma injection. J Neurosci Res 1999;57:388-398.

Hatherley D, Barclay AN. The CD200 and CD200 receptor cell surface proteins interact through their N-terminal immunoglobulin-like domains. Eur J Immunol 2004;34:1688-1694.

Hatori K, Nagai A, Heisel R, Ryu JK, Kim SU. Fractalkine and fractalkine receptors in human neurons and glial cells. J Neurosci Res 2002;69:418-426.

Hausler KG, Prinz M, Nolte C et al. Interferon-gamma differentially modulates the release of cytokines and chemokines in lipopolysaccharide- and pneumococcal cell wall-stimulated mouse microglia and macrophages. Eur J Neurosci 2002;16:2113-2122.

Haynes SE, Hollopeter G, Yang G et al. The P2Y12 receptor regulates microglial activation by extracellular nucleotides. Nat Neurosci 2006;9:1512-1519.

Heine H, Ulmer AJ, El-Samalouti VT, Lentschat A, Hamann L. Decay-accelerating factor (DAF/CD55) is a functional active element of the LPS receptor complex. J Endotoxin Res 2001;7:227-231.

Heinemann U, Lux HD. Undershoots following stimulus-induced rises of extracellular potassium concentration in cerebral cortex of cat. Brain Res 1975;93:63-76.

Heinemann U, Lux HD. Ceiling of stimulus induced rises in extracellular potassium concentration in the cerebral cortex of cat. Brain Res 1977;120:231-249.

Heinemann U, Lux HD, Gutnick MJ. Extracellular free calcium and potassium during paroxsmal activity in the cerebral cortex of the cat. Exp Brain Res 1977;27:237-243.

Heinemann U, Gutnick MJ. Relation between extracellular potassium concentration and neuronal activities in cat thalamus (VPL) during projection of cortical epileptiform discharge. Electroencephalogr Clin Neurophysiol 1979;47:345-347.

Heinemann U, Louvel J. Changes in [Ca2+]o and [K+]o during repetitive electrical stimulation and during pentetrazol induced seizure activity in the sensorimotor cortex of cats. Pflugers Arch 1983;398:310-317.

Heinemann U, Arens J. Production and calibration of ion-senstitive microelectrodes. In: Kettenmann H, Grantyn R, (eds): Practical electrophysiological methods: a guide for in vitro studies in cellular neurobiology.New York, USA: Wiley-Liss, Inc., 1992

Heinemann U, Gabriel S, Jauch R et al. Alterations of glial cell function in temporal lobe epilepsy. Epilepsia 2000;41 Suppl 6:S185-S189.

Heinemann U, Kaufer D, Friedman A. Blood-brain barrier dysfunction, TGFbeta signaling, and astrocyte dysfunction in epilepsy. Glia 2012;60:1251-1257.

Hellstrom IC, Danik M, Luheshi GN, Williams S. Chronic LPS exposure produces changes in intrinsic membrane properties and a sustained IL-beta-dependent increase in GABAergic inhibition in hippocampal CA1 pyramidal neurons. Hippocampus 2005;15:656-664.

Helmy A, De Simoni MG, Guilfoyle MR, Carpenter KL, Hutchinson PJ. Cytokines and innate inflammation in the pathogenesis of human traumatic brain injury. Prog Neurobiol 2011;95:352-372.

Helmy A, Carpenter KL, Menon DK, Pickard JD, Hutchinson PJ. The cytokine response to human traumatic brain injury: temporal profiles and evidence for cerebral parenchymal production. J Cereb Blood Flow Metab 2011;31:658-670.

Henderson AP, Barnett MH, Parratt JD, Prineas JW. Multiple sclerosis: distribution of inflammatory cells in newly forming lesions. Ann Neurol 2009;66:739-753.

Heo Y, Zhang Y, Gao D, Miller VM, Lawrence DA. Aberrant immune responses in a mouse with behavioral disorders. PLoS One 2011;6:e20912.

Heppner FL, Skutella T, Hailer NP, Haas D, Nitsch R. Activated microglial cells migrate towards sites of excitotoxic neuronal injury inside organotypic hippocampal slice cultures. Eur J Neurosci 1998;10:3284-3290.

Hertz L. Possible role of neuroglia: a potassium-mediated neuronal--neuroglial--neuronal impulse transmission system. Nature 1965;206:1091-1094.

Hill M. UNSW Embryology, Carnegie Stage Comparision.2008. (Accessed 13-7-2012 at http://embryology.med.unsw.edu.au/OtherEmb/CStages.htm.)

Hinterkeuser S, Schroder W, Hager G et al. Astrocytes in the hippocampus of patients with temporal lobe epilepsy display changes in potassium conductances. Eur J Neurosci 2000;12:2087-2096.

Hinze A, Stolzing A. Differentiation of mouse bone marrow derived stem cells toward microglia-like cells. BMC Cell Biol 2011;12:35.

Hoek RM, Ruuls SR, Murphy CA et al. Down-regulation of the macrophage lineage through interaction with OX2 (CD200). Science 2000;290:1768-1771.

Holt GR, Koch C. Electrical interactions via the extracellular potential near cell bodies. J Comput Neurosci 1999;6:169-184.

Holthoff K, Witte OW. Directed spatial potassium redistribution in rat neocortex. Glia 2000;29:288-292.

Holtmaat A, De P, V, Wilbrecht L, Knott GW. Imaging of experience-dependent structural plasticity in the mouse neocortex in vivo. Behav Brain Res 2008;192:20-25.

Holtmaat A, Svoboda K. Experience-dependent structural synaptic plasticity in the mammalian brain. Nat Rev Neurosci 2009;10:647-658.

Honda S, Sasaki Y, Ohsawa K et al. Extracellular ATP or ADP induce chemotaxis of cultured microglia through Gi/o-coupled P2Y receptors. J Neurosci 2001;21:1975-1982.

Howard CV, Reed MG. Unbiased Stereology: Three-Dimensional Measurement in Microscopy 2nd ed. Oxon, UK: Garland Science/BIOS Scientific publishers, 2005.

Howell OW, Rundle JL, Garg A et al. Activated microglia mediate axoglial disruption that contributes to axonal injury in multiple sclerosis. J Neuropathol Exp Neurol 2010;69:1017-1033.

Huchzermeyer C, Albus K, Gabriel HJ et al. Gamma oscillations and spontaneous network activity in the hippocampus are highly sensitive to decreases in pO2 and concomitant changes in mitochondrial redox state. J Neurosci 2008;28:1153-1162.

Hughes MM, Field RH, Perry VH, Murray CL, Cunningham C. Microglia in the degenerating brain are capable of phagocytosis of beads and of apoptotic cells, but do not efficiently remove PrPSc, even upon LPS stimulation. Glia 2010;58:2017-2030.

Hundhausen C, Misztela D, Berkhout TA et al. The disintegrin-like metalloproteinase ADAM10 is involved in constitutive cleavage of CX3CL1 (fractalkine) and regulates CX3CL1-mediated cell-cell adhesion. Blood 2003;102:1186-1195.

Hung J, Chansard M, Ousman SS, Nguyen MD, Colicos MA. Activation of microglia by neuronal activity: results from a new in vitro paradigm based on neuronal-silicon interfacing technology. Brain Behav Immun 2010;24:31-40.

Huuskonen J, Suuronen T, Miettinen R, van Groen T, Salminen A. A refined in vitro model to study inflammatory responses in organotypic membrane culture of postnatal rat hippocampal slices. J Neuroinflammation 2005;2:25.

Hwang J, Zheng LT, Ock J et al. Inhibition of glial inflammatory activation and neurotoxicity by tricyclic antidepressants. Neuropharmacology 2008;55:826-834.

Hwang J, Zheng LT, Ock J, Lee MG, Suk K. Anti-inflammatory effects of m-chlorophenylpiperazine in brain glia cells. Int Immunopharmacol 2008;8:1686-1694.

Ilschner S, Ohlemeyer C, Gimpl G, Kettenmann H. Modulation of potassium currents in cultured murine microglial cells by receptor activation and intracellular pathways. Neuroscience 1995;66:983-1000.

Irie-Sasaki J, Sasaki T, Matsumoto W et al. CD45 is a JAK phosphatase and negatively regulates cytokine receptor signalling. Nature 2001;409:349-354.

Ito D, Imai Y, Ohsawa K et al. Microglia-specific localisation of a novel calcium binding protein, Iba1. Brain Res Mol Brain Res 1998;57:1-9.

Iyer AM, Zurolo E, Boer K et al. Tissue plasminogen activator and urokinase plasminogen activator in human epileptogenic pathologies. Neuroscience 2010;167:929-945.

Jakubs K, Bonde S, Iosif RE et al. Inflammation regulates functional integration of neurons born in adult brain. J Neurosci 2008;28:12477-12488.

Jankowsky JL, Derrick BE, Patterson PH. Cytokine responses to LTP induction in the rat hippocampus: a comparison of in vitro and in vivo techniques. Learn Mem 2000;7:400-412.

Jarvela JT, Lopez-Picon FR, Plysjuk A, Ruohonen S, Holopainen IE. Temporal profiles of age-dependent changes in cytokine mRNA expression and glial cell activation after status epilepticus in postnatal rat hippocampus. J Neuroinflammation 2011;8:29.

Jauch R, Windmüller O, Lehmann TN, Heinemann U, Gabriel S. Effects of barium, furosemide, ouabaine and 4,4'-diisothiocyanatostilbene-2,2'-disulfonic acid (DIDS) on ionophoretically-induced changes in extracellular potassium concentration in hippocampal slices from rats and from patients with epilepsy. Brain Res 2002;925:18-27.

Jenmalm MC, Cherwinski H, Bowman EP, Phillips JH, Sedgwick JD. Regulation of myeloid cell function through the CD200 receptor. J Immunol 2006;176:191-199.

Jester JM, Campbell LW, Sejnowski TJ. Associative EPSP-spike potentiation induced by pairing orthodromic and antidromic stimulation in rat hippocampal slices. J Physiol 1995;484 (Pt 3):689-705.

Jinno S, Fleischer F, Eckel S, Schmidt V, Kosaka T. Spatial arrangement of microglia in the mouse hippocampus: a stereological study in comparison with astrocytes. Glia 2007;55:1334-1347.

Jo JH, Park EJ, Lee JK, Jung MW, Lee CJ. Lipopolysaccharide inhibits induction of long-term potentiation and depression in the rat hippocampal CA1 area. Eur J Pharmacol 2001;422:69-76.

Johansson S, Bohman S, Radesater AC, Oberg C, Luthman J. Salmonella lipopolysaccharide (LPS) mediated neurodegeneration in hippocampal slice cultures. Neurotox Res 2005;8:207-220.

Johnson EA, Kan RK. The acute phase response and soman-induced status epilepticus: temporal, regional and cellular changes in rat brain cytokine concentrations. J Neuroinflammation 2010;7:40.

Johnston D, Wu Y. Extracellular field recordings. Foundations of Cellular Neurophysiology.Cambridge, MA, USA: MIT Press, 1994: pp 423-439

Johnston D, Amaral DG. Hippocampus. In: Shepherd GM, (ed): The synaptic organization of the brain. 5th ed.New York, USA: Oxford University Press, 2003

Juckel G, Manitz MP, Brune M et al. Microglial activation in a neuroinflammational animal model of schizophrenia--a pilot study. Schizophr Res 2011;131:96-100.

Jung KH, Chu K, Lee ST et al. Molecular alterations underlying epileptogenesis after prolonged febrile seizure and modulation by erythropoietin. Epilepsia 2011;52:541-550.

Junker A, Krumbholz M, Eisele S et al. MicroRNA profiling of multiple sclerosis lesions identifies modulators of the regulatory protein CD47. Brain 2009;132:3342-3352.

Jurgens HA, Johnson RW. Dysregulated neuronal-microglial cross-talk during aging, stress and inflammation. Exp Neurol 2010.

Kajikawa Y, Schroeder CE. How local is the local field potential? Neuron 2011;72:847-858.

Kalmar B, Kittel A, Lemmens R, Kornyei Z, Madarasz E. Cultured astrocytes react to LPS with increased cyclooxygenase activity and phagocytosis. Neurochem Int 2001;38:453-461.

Kann O, Schuchmann S, Buchheim K, Heinemann U. Coupling of neuronal activity and mitochondrial metabolism as revealed by NAD(P)H fluorescence signals in organotypic hippocampal slice cultures of the rat. Neuroscience 2003;119:87-100.

Kann O, Kovacs R, Heinemann U. Metabotropic receptor-mediated Ca2+ signaling elevates mitochondrial Ca2+ and stimulates oxidative metabolism in hippocampal slice cultures. J Neurophysiol 2003;90:613-621.

Kann O. The energy demand of fast neuronal network oscillations: insights from brain slice preparations. Front Pharmacol 2011;2:90.

Kato TA, Monji A, Mizoguchi Y et al. Anti-Inflammatory properties of antipsychotics via microglia modulations: are antipsychotics a 'fire extinguisher' in the brain of schizophrenia? Mini Rev Med Chem 2011;11:565-574.

Kawai T, Akira S. The roles of TLRs, RLRs and NLRs in pathogen recognition. Int Immunol 2009;21:317-337.

Kennedy DW, Abkowitz JL. Kinetics of central nervous system microglial and macrophage engraftment: analysis using a transgenic bone marrow transplantation model. Blood 1997;90:986-993.

Kettenmann H, Hoppe D, Gottmann K, Banati R, Kreutzberg G. Cultured microglial cells have a distinct pattern of membrane channels different from peritoneal macrophages. J Neurosci Res 1990;26:278-287.

Kettenmann H, Hanisch UK, Noda M, Verkhratsky A. Physiology of microglia. Physiol Rev 2011;91:461-553.

Kim JM, Lee P, Son D, Kim H, Kim SY. Falcarindiol inhibits nitric oxide-mediated neuronal death in lipopolysaccharide-treated organotypic hippocampal cultures. Neuroreport 2003;14:1941-1944.

Kim WG, Mohney RP, Wilson B et al. Regional difference in susceptibility to lipopolysaccharide-induced neurotoxicity in the rat brain: role of microglia. J Neurosci 2000;20:6309-6316.

Klegeris A, Bissonnette CJ, McGeer PL. Reduction of human monocytic cell neurotoxicity and cytokine secretion by ligands of the cannabinoid-type CB2 receptor. Br J Pharmacol 2003;139:775-786.

Knott G, Holtmaat A. Dendritic spine plasticity-current understanding from in vivo studies. Brain Res Rev 2008;58:282-289.

Koning N, Bo L, Hoek RM, Huitinga I. Downregulation of macrophage inhibitory molecules in multiple sclerosis lesions. Ann Neurol 2007;62:504-514.

Koning N, Swaab DF, Hoek RM, Huitinga I. Distribution of the immune inhibitory molecules CD200 and CD200R in the normal central nervous system and multiple sclerosis lesions suggests neuron-glia and glia-glia interactions. J Neuropathol Exp Neurol 2009;68:159-167.

Kovacs R, Rabanus A, Otahal J et al. Endogenous nitric oxide is a key promoting factor for initiation of seizure-like events in hippocampal and entorhinal cortex slices. J Neurosci 2009;29:8565-8577.

Krasowska-Zoladek A, Banaszewska M, Kraszpulski M, Konat GW. Kinetics of inflammatory response of astrocytes induced by TLR 3 and TLR4 ligation. J Neurosci Res 2007;85:205-212.

Kraushaar U, Jonas P. Efficacy and stability of quantal GABA release at a hippocampal interneuron-principal neuron synapse. J Neurosci 2000;20:5594-5607.

Kreutzberg GW. Microglia: a sensor for pathological events in the CNS. Trends Neurosci 1996;19:312-318.

Kristensen BW, Noraberg J, Zimmer J. Comparison of excitotoxic profiles of ATPA, AMPA, KA and NMDA in organotypic hippocampal slice cultures. Brain Res 2001;917:21-44.

Kuhn SA, van Landeghem FK, Zacharias R et al. Microglia express GABA(B) receptors to modulate interleukin release. Mol Cell Neurosci 2004;25:312-322.

Lafon M, Megret F, Lafage M, Prehaud C. The innate immune facet of brain: human neurons express TLR-3 and sense viral dsRNA. J Mol Neurosci 2006;29:185-194.

Lawson LJ, Perry VH, Dri P, Gordon S. Heterogeneity in the distribution and morphology of microglia in the normal adult mouse brain. Neuroscience 1990;39:151-170.

Lawson LJ, Perry VH, Gordon S. Turnover of resident microglia in the normal adult mouse brain. Neuroscience 1992;48:405-415.

Lee J, Auyeung WW, Mattson MP. Interactive effects of excitotoxic injury and dietary restriction on microgliosis and neurogenesis in the hippocampus of adult mice. Neuromolecular Med 2003;4:179-196.

Lee KH, Won R, Kim UJ et al. Neuroprotective effects of FK506 against excitotoxicity in organotypic hippocampal slice culture. Neurosci Lett 2010;474:126-130.

Lee SC, Liu W, Brosnan CF, Dickson DW. GM-CSF promotes proliferation of human fetal and adult microglia in primary cultures. Glia 1994;12:309-318.

Lehnardt S, Lachance C, Patrizi S et al. The toll-like receptor TLR4 is necessary for lipopolysaccharide-induced oligodendrocyte injury in the CNS. J Neurosci 2002;22:2478-2486.

Lehnardt S, Massillon L, Follett P et al. Activation of innate immunity in the CNS triggers neurodegeneration through a Toll-like receptor 4-dependent pathway. Proc Natl Acad Sci U S A 2003;100:8514-8519.

Lemke R, Hartlage-Rubsamen M, Schliebs R. Differential injury-dependent glial expression of interleukins-1 alpha, beta, and interleukin-6 in rat brain. Glia 1999;27:75-87.

Leonoudakis D, Braithwaite SP, Beattie MS, Beattie EC. TNFalpha-induced AMPA-receptor trafficking in CNS neurons; relevance to excitotoxicity? Neuron Glia Biol 2004;1:263-273.

Levesque S, Wilson B, Gregoria V et al. Reactive microgliosis: extracellular micro-calpain and microglia-mediated dopaminergic neurotoxicity. Brain 2010;133:808-821.

Li F, Lu J, Wu CY et al. Expression of Kv1.2 in microglia and its putative roles in modulating production of proinflammatory cytokines and reactive oxygen species. J Neurochem 2008;106:2093-2105.

Li L, Lu J, Tay SS, Moochhala SM, He BP. The function of microglia, either neuroprotection or neurotoxicity, is determined by the equilibrium among factors released from activated microglia in vitro. Brain Res 2007;1159:8-17.

Li XZ, Bai LM, Yang YP et al. Effects of IL-6 secreted from astrocytes on the survival of dopaminergic neurons in lipopolysaccharide-induced inflammation. Neurosci Res 2009;65:252-258.

Liaury K, Miyaoka T, Tsumori T et al. Morphological features of microglial cells in the hippocampal dentate gyrus of Gunn rat: a possible schizophrenia animal model. J Neuroinflammation 2012;9:56.

Lim JE, Song M, Jin J et al. The effects of MyD88 deficiency on exploratory activity, anxiety, motor coordination, and spatial learning in C57BL/6 and APPswe/PS1dE9 mice. Behav Brain Res 2012;227:36-42.

Lim NK, Villemagne VL, Soon CP et al. Investigation of matrix metalloproteinases, MMP-2 and MMP-9, in plasma reveals a decrease of MMP-2 in Alzheimer's disease. J Alzheimers Dis 2011;26:779-786.

Linden H, Tetzlaff T, Potjans TC et al. Modeling the spatial reach of the LFP. Neuron 2011;72:859-872.

Liu M, Bing G. Lipopolysaccharide animal models for Parkinson's disease. Parkinsons Dis 2011;2011:327089.

Liu S, Liu Y, Hao W et al. TLR2 is a primary receptor for Alzheimer's amyloid beta peptide to trigger neuroinflammatory activation. J Immunol 2012;188:1098-1107.

Longo B, Romariz S, Blanco MM et al. Distribution and proliferation of bone marrow cells in the brain after pilocarpine-induced status epilepticus in mice. Epilepsia 2010;51:1628-1632.

Lu X, Ma L, Ruan L et al. Resveratrol differentially modulates inflammatory responses of microglia and astrocytes. J Neuroinflammation 2010;7:46.

Lux HD, Neher E. The equilibration time course of $(K^+)_o$ in cat cortex. Exp Brain Res 1973;17:190-205.

Lyons SA, Pastor A, Ohlemeyer C et al. Distinct physiologic properties of microglia and blood-borne cells in rat brain slices after permanent middle cerebral artery occlusion. J Cereb Blood Flow Metab 2000;20:1537-1549.

Maciejewski-Lenoir D, Chen S, Feng L, Maki R, Bacon KB. Characterization of fractalkine in rat brain cells: migratory and activation signals for CX3CR-1-expressing microglia. J Immunol 1999;163:1628-1635.

Madhusudan A, Vogel P, Knuesel I. Impact of Prenatal Immune System Disturbances on Brain Development. J Neuroimmune Pharmacol 2012; [Epub ahead of print].

Maezawa I, Calafiore M, Wulff H, Jin LW. Does microglial dysfunction play a role in autism and Rett syndrome? Neuron Glia Biol 2012;1-13.

Mahe C, Loetscher E, Dev KK et al. Serotonin 5-HT7 receptors coupled to induction of interleukin-6 in human microglial MC-3 cells. Neuropharmacology 2005;49:40-47.

Majewska AK, Newton JR, Sur M. Remodeling of synaptic structure in sensory cortical areas in vivo. J Neurosci 2006;26:3021-3029.

Marder CP, Buonomano DV. Differential effects of short- and long-term potentiation on cell firing in the CA1 region of the hippocampus. J Neurosci 2003;23:112-121.

Marin-Teva JL, Almendros A, Calvente R, Cuadros MA, Navascues J. Tangential migration of ameboid microglia in the developing quail retina: mechanism of migration and migratory behavior. Glia 1998;22:31-52.

Maroso M, Balosso S, Ravizza T et al. Interleukin-1 type 1 receptor/Toll-like receptor signalling in epilepsy: the importance of IL-1beta and high-mobility group box 1. J Intern Med 2011;270:319-326.

Maroso M, Balosso S, Ravizza T et al. Interleukin-1beta biosynthesis inhibition reduces acute seizures and drug resistant chronic epileptic activity in mice. Neurotherapeutics 2011;8:304-315.

Massengale M, Wagers AJ, Vogel H, Weissman IL. Hematopoietic cells maintain hematopoietic fates upon entering the brain. J Exp Med 2005;201:1579-1589.

Mastroeni D, Grover A, Leonard B et al. Microglial responses to dopamine in a cell culture model of Parkinson's disease. Neurobiol Aging 2009;30:1805-1817.

Matsumoto H, Kumon Y, Watanabe H et al. Antibodies to CD11b, CD68, and lectin label neutrophils rather than microglia in traumatic and ischemic brain lesions. J Neurosci Res 2007;85:994-1009.

Matsuo M, Hamasaki Y, Fujiyama F, Miyazaki S. Eicosanoids are produced by microglia, not by astrocytes, in rat glial cell cultures. Brain Res 1995;685:201-204.

Mattson MP. Glutamate and neurotrophic factors in neuronal plasticity and disease. Ann N Y Acad Sci 2008;1144:97-112.

Matveev V, Wang XJ. Differential short-term synaptic plasticity and transmission of complex spike trains: to depress or to facilitate? Cereb Cortex 2000;10:1143-1153.

Matveev V, Wang XJ. Implications of all-or-none synaptic transmission and short-term depression beyond vesicle depletion: a computational study. J Neurosci 2000;20:1575-1588.

McKercher SR, Torbett BE, Anderson KL et al. Targeted disruption of the PU.1 gene results in multiple hematopoietic abnormalities. EMBO J 1996;15:5647-5658.

Mellentin C, Möller M, Jahnsen H. Properties of long-term synaptic plasticity and metaplasticity in organotypic slice cultures of rat hippocampus. Exp Brain Res 2006;170:522-531.

Mertsch K, Hanisch UK, Kettenmann H, Schnitzer J. Characterization of microglial cells and their response to stimulation in an organotypic retinal culture system. J Comp Neurol 2001;431:217-227.

Merz F, Müller M, Taucher-Scholz G et al. Tissue slice cultures from humans or rodents: a new tool to evaluate biological effects of heavy ions. Radiat Environ Biophys 2010;49:457-462.

Minas K, Liversidge J. Is the CD200/CD200 receptor interaction more than just a myeloid cell inhibitory signal? Crit Rev Immunol 2006;26:213-230.

Mirrione MM, Konomos DK, Gravanis I et al. Microglial ablation and lipopolysaccharide preconditioning affects pilocarpine-induced seizures in mice. Neurobiol Dis 2010;39:85-97.

Mitchell SJ, Silver RA. Shunting inhibition modulates neuronal gain during synaptic excitation. Neuron 2003;38:433-445.

Mittelbronn M, Dietz K, Schluesener HJ, Meyermann R. Local distribution of microglia in the normal adult human central nervous system differs by up to one order of magnitude. Acta Neuropathol 2001;101:249-255.

Mitzdorf U. Current source-density method and application in cat cerebral cortex: investigation of evoked potentials and EEG phenomena. Physiol Rev 1985;65:37-100.

Mizuno T, Yoshihara Y, Kagamiyama H et al. Neuronal adhesion molecule telencephalin induces rapid cell spreading of microglia. Brain Res 1999;849:58-66.

Mizuno T, Kawanokuchi J, Numata K, Suzumura A. Production and neuroprotective functions of fractalkine in the central nervous system. Brain Res 2003;979:65-70.

Mizuno T, Kurotani T, Komatsu Y et al. Neuroprotective role of phosphodiesterase inhibitor ibudilast on neuronal cell death induced by activated microglia. Neuropharmacology 2004;46:404-411.

Möller JC, Klein MA, Haas S et al. Regulation of thrombospondin in the regenerating mouse facial motor nucleus. Glia 1996;17:121-132.

Möller T, Kann O, Verkhratsky A, Kettenmann H. Activation of mouse microglial cells affects P2 receptor signaling. Brain Res 2000;853:49-59.

Möller T, Hanisch UK, Ransom BR. Thrombin-induced activation of cultured rodent microglia. J Neurochem 2000;75:1539-1547.

Möller T, Weinstein JR, Hanisch UK. Activation of microglial cells by thrombin: past, present, and future. Semin Thromb Hemost 2006;32 Suppl 1:69-76.

Monier A, Adle-Biassette H, Delezoide AL et al. Entry and distribution of microglial cells in human embryonic and fetal cerebral cortex. J Neuropathol Exp Neurol 2007;66:372-382.

Monji A, Kato TA, Mizoguchi Y et al. Neuroinflammation in schizophrenia especially focused on the role of microglia. Prog Neuropsychopharmacol Biol Psychiatry 2011.

Moon JH, Kim SY, Lee HG, Kim SU, Lee YB. Activation of nicotinic acetylcholine receptor prevents the production of reactive oxygen species in fibrillar beta amyloid peptide (1-42)-stimulated microglia. Exp Mol Med 2008;40:11-18.

Morgan JT, Chana G, Pardo CA et al. Microglial activation and increased microglial density observed in the dorsolateral prefrontal cortex in autism. Biol Psychiatry 2010;68:368-376.

Moriguchi S, Mizoguchi Y, Tomimatsu Y et al. Potentiation of NMDA receptor-mediated synaptic responses by microglia. Brain Res Mol Brain Res 2003;119:160-169.

Mott RT, Ait-Ghezala G, Town T et al. Neuronal expression of CD22: novel mechanism for inhibiting microglial proinflammatory cytokine production. Glia 2004;46:369-379.

Mrak RE. Microglia in Alzheimer brain: a neuropathological perspective. Int J Alzheimers Dis 2012;2012:165021.

Müller D, Toni N, Buchs PA. Spine changes associated with long-term potentiation. Hippocampus 2000;10:596-604.

Müller N, Myint AM, Schwarz MJ. Inflammation in schizophrenia. Adv Protein Chem Struct Biol 2012;88:49-68.

Najjar S, Pearlman D, Miller DC, Devinsky O. Refractory epilepsy associated with microglial activation. Neurologist 2011;17:249-254.

Nakajima K, Shimojo M, Hamanoue M et al. Identification of elastase as a secretory protease from cultured rat microglia. J Neurochem 1992;58:1401-1408.

Nakajima K, Honda S, Tohyama Y et al. Neurotrophin secretion from cultured microglia. J Neurosci Res 2001;65:322-331.

Nakamura Y, Si QS, Kataoka K. Lipopolysaccharide-induced microglial activation in culture: temporal profiles of morphological change and release of cytokines and nitric oxide. Neurosci Res 1999;35:95-100.

Nathan C, Müller WA. Putting the brakes on innate immunity: a regulatory role for CD200? Nat Immunol 2001;2:17-19.

Neher JJ, Neniskyte U, Zhao JW et al. Inhibition of microglial phagocytosis is sufficient to prevent inflammatory neuronal death. J Immunol 2011;186:4973-4983.

Neumann H, Boucraut J, Hahnel C, Misgeld T, Wekerle H. Neuronal control of MHC class II inducibility in rat astrocytes and microglia. Eur J Neurosci 1996;8:2582-2590.

Neumann H. Control of glial immune function by neurons. Glia 2001;36:191-199.

Neumann J, Gunzer M, Gutzeit HO et al. Microglia provide neuroprotection after ischemia. FASEB J 2006;20:714-716.

Nicholls DG. Mitochondrial dysfunction and glutamate excitotoxicity studied in primary neuronal cultures. Curr Mol Med 2004;4:149-177.

Nimmerjahn A, Kirchhoff F, Helmchen F. Resting microglial cells are highly dynamic surveillants of brain parenchyma in vivo. Science 2005;308:1314-1318.

Nishiyori A, Minami M, Ohtani Y et al. Localization of fractalkine and CX3CR1 mRNAs in rat brain: does fractalkine play a role in signaling from neuron to microglia? FEBS Lett 1998;429:167-172.

Nitschke L. CD22 and Siglec-G: B-cell inhibitory receptors with distinct functions. Immunol Rev 2009;230:128-143.

Nizri E, Irony-Tur-Sinai M, Faranesh N et al. Suppression of neuroinflammation and immunomodulation by the acetylcholinesterase inhibitor rivastigmine. J Neuroimmunol 2008;203:12-22.

Noda M, Nakanishi H, Nabekura J, Akaike N. AMPA-kainate subtypes of glutamate receptor in rat cerebral microglia. J Neurosci 2000;20:251-258.

Noraberg J, Kristensen BW, Zimmer J. Markers for neuronal degeneration in organotypic slice cultures. Brain Res Brain Res Protoc 1999;3:278-290.

Noraberg J. Organotypic brain slice cultures: an efficient and reliable method for neurotoxicological screening and mechanistic studies. Altern Lab Anim 2004;32:329-337.

Noraberg J, Poulsen FR, Blaabjerg M et al. Organotypic hippocampal slice cultures for studies of brain damage, neuroprotection and neurorepair. Curr Drug Targets CNS Neurol Disord 2005;4:435-452.

Norenberg W, Gebicke-Haerter PJ, Illes P. Inflammatory stimuli induce a new K+ outward current in cultured rat microglia. Neurosci Lett 1992;147:171-174.

Norenberg W, Gebicke-Haerter PJ, Illes P. Voltage-dependent potassium channels in activated rat microglia. J Physiol 1994;475:15-32.

Ohsawa K, Kohsaka S. Dynamic motility of microglia: Purinergic modulation of microglial movement in the normal and pathological brain. Glia 2011;59:1793-1799.

Oka S, Mori K, Watanabe Y. Mammalian telencephalic neurons express a segment-specific membrane glycoprotein, telencephalin. Neuroscience 1990;35:93-103.

Okubo Y, Iino M. Visualization of glutamate as a volume transmitter. J Physiol 2011;589:481-488.

Okun E, Griffioen KJ, Mattson MP. Toll-like receptor signaling in neural plasticity and disease. Trends Neurosci 2011;34:269-281.

Olah M, Biber K, Vinet J, Boddeke HW. Microglia phenotype diversity. CNS Neurol Disord Drug Targets 2011;10:108-118.

Olson JK, Miller SD. Microglia initiate central nervous system innate and adaptive immune responses through multiple TLRs. J Immunol 2004;173:3916-3924.

Oorschot DE, Peterson DA, Jones DG. Neurite growth from, and neuronal survival within, cultured explants of the nervous system: a critical review of morphometric and stereological methods, and suggestions for the future. Prog Neurobiol 1991;37:525-546.

Opitz-Araya X, Barria A. Organotypic hippocampal slice cultures. J Vis Exp 2011;48:pii 2462.

Orkand RK, Nicholls JG, Kuffler SW. Effect of nerve impulses on the membrane potential of glial cells in the central nervous system of amphibia. J Neurophysiol 1966;29:788-806.

Orr AG, Orr AL, Li XJ, Gross RE, Traynelis SF. Adenosine A(2A) receptor mediates microglial process retraction. Nat Neurosci 2009;12:872-878.

Ovanesov MV, Sauder C, Rubin SA et al. Activation of microglia by borna disease virus infection: in vitro study. J Virol 2006;80:12141-12148.

Pan B, Zucker RS. A general model of synaptic transmission and short-term plasticity. Neuron 2009;62:539-554.

Panama BK, Latour-Villamil D, Farman GP et al. Nuclear factor kappaB downregulates the transient outward potassium current I(to,f) through control of KChIP2 expression. Circ Res 2011;108:537-543.

Paolicelli RC, Bolasco G, Pagani F et al. Synaptic pruning by microglia is necessary for normal brain development. Science 2011;333:1456-1458.

Park HY, Park JY, Kim JW et al. Differential expression of dendritic cell markers by all-trans retinoic acid on human acute promyelocytic leukemic cell line. Int Immunopharmacol 2004;4:1587-1601.

Park KM, Bowers WJ. Tumor necrosis factor-alpha mediated signaling in neuronal homeostasis and dysfunction. Cell Signal 2010;22:977-983.

Park KW, Lee HG, Jin BK, Lee YB. Interleukin-10 endogenously expressed in microglia prevents lipopolysaccharide-induced neurodegeneration in the rat cerebral cortex in vivo. Exp Mol Med 2007;39:812-819.

Penninger JM, Irie-Sasaki J, Sasaki T, Oliveira-dos-Santos AJ. CD45: new jobs for an old acquaintance. Nat Immunol 2001;2:389-396.

Perera PY, Mayadas TN, Takeuchi O et al. CD11b/CD18 acts in concert with CD14 and Toll-like receptor (TLR) 4 to elicit full lipopolysaccharide and taxol-inducible gene expression. J Immunol 2001;166:574-581.

Pernot F, Heinrich C, Barbier L et al. Inflammatory changes during epileptogenesis and spontaneous seizures in a mouse model of mesiotemporal lobe epilepsy. Epilepsia 2011;52:2315-2325.

Perry VH, Nicoll JA, Holmes C. Microglia in neurodegenerative disease. Nat Rev Neurol 2010;6:193-201.

Petrova LN, Grigor'ev VV, Bachurin SO. Effect of interleukin-1beta on NMDA-induced 45Ca2+ uptake by synaptosomes of rat brain cortex. Bull Exp Biol Med 2005;140:693-694.

Pintado C, Revilla E, Vizuete ML et al. Regional difference in inflammatory response to LPS-injection in the brain: role of microglia cell density. J Neuroimmunol 2011;238:44-51.

Plata-Salaman CR, Ffrench-Mullen JM. Interleukin-1 beta depresses calcium currents in CA1 hippocampal neurons at pathophysiological concentrations. Brain Res Bull 1992;29:221-223.

Plata-Salaman CR, Ffrench-Mullen JM. Interleukin-1 beta inhibits Ca2+ channel currents in hippocampal neurons through protein kinase C. Eur J Pharmacol 1994;266:1-10.

Pocock JM, Kettenmann H. Neurotransmitter receptors on microglia. Trends Neurosci 2007;30:527-535.

Polazzi E, Contestabile A. Reciprocal interactions between microglia and neurons: from survival to neuropathology. Rev Neurosci 2002;13:221-242.

Polazzi E, Monti B. Microglia and neuroprotection: from in vitro studies to therapeutic applications. Prog Neurobiol 2010;92:293-315.

Prehaud C, Megret F, Lafage M, Lafon M. Virus infection switches TLR-3-positive human neurons to become strong producers of beta interferon. J Virol 2005;79:12893-12904.

Priller J, Flügel A, Wehner T et al. Targeting gene-modified hematopoietic cells to the central nervous system: use of green fluorescent protein uncovers microglial engraftment. Nat Med 2001;7:1356-1361.

Prince DA, Lux HD, Neher E. Measurement of extracellular potassium activity in cat cortex. Brain Res 1973;50:489-495.

Prinz M, Kann O, Draheim HJ et al. Microglial activation by components of gram-positive and -negative bacteria: distinct and common routes to the induction of ion channels and cytokines. J Neuropathol Exp Neurol 1999;58:1078-1089.

Ralay Ranaivo H, Hodge JN, Choi N, Wainwright MS. Albumin induces upregulation of matrix metalloproteinase-9 in astrocytes via MAPK and reactive oxygen species-dependent pathways. J Neuroinflammation 2012;9:68.

Ramirez BG, Blazquez C, Gomez del PT, Guzman M, de Ceballos ML. Prevention of Alzheimer's disease pathology by cannabinoids: neuroprotection mediated by blockade of microglial activation. J Neurosci 2005;25:1904-1913.

Ransohoff RM, Perry VH. Microglial physiology: unique stimuli, specialized responses. Annu Rev Immunol 2009;27:119-145.

Ransohoff RM, Cardona AE. The myeloid cells of the central nervous system parenchyma. Nature 2010;468:253-262.

Ransom CB, Ransom BR, Sontheimer H. Activity-dependent extracellular K+ accumulation in rat optic nerve: the role of glial and axonal Na+ pumps. J Physiol 2000;522 Pt 3:427-442.

Rasch M, Logothetis NK, Kreiman G. From neurons to circuits: linear estimation of local field potentials. J Neurosci 2009;29:13785-13796.

Rasch MJ, Gretton A, Murayama Y, Maass W, Logothetis NK. Inferring spike trains from local field potentials. J Neurophysiol 2008;99:1461-1476.

Ravizza T, Rizzi M, Perego C et al. Inflammatory response and glia activation in developing rat hippocampus after status epilepticus. Epilepsia 2005;46 Suppl 5:113-117.

Reed R, Marks RJ, Oh S. Similarities of error regularization, sigmoid gain scaling, target smoothing, and training with jitter. IEEE Trans Neural Netw 1995;6:529-538.

Regen T, van Rossum D, Scheffel J et al. CD14 and TRIF govern distinct responsiveness and responses in mouse microglial TLR4 challenges by structural variants of LPS. Brain Behav Immun 2011;25:957-970.

Reis e Sousa. Dendritic cells in a mature age. Nat Rev Immunol 2006;6:476-483.

Ren WJ, Liu Y, Zhou LJ et al. Peripheral nerve injury leads to working memory deficits and dysfunction of the hippocampus by upregulation of TNF-alpha in rodents. Neuropsychopharmacology 2011;36:979-992.

Rezaie P, Male D. Colonisation of the developing human brain and spinal cord by microglia: a review. Microsc Res Tech 1999;45:359-382.

Ribes S, Ebert S, Czesnik D et al. Toll-like receptor prestimulation increases phagocytosis of Escherichia coli DH5alpha and Escherichia coli K1 strains by murine microglial cells. Infect Immun 2009;77:557-564.

Richwine AF, Parkin AO, Buchanan JB et al. Architectural changes to CA1 pyramidal neurons in adult and aged mice after peripheral immune stimulation. Psychoneuroendocrinology 2008;33:1369-1377.

Rizzi M, Perego C, Aliprandi M et al. Glia activation and cytokine increase in rat hippocampus by kainic acid-induced status epilepticus during postnatal development. Neurobiol Dis 2003;14:494-503.

Rizzoli SO, Betz WJ. Synaptic vesicle pools. Nat Rev Neurosci 2005;6:57-69.

Rochefort N, Quenech'du N, Watroba L et al. Microglia and astrocytes may participate in the shaping of visual callosal projections during postnatal development. J Physiol Paris 2002;96:183-192.

Rochefort N, Quenech'du N, Watroba L et al. Microglia and astrocytes may participate in the shaping of visual callosal projections during postnatal development. J Physiol Paris 2002;96:183-192.

Rochefort N, Quenech'du N, Watroba L et al. Microglia and astrocytes may participate in the shaping of visual callosal projections during postnatal development. J Physiol Paris 2002;96:183-192.

Rodgers KM, Hutchinson MR, Northcutt A et al. The cortical innate immune response increases local neuronal excitability leading to seizures. Brain 2009;132:2478-2486.

Rosenberg GA, Cunningham LA, Wallace J et al. Immunohistochemistry of matrix metalloproteinases in reperfusion injury to rat brain: activation of MMP-9 linked to stromelysin-1 and microglia in cell cultures. Brain Res 2001;893:104-112.

Rosi S. Neuroinflammation and the plasticity-related immediate-early gene Arc. Brain Behav Immun 2011;25 Suppl 1:S39-S49.

Rossaint J, Rossaint R, Weis J et al. Propofol: neuroprotection in an in vitro model of traumatic brain injury. Crit Care 2009;13:R61.

Rothstein JD, Patel S, Regan MR et al. Beta-lactam antibiotics offer neuroprotection by increasing glutamate transporter expression. Nature 2005;433:73-77.

Roy A, Fung YK, Liu X, Pahan K. Up-regulation of microglial CD11b expression by nitric oxide. J Biol Chem 2006;281:14971-14980.

Ruiz A, Matute C, Alberdi E. Endoplasmic reticulum Ca(2+) release through ryanodine and IP(3) receptors contributes to neuronal excitotoxicity. Cell Calcium 2009;46:273-281.

Rupalla K, Allegrini PR, Sauer D, Wiessner C. Time course of microglia activation and apoptosis in various brain regions after permanent focal cerebral ischemia in mice. Acta Neuropathol 1998;96:172-178.

Ryu JK, McLarnon JG. A leaky blood-brain barrier, fibrinogen infiltration and microglial reactivity in inflamed Alzheimer's disease brain. J Cell Mol Med 2009;13:2911-2925.

Ryu JK, Davalos D, Akassoglou K. Fibrinogen signal transduction in the nervous system. J Thromb Haemost 2009;7 Suppl 1:151-154.

Ryu JK, McLarnon JG. A leaky blood-brain barrier, fibrinogen infiltration and microglial reactivity in inflamed Alzheimer's disease brain. J Cell Mol Med 2009;13:2911-2925.

Sanchez-Lopez A, Cuadros MA, Calvente R et al. Radial migration of developing microglial cells in quail retina: a confocal microscopy study. Glia 2004;46:261-273.

Santello M, Bezzi P, Volterra A. TNFalpha controls glutamatergic gliotransmission in the hippocampal dentate gyrus. Neuron 2011;69:988-1001.

Sarnowska A, Jurga M, Buzanska L et al. Bilateral interaction between cord blood-derived human neural stem cells and organotypic rat hippocampal culture. Stem Cells Dev 2009;18:1191-1200.

Sasaki T, Sasaki-Irie J, Penninger JM. New insights into the transmembrane protein tyrosine phosphatase CD45. Int J Biochem Cell Biol 2001;33:1041-1046.

Saura J. Microglial cells in astroglial cultures: a cautionary note. J Neuroinflammation 2007;4:26.

Schilling M, Besselmann M, Leonhard C et al. Microglial activation precedes and predominates over macrophage infiltration in transient focal cerebral ischemia: a study in green fluorescent protein transgenic bone marrow chimeric mice. Exp Neurol 2003;183:25-33.

Schilling M, Strecker JK, Ringelstein EB, Schabitz WR, Kiefer R. The role of CC chemokine receptor 2 on microglia activation and blood-borne cell recruitment after transient focal cerebral ischemia in mice. Brain Res 2009;1289:79-84.

Schilling T, Nitsch R, Heinemann U, Haas D, Eder C. Astrocyte-released cytokines induce ramification and outward K+ channel expression in microglia via distinct signalling pathways. Eur J Neurosci 2001;14:463-473.

Schilling T, Eder C. Ion channel expression in resting and activated microglia of hippocampal slices from juvenile mice. Brain Res 2007;1186:21-28.

Schmidtmayer J, Jacobsen C, Miksch G, Sievers J. Blood monocytes and spleen macrophages differentiate into microglia-like cells on monolayers of astrocytes: membrane currents. Glia 1994;12:259-267.

Schmued LC, Albertson C, Slikker W, Jr. Fluoro-Jade: a novel fluorochrome for the sensitive and reliable histochemical localization of neuronal degeneration. Brain Res 1997;751:37-46.

Schmued LC, Hopkins KJ. Fluoro-Jade B: a high affinity fluorescent marker for the localization of neuronal degeneration. Brain Res 2000;874:123-130.

Schmued LC, Hopkins KJ. Fluoro-Jade: novel fluorochromes for detecting toxicant-induced neuronal degeneration. Toxicol Pathol 2000;28:91-99.

Schmued LC, Stowers CC, Scallet AC, Xu L. Fluoro-Jade C results in ultra high resolution and contrast labeling of degenerating neurons. Brain Res 2005;1035:24-31.

Schroder W, Hinterkeuser S, Seifert G et al. Functional and molecular properties of human astrocytes in acute hippocampal slices obtained from patients with temporal lobe epilepsy. Epilepsia 2000;41 Suppl 6:S181-S184.

Schwartz M, Butovsky O, Bruck W, Hanisch UK. Microglial phenotype: is the commitment reversible? Trends Neurosci 2006;29:68-74.

Seifert G, Steinhäuser C. Ionotropic glutamate receptors in astrocytes. Prog Brain Res 2001;132:287-299.

Serantes R, Arnalich F, Figueroa M et al. Interleukin-1beta enhances GABAA receptor cell-surface expression by a phosphatidylinositol 3-kinase/Akt pathway: relevance to sepsis-associated encephalopathy. J Biol Chem 2006;281:14632-14643.

Sgroi D, Stamenkovic I. The B-cell adhesion molecule CD22 is cross-species reactive and recognizes distinct sialoglycoproteins on different functional T-cell sub-populations. Scand J Immunol 1994;39:433-438.

Shankaran M, Marino ME, Busch R et al. Measurement of brain microglial proliferation rates in vivo in response to neuroinflammatory stimuli: application to drug discovery. J Neurosci Res 2007;85:2374-2384.

Shapiro LA, Perez ZD, Foresti ML, Arisi GM, Ribak CE. Morphological and ultrastructural features of Iba1-immunolabeled microglial cells in the hippocampal dentate gyrus. Brain Res 2009;1266:29-36.

Sheehan JJ, Tsirka SE. Fibrin-modifying serine proteases thrombin, tPA, and plasmin in ischemic stroke: a review. Glia 2005;50:340-350.

Sholl DA. Dendritic organization in the neurons of the visual and motor cortices of the cat. J Anat 1953;87:387-406.

Shytle RD, Mori T, Townsend K et al. Cholinergic modulation of microglial activation by alpha 7 nicotinic receptors. J Neurochem 2004;89:337-343.

Singer W, Lux HD. Presynaptic depolarization and extracellular potassium in the cat lateral geniculate nucleus. Brain Res 1973;64:17-33.

Siskova Z, Page A, O'Connor V, Perry VH. Degenerating synaptic boutons in prion disease: microglia activation without synaptic stripping. Am J Pathol 2009;175:1610-1621.

Skibo GG, Nikonenko IR, Savchenko VL, McKanna JA. Microglia in organotypic hippocampal slice culture and effects of hypoxia: ultrastructure and lipocortin-1 immunoreactivity. Neuroscience 2000;96:427-438.

Skou JC, Butler KW, Hansen O. The effect of magnesium, ATP, P i , and sodium on the inhibition of the (Na + + K +)-activated enzyme system by g-strophanthin. Biochim Biophys Acta 1971;241:443-461.

Sola C, Casal C, Tusell JM, Serratosa J. Astrocytes enhance lipopolysaccharide-induced nitric oxide production by microglial cells. Eur J Neurosci 2002;16:1275-1283.

Soulet D, Rivest S. Bone-marrow-derived microglia: myth or reality? Curr Opin Pharmacol 2008;8:508-518.

Soulet D, Rivest S. Microglia. Curr Biol 2008;18:R506-R508.

Squire LR, Bloom FE, McConnel SK et al. Electrotonic properties of axons and dendrites. In: Squire LR, Bloom FE, McConnel SK, Roberts JL, Spitzer NC, Zigmond MJ, (eds): Fundamental neuroscience. 2nd ed.London, UK: Academic Press, 2003

Sriram S. Role of glial cells in innate immunity and their role in CNS demyelination. J Neuroimmunol 2011;239:13-20.

Stamenkovic I, Sgroi D, Aruffo A, Sy MS, Anderson T. The B lymphocyte adhesion molecule CD22 interacts with leukocyte common antigen CD45RO on T cells and alpha 2-6 sialyltransferase, CD75, on B cells. Cell 1991;66:1133-1144.

Steinert JR, Robinson SW, Tong H et al. Nitric oxide is an activity-dependent regulator of target neuron intrinsic excitability. Neuron 2011;71:291-305.

Stella N. Endocannabinoid signaling in microglial cells. Neuropharmacology 2009;56 Suppl 1:244-253.

Stellwagen D, Beattie EC, Seo JY, Malenka RC. Differential regulation of AMPA receptor and GABA receptor trafficking by tumor necrosis factor-alpha. J Neurosci 2005;25:3219-3228.

Stellwagen D, Malenka RC. Synaptic scaling mediated by glial TNF-alpha. Nature 2006;440:1054-1059.

Stence N, Waite M, Dailey ME. Dynamics of microglial activation: a confocal time-lapse analysis in hippocampal slices. Glia 2001;33:256-266.

Stern EL, Quan N, Proescholdt MG, Herkenham M. Spatiotemporal induction patterns of cytokine and related immune signal molecule mRNAs in response to intrastriatal injection of lipopolysaccharide. J Neuroimmunol 2000;106:114-129.

Stoppini L, Buchs PA, Müller D. A simple method for organotypic cultures of nervous tissue. J Neurosci Methods 1991;37:173-182.

Streit WJ, Kreutzberg GW. Lectin binding by resting and reactive microglia. J Neurocytol 1987;16:249-260.

Streit WJ. Microglial-neuronal interactions. J Chem Neuroanat 1993;6:261-266.

Streit WJ, Graeber MB. Heterogeneity of microglial and perivascular cell populations: insights gained from the facial nucleus paradigm. Glia 1993;7:68-74.

Streit WJ, Walter SA, Pennell NA. Reactive microgliosis. Prog Neurobiol 1999;57:563-581.

Streit WJ. Microglia as neuroprotective, immunocompetent cells of the CNS. Glia 2002;40:133-139.

Streit WJ. Microglial cells. In: Kettenmann H, Ransom BR, (eds): Neuroglia. 1st ed.New York: Oxford University Press, 2005

Su T, Paradiso B, Long YS, Liao WP, Simonato M. Evaluation of cell damage in organotypic hippocampal slice culture from adult mouse: a potential model system to study neuroprotection. Brain Res 2011;1385:68-76.

Sugama S, Takenouchi T, Fujita M, Kitani H, Hashimoto M. Cold stress induced morphological microglial activation and increased IL-1beta expression in astroglial cells in rat brain. J Neuroimmunol 2011;233:29-36.

Sun J, Zhang X, Broderick M, Fein H. Measurement of Nitric Oxide Production in Biological Systems by Using Griess Reaction Assay. Sensors 2003;3:276-284.

Sundstrom L, Morrison B, III, Bradley M, Pringle A. Organotypic cultures as tools for functional screening in the CNS. Drug Discov Today 2005;10:993-1000.

Sunico CR, Portillo F, Gonzalez-Forero D, Moreno-Lopez B. Nitric-oxide-directed synaptic remodeling in the adult mammal CNS. J Neurosci 2005;25:1448-1458.

Svensson M, Aldskogius H. Synaptic density of axotomized hypoglossal motorneurons following pharmacological blockade of the microglial cell proliferation. Exp Neurol 1993;120:123-131.

Takahashi H, Magee JC. Pathway interactions and synaptic plasticity in the dendritic tuft regions of CA1 pyramidal neurons. Neuron 2009;62:102-111.

Tan J, Town T, Mori T et al. CD45 opposes beta-amyloid peptide-induced microglial activation via inhibition of p44/42 mitogen-activated protein kinase. J Neurosci 2000;20:7587-7594.

Tan J, Town T, Mullan M. CD45 inhibits CD40L-induced microglial activation via negative regulation of the Src/p44/42 MAPK pathway. J Biol Chem 2000;275:37224-37231.

Tanaka K, Okada Y, Kanno T et al. A dopamine receptor antagonist L-745,870 suppresses microglia activation in spinal cord and mitigates the progression in ALS model mice. Exp Neurol 2008;211:378-386.

Tang SC, Arumugam TV, Xu X et al. Pivotal role for neuronal Toll-like receptors in ischemic brain injury and functional deficits. Proc Natl Acad Sci U S A 2007;104:13798-13803.

Tang SC, Lathia JD, Selvaraj PK et al. Toll-like receptor-4 mediates neuronal apoptosis induced by amyloid beta-peptide and the membrane lipid peroxidation product 4-hydroxynonenal. Exp Neurol 2008;213:114-121.

Taylor DL, Diemel LT, Cuzner ML, Pocock JM. Activation of group II metabotropic glutamate receptors underlies microglial reactivity and neurotoxicity following stimulation with chromogranin A, a peptide up-regulated in Alzheimer's disease. J Neurochem 2002;82:1179-1191.

Taylor DL, Diemel LT, Pocock JM. Activation of microglial group III metabotropic glutamate receptors protects neurons against microglial neurotoxicity. J Neurosci 2003;23:2150-2160.

Taylor DL, Jones F, Kubota ES, Pocock JM. Stimulation of microglial metabotropic glutamate receptor mGlu2 triggers tumor necrosis factor alpha-induced neurotoxicity in concert with microglial-derived Fas ligand. J Neurosci 2005;25:2952-2964.

Tedder TF, Tuscano J, Sato S, Kehrl JH. CD22, a B lymphocyte-specific adhesion molecule that regulates antigen receptor signaling. Annu Rev Immunol 1997;15:481-504.

Tetreault NA, Hakeem AY, Jiang S et al. Microglia in the Cerebral Cortex in Autism. J Autism Dev Disord 2012.

Thams S, Oliveira A, Cullheim S. MHC class I expression and synaptic plasticity after nerve lesion. Brain Res Rev 2008;57:265-269.

Theiler K. The house mouse; development and normal stages from fertilization to 4 weeks of age. Berlin-Heidelberg-New York: Springer Verlag, 1972.

Thellung S, Corsaro A, Villa V et al. Amino-terminally truncated prion protein PrP90-231 induces microglial activation in vitro. Ann N Y Acad Sci 2007;1096:258-270.

Tian L, Lappalainen J, Autero M et al. Shedded neuronal ICAM-5 suppresses T-cell activation. Blood 2008;111:3615-3625.

Tomimatsu Y, Idemoto S, Moriguchi S, Watanabe S, Nakanishi H. Proteases involved in long-term potentiation. Life Sci 2002;72:355-361.

Tomozawa Y, Yabuuchi K, Inoue T, Satoh M. Participation of cAMP and cAMP-dependent protein kinase in beta-adrenoceptor-mediated interleukin-1 beta mRNA induction in cultured microglia. Neurosci Res 1995;22:399-409.

Trachtenberg JT, Chen BE, Knott GW et al. Long-term in vivo imaging of experience-dependent synaptic plasticity in adult cortex. Nature 2002;420:788-794.

Trapp BD, Wujek JR, Criste GA et al. Evidence for synaptic stripping by cortical microglia. Glia 2007;55:360-368.

Tremblay ME, Majewska AK. A role for microglia in synaptic plasticity? Commun Integr Biol 2011;4:220-222.

Ulvestad E, Williams K, Bjerkvig R et al. Human microglial cells have phenotypic and functional characteristics in common with both macrophages and dendritic antigen-presenting cells. J Leukoc Biol 1994;56:732-740.

Ulvestad E, Williams K, Bo L et al. HLA class II molecules (HLA-DR, -DP, -DQ) on cells in the human CNS studied in situ and in vitro. Immunology 1994;82:535-541.

Ulvestad E, Williams K, Matre R et al. Fc receptors for IgG on cultured human microglia mediate cytotoxicity and phagocytosis of antibody-coated targets. J Neuropathol Exp Neurol 1994;53:27-36.

van Noort JM, Baker D, Amor S. Mechanisms in the development of multiple sclerosis lesions: reconciling autoimmune and neurodegenerative factors. CNS Neurol Disord Drug Targets 2012;11:556-569.

van der Valk J, Brunner D, De SK et al. Optimization of chemically defined cell culture media--replacing fetal bovine serum in mammalian in vitro methods. Toxicol In Vitro 2010;24:1053-1063.

van Neerven S, Nemes A, Imholz P et al. Inflammatory cytokine release of astrocytes in vitro is reduced by all-trans retinoic acid. J Neuroimmunol 2010;229:169-179.

Velez-Fort M, Audinat E, Angulo MC. Central role of GABA in neuron-glia interactions. Neuroscientist 2012;18:237-250.

Verkhratsky A. Physiology of neuronal-glial networking. Neurochem Int 2010;57:332-343.

Visentin S, Renzi M, Levi G. Altered outward-rectifying K(+) current reveals microglial activation induced by HIV-1 Tat protein. Glia 2001;33:181-190.

Viviani B, Bartesaghi S, Gardoni F et al. Interleukin-1beta enhances NMDA receptor-mediated intracellular calcium increase through activation of the Src family of kinases. J Neurosci 2003;23:8692-8700.

Viviani B, Gardoni F, Marinovich M. Cytokines and neuronal ion channels in health and disease. Int Rev Neurobiol 2007;82:247-263.

Vogt C, Hailer NP, Ghadban C, Korf HW, Dehghani F. Successful inhibition of excitotoxic neuronal damage and microglial activation after delayed application of interleukin-1 receptor antagonist. J Neurosci Res 2008;86:3314-3321.

von Zahn J, Möller T, Kettenmann H, Nolte C. Microglial phagocytosis is modulated by pro- and anti-inflammatory cytokines. Neuroreport 1997;8:3851-3856.

Vornov JJ, Tasker RC, Park J. Neurotoxicity of acute glutamate transport blockade depends on coactivation of both NMDA and AMPA/Kainate receptors in organotypic hippocampal cultures. Exp Neurol 1995;133:7-17.

Wahab A, Albus K, Heinemann U. Age- and region-specific effects of anticonvulsants and bumetanide on 4-aminopyridine-induced seizure-like events in immature rat hippocampal-entorhinal cortex slices. Epilepsia 2011;52:94-103.

Walker JA, Smith KG. CD22: an inhibitory enigma. Immunology 2008;123:314-325.

Wallraff A, Kohling R, Heinemann U et al. The impact of astrocytic gap junctional coupling on potassium buffering in the hippocampus. J Neurosci 2006;26:5438-5447.

Walter L, Franklin A, Witting A et al. Nonpsychotropic cannabinoid receptors regulate microglial cell migration. J Neurosci 2003;23:1398-1405.

Walter P, Ron D. The unfolded protein response: from stress pathway to homeostatic regulation. Science 2011;334:1081-1086.

Wang D, Lu H, Xu T. Mediation by calcium/calmodulin-dependent protein kinase II of suppression of GABA(A) receptors by NMDA. Sci China C Life Sci 2000;43:655-662.

Wang K, Bekar LK, Furber K, Walz W. Vimentin-expressing proximal reactive astrocytes correlate with migration rather than proliferation following focal brain injury. Brain Res 2004;1024:193-202.

Wang Q, Liu L, Pei L et al. Control of synaptic strength, a novel function of Akt. Neuron 2003;38:915-928.

Wang Q, Yu S, Simonyi A, Sun GY, Sun AY. Kainic acid-mediated excitotoxicity as a model for neurodegeneration. Mol Neurobiol 2005;31:3-16.

Wang Q, Andreasson K. The organotypic hippocampal slice culture model for examining neuronal injury. J Vis Exp 2010.

Watanabe T, Fan J. Atherosclerosis and inflammation mononuclear cell recruitment and adhesion molecules with reference to the implication of ICAM-1/LFA-1 pathway in atherogenesis. Int J Cardiol 1998;66 Suppl 1:S45-S53.

Webb M, Barclay AN. Localisation of the MRC OX-2 glycoprotein on the surfaces of neurones. J Neurochem 1984;43:1061-1067.

Weibel ER. Morphometry of the human lung: the state of the art after two decades. Bull Eur Physiopathol Respir 1979;15:999-1013.

Weis C, Humpel C. Evidence that toxicity of lipopolysaccharide upon cholinergic basal forebrain neurons requires the presence of glial cells in vitro. Brain Res Bull 2002;58:91-98.

Weissenbock H, Hornig M, Hickey WF, Lipkin WI. Microglial activation and neuronal apoptosis in Bornavirus infected neonatal Lewis rats. Brain Pathol 2000;10:260-272.

Wenzel HJ, Tamse CT, Schwartzkroin PA. Dentate development in organotypic hippocampal slice cultures from p35 knockout mice. Dev Neurosci 2007;29:99-112.

Wesseling JF, Lo DC. Limit on the role of activity in controlling the release-ready supply of synaptic vesicles. J Neurosci 2002;22:9708-9720.

West MJ, Slomianka L, Gundersen HJ. Unbiased stereological estimation of the total number of neurons in thesubdivisions of the rat hippocampus using the optical fractionator 1. Anat Rec 1991;231:482-497.

West MJ. Design-based stereological methods for counting neurons. Prog Brain Res 2002;135:43-51.

Wheeler D, Knapp E, Bandaru VV et al. Tumor necrosis factor-alpha-induced neutral sphingomyelinase-2 modulates synaptic plasticity by controlling the membrane insertion of NMDA receptors. J Neurochem 2009;109:1237-1249.

Williamson LL, Sholar PW, Mistry RS, Smith SH, Bilbo SD. Microglia and memory: modulation by early-life infection. J Neurosci 2011;31:15511-15521.

Wirenfeldt M, Babcock AA, Ladeby R et al. Reactive microgliosis engages distinct responses by microglial subpopulations after minor central nervous system injury. J Neurosci Res 2005;82:507-514.

Wirenfeldt M, Dissing-Olesen L, Anne BA et al. Population control of resident and immigrant microglia by mitosis and apoptosis. Am J Pathol 2007;171:617-631.

Wirenfeldt M, Babcock AA, Vinters HV. Microglia - insights into immune system structure, function, and reactivity in the central nervous system. Histol Histopathol 2011;26:519-530.

Witschi E. Development: Rat. In: Altman PL, Dittmer DS, (eds): Growth including reproduction and morphological development.Washington., D.C.: Fed Am Soc Exp Biol, 1962

Wright GJ, Cherwinski H, Foster-Cuevas M et al. Characterization of the CD200 receptor family in mice and humans and their interactions with CD200. J Immunol 2003;171:3034-3046.

Wu CH, Wen CY, Shieh JY, Ling EA. Down-regulation of membrane glycoprotein in amoeboid microglia transforming into ramified microglia in postnatal rat brain. J Neurocytol 1994;23:258-269.

Wu CH, Chien HF, Chang CY, Ling EA. Heterogeneity of antigen expression and lectin labeling on microglial cells in the olfactory bulb of adult rats. Neurosci Res 1997;28:67-75.

Wu CH, Chien HF, Chang CY, Chen SH, Huang YS. Response of amoeboid and differentiating ramified microglia to glucocorticoids in postnatal rats: a lectin histochemical and ultrastructural study. Neurosci Res 2001;40:235-244.

Wynne AM, Henry CJ, Huang Y, Cleland A, Godbout JP. Protracted downregulation of CX3CR1 on microglia of aged mice after lipopolysaccharide challenge. Brain Behav Immun 2010;24:1190-1201.

Yamada J, Sawada M, Nakanishi H. Cell cycle-dependent regulation of kainate-induced inward currents in microglia. Biochem Biophys Res Commun 2006;349:913-919.

Yang H. Structure, Expression, and Function of ICAM-5. Comp Funct Genomics 2012;2012:368938.

Yang S, Liu ZW, Wen L et al. Interleukin-1beta enhances NMDA receptor-mediated current but inhibits excitatory synaptic transmission. Brain Res 2005;1034:172-179.

Yeo SI, Kim JE, Ryu HJ et al. The roles of fractalkine/CX3CR1 system in neuronal death following pilocarpine-induced status epilepticus. J Neuroimmunol 2011;234:93-102.

Young AM, Campbell E, Lynch S, Suckling J, Powis SJ. Aberrant NF-kappaB expression in autism spectrum condition: a mechanism for neuroinflammation. Front Psychiatry 2011;2:27.

Zattoni M, Mura ML, Deprez F et al. Brain infiltration of leukocytes contributes to the pathophysiology of temporal lobe epilepsy. J Neurosci 2011;31:4037-4050.

Zhang D, Hu X, Qian L et al. Microglial MAC1 receptor and PI3K are essential in mediating beta-amyloid peptide-induced microglial activation and subsequent neurotoxicity. J Neuroinflammation 2011;8:3.

Zhang L, McLarnon JG, Goghari V et al. Cholinergic agonists increase intracellular Ca2+ in cultured human microglia. Neurosci Lett 1998;255:33-36.

Zhang L, Berta T, Xu ZZ et al. TNF-alpha contributes to spinal cord synaptic plasticity and inflammatory pain: distinct role of TNF receptor subtypes 1 and 2. Pain 2011;152:419-427.

Zhang R, Yamada J, Hayashi Y et al. Inhibition of NMDA-induced outward currents by interleukin-1beta in hippocampal neurons. Biochem Biophys Res Commun 2008;372:816-820.

Zhang R, Sun L, Hayashi Y et al. Acute p38-mediated inhibition of NMDA-induced outward currents in hippocampal CA1 neurons by interleukin-1beta. Neurobiol Dis 2010;38:68-77.

Zhang RX, Li A, Liu B et al. IL-1ra alleviates inflammatory hyperalgesia through preventing phosphorylation of NMDA receptor NR-1 subunit in rats. Pain 2008;135:232-239.

Zhang RX, Liu B, Li A et al. Interleukin 1beta facilitates bone cancer pain in rats by enhancing NMDA receptor NR-1 subunit phosphorylation. Neuroscience 2008;154:1533-1538.

Zhang W, Linden DJ. The other side of the engram: experience-driven changes in neuronal intrinsic excitability. Nat Rev Neurosci 2003;4:885-900.

Zhang W, Wang T, Pei Z et al. Aggregated alpha-synuclein activates microglia: a process leading to disease progression in Parkinson's disease. FASEB J 2005;19:533-542.

Zhang XM, Zhu J. Kainic Acid-induced neurotoxicity: targeting glial responses and glia-derived cytokines. Curr Neuropharmacol 2011;9:388-398.

Zhang Y, Saccani S, Shin H, Nikolajczyk BS. Dynamic protein associations define two phases of IL-1beta transcriptional activation. J Immunol 2008;181:503-512.

Zheng H, Zhu W, Zhao H et al. Kainic acid-activated microglia mediate increased excitability of rat hippocampal neurons in vitro and in vivo: crucial role of interleukin-1beta. Neuroimmunomodulation 2010;17:31-38.

Zheng XY, Zhang HL, Luo Q, Zhu J. Kainic acid-induced neurodegenerative model: potentials and limitations. J Biomed Biotechnol 2011;2011:457079.

Zhou Y, Wang Y, Kovacs M, Jin J, Zhang J. Microglial activation induced by neurodegeneration: a proteomic analysis. Mol Cell Proteomics 2005;4:1471-1479.

Zhu W, Zheng H, Shao X et al. Excitotoxicity of TNFalpha derived from KA activated microglia on hippocampal neurons in vitro and in vivo. J Neurochem 2010;114:386-396.

Zimmer J, Gähwiler BH. Cellular and connective organization of slice cultures of the rat hippocampus and fascia dentata. J Comp Neurol 1984;228:432-446.

Zimmer J, Kristensen BW, Jakobsen B, Noraberg J. Excitatory amino acid neurotoxicity and modulation of glutamate receptor expression in organotypic brain slice cultures. Amino Acids 2000;19:7-21.

Zucker RS. Short-term synaptic plasticity. Annu Rev Neurosci 1989;12:13-31.

Zucker RS, Regehr WG. Short-term synaptic plasticity. Annu Rev Physiol 2002;64:355-405.

Zujovic V, Benavides J, Vige X, Carter C, Taupin V. Fractalkine modulates TNF-alpha secretion and neurotoxicity induced by microglial activation. Glia 2000;29:305-315.

Zujovic V, Taupin V. Use of cocultured cell systems to elucidate chemokine-dependent neuronal/microglial interactions: control of microglial activation. Methods 2003;29:345-350.

Zurolo E, Iyer A, Maroso M et al. Activation of Toll-like receptor, RAGE and HMGB1 signalling in malformations of cortical development. Brain 2011;134:1015-1032.

8. CURRICULUM VITAE

Mein Lebenslauf wird aus datenschutzrechtlichen Gründen in der elektronischen Version meiner Arbeit nicht veröffentlicht.

Mein Lebenslauf wird aus datenschutzrechtlichen Gründen in der elektronischen Version meiner Arbeit nicht veröffentlicht.

9. PUBLICATION LIST

PUBLICATIONS IN SCIENTIFIC JOURNALS

- Assimakopoulos SF, Papageorgiou I, Charonis A. Intestinal Tight Junctions: a molecular approach and clinical implications. World J Gastroint Pathol, 2011; 2(6):123-37 [Review]
- Kann O, Taubenberger N, Huchzermeyer C, Papageorgiou IE, Benninger F, Heinemann U, Kovács R. Muscarinic receptor activation determines the effects of store-operated Ca2+-entry on excitability and energy metabolism in pyramidal neurons. Cell Calcium, 2012; 51(1): 40-50
- Papageorgiou IE, Gabriel S, Fetani AF, Kann O, Heinemann U. Redistribution of astrocytic glutamine synthetase in the hippocampus of chronic epileptic rats. Glia, 2011; 59(11):1706-18
- Kovacs R, Papageorgiou IE, Heinemann U. Slice cultures as a model to study neurovascular coupling and blood brain barrier in vitro. Cardiovasc. Psychiatry Neurol., 2011; Volume 2011: Article ID 646958
- Psilopanagioti A, Malliaris P, Papageorgiou I, Alexopoulos P, Papavassiliou AG, Dougenis D. Mechanical circulatory support: a clinical and molecular approach. Arch. Hellen. Med., 2004; 21(1): 13-25 [Review] [Article in Greek]
- Papageorgiou I, Charonis A. Tight Junctions: A molecular approach. Arch. Hellen. Med. 2002; 20SA: 112-25 [Review]
- Papageorgiou I, Charonis A. Hemidesmosomes. Iatriki 2002; 81(5): 389-402 [Review] [Article in Greek]

PUBLICATIONS IN SCIENTIFIC MEETINGS

ORAL PRESENTATIONS

- Papageorgiou I. Microglia cell influence on neuronal excitability. In: Junior Neuroscientists meeting on epilepsy. Sept 2011, Berlin, Germany
- Papageorgiou I. Microglia: role in epilepsy. Insights from a microglia depletion model. In: 2nd PhD Student Meeting of the Transregional Research Consortium SFB/TR3 ‘Mesial Temporal Lobe Epilepsies’. May 2010, Bonn, Germany
- Papageorgiou I. SFB-TR3, D12 project: Free radical formation and mitochondrial damage as a key factor in epileptogenesis.In: 1st PhD Student Meeting of the

Transregional Research Consortium SFB/TR3 ‘Mesial Temporal Lobe Epilepsies’. May 2009, Bonn, Germany

- Papageorgiou I, Avgeris P, Papadimitriou E, Boulis S, Tzoumakas K. Comparative rehabilitation of Colle’s fracture: Röntgen guided closed reduction versus external osteosynthesis.In: 14th Congress of Medico surgical Association of Corfu, March 2006, Corfu, Greece

POSTER PRESENTATIONS

- Papageorgiou IE, Scheffel J, Hanisch U-K, Kann O. Lipopolysaccharide activated microglial cells induce moderate changes in neuronal function: a long-term exposure study in organotypic hippocampal cultures. In: 8th FENS Forum, July 2012, Barcelona, Spain
- Papageorgiou IE, Kann O. Microglia (brain macrophages): vectors of inflammation but not necessarily of neurotoxicity. Insights from organotypic slice cultures. In: 12th Annual IZN retreat, July 2012, Kloster Schöntal, Heidelberg, Germany
- Papageorgiou IE, Kann O. Chronic lipopolysaccharide exposure of organotypic hipppocampal slice cultures induces microglial activation without neurotoxic impact. In: 91st Annual meeting of the German Physiologic society, March 2012, Dresden, Gemany
- Papageorgiou IE, Fetani AF, Kann O, Heinemann U. Microglia in epilepsy are activated in a region specific manner : a morphologic analysis in the epileptic rat hippocampus. In: 29th International Epilepsy Congress, Aug 2011, Rome, Italy
- Papageorgiou IE, Kann O. Organotypic hippocampal slice cultures as electrophysiological model for studying microglia activation. In: FENS IBRO Summer School ‘Metabolic aspects of chronic brain diseases’, July 2011, Reisensburg/Günzburg, Germany
- Papageorgiou IE, Eom G, Heppner FL, Kann O. In vivo microglia depletion modifies short term plasticity in the Schaffer collateral pathway of mouse hippocampus. In: 33rd Göttingen Neurobiology Conference & 9th Meeting of the German Neuroscience Society, March 2011, Göttingen, Germany
- Papageorgiou IE, Gabriel S, Kann O, Heinemann U. Redistribution of glutamine synthetase in temporal lobe epilepsy: evidence from the rat pilocarpine model. In: Berlin Brain Days 2010, Nov 2010, Berlin, Germany

- Papageorgiou IE, Kann O, Gabriel S, Heinemann U. Glutamine synthetase in a temporal lobe epilepsy model exhibits modified subcellular expression pattern. In: 9th European Congress on Epileptology, June 2010, Rhodes, Greece
- Papageorgiou I, Eom G, Huchzermeyer C, Kaelin RE, Heppner FL, Kann O. Microglia cell ablation in a transgenic mouse model: Electrophysiological properties. In: Berlin Brain Days 2009, Dec 2009, Berlin, Germany
- Eom GD*, Papageorgiou I*, Kälin RE, Kann O, Heppner FL (*equal contribution). Functional characterization of neuronal electrophysiological properties upon in vivo microglial ablation. In: 54th Annual Meeting of the DGNN, Sept 2009, Düsseldorf, Germany

10. ERKLÄRUNG

Ich, Ismini Papageorgiou, erkläre, dass ich die vorgelegte Dissertation mit dem Thema: ‚Influence of microglial activation on neuronal survival and excitability' selbst verfasst und keine anderen als die angegebenen Quellen und Hilfsmittel benutzt, ohne die (unzulässige) Hilfe Dritter verfasst und auch in Teilen keine Kopien anderer Arbeiten dargestellt habe.

Datum Unterschrift